UNIVERSITY
OF TRENTO - Italy
DEPARTMENT OF INDUSTRIAL ENGINEERING

XXIX cycle

Doctoral School in Materials, Mechatronics and System Engineering

Cell-laden hydrogels for biofabrication: matrices processing and cryopreservation

Nicola Cagol

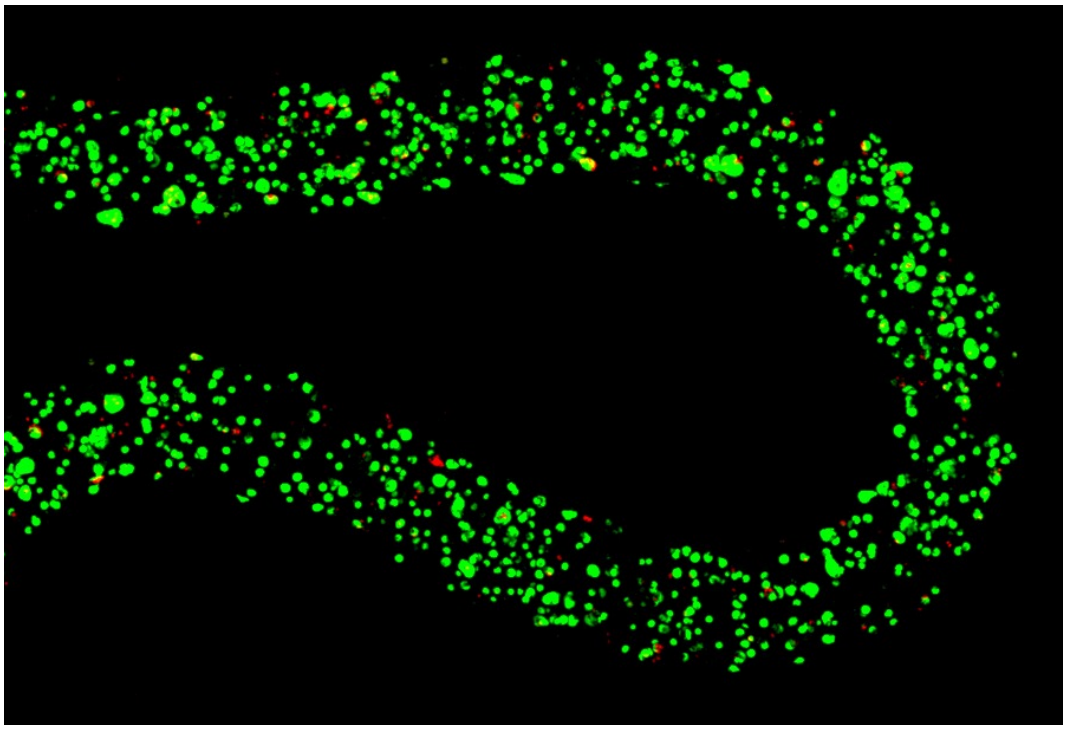

Trento, March 2018

Cell-laden hydrogels for biofabrication: matrices processing and cryopreservation

Nicola Cagol
nicola.cagol@unitn.it

Advisors

Prof. Claudio Migliaresi
Department of Industrial Engineering
University of Trento, Italy.

Dr. Devid Maniglio
Department of Industrial Engineering
University of Trento, Italy.

Doctoral Committee

Prof. Gilson Khang
Chonbuk National University, South Korea

Prof. Julio San Roman
CSIC, Spain

University of Trento,
Department of Industrial Engineering
March 2018

dedicated to those who believe in me

Table of content

Preface

In this dissertation, a report of my PhD research activity is provided. The activity was carried out in Biotech Research Center, part of the Industrial Engineering Department, of the University of Trento (Italy), under the supervision of Prof. Claudio Migliaresi and Dr. Devid Maniglio.

Biofabrication, an approach to the bottom-up paradigm of tissue engineering, represent the research topic. This technology is defined as the production of complex biological constructs using cells, components of the ECM, biomolecules and biomaterials that are assembled with different techniques in an engineered tissue fragment. The general aim of the work was to address some of the problems that currently limited the development and applicability of biofabrication. In particular, two issues were considered in the experimental part: the cryopreservation of cell-laden hydrogel constructs and the development of novel building blocks containing cells using alginate-based hydrogels. Alginate was the material of choice for investigation, as an accepted support for different tissue engineering applications that can sustain several modification and fabrication methods.

In the first chapter, the concepts of bottom up tissue engineering and biofabrication are introduced. The role and state of the art of hydrogels to manufacture cell-laden building blocks, the techniques for cell encapsulation and the commonly used fabrication strategies for biofabrication and bioprinting are reviewed together with their applications. Moreover, the limitations that currently restrict the applicability of hydrogel-based tissue engineering are discussed.

In chapter two, the role of alginate hydrogels in tissue engineering and biofabrication is described. In particular, its chemical content, crosslinking behavior, manufacturing capacity and applications are reviewed with emphasis on

the possible modification of alginate hydrogels in order to enhance biocompatibility and functionality of encapsulated cells.

The experimental part is described in the following chapters. Chapter three introduces the concept of cryopreservation, and in particular the issues concerning preservation of cell-laden building blocks. Subsequently, the impact of cryopreservation on the viability and functionality of cells encapsulated in alginate matrices is evaluated comparing different cryoprotective agents. The experimental methods for manufacturing and preserving cell-laden alginate fibers and for performing the biological and structural tests are reported. The results are presented, discussed and compared with the state of the art.

In chapter four, a novel method for encapsulating cells within alginate-based hydrogel films with micrometer thickness is described. The procedure for immobilizing cells within hydrogel films with different composition is described, together with the performed biological assays aimed at selecting the best matrix composition. The results are reported and discussed, emphasizing the potential applications and future developments of the proposed method.

Chapter 1.
Hydrogel based Biofabrication for Tissue Engineering and Regenerative Medicine

In this chapter, the use of hydrogels for cell culture will be introduced. The concept of tissue engineering, biofabrication, cell encapsulation and bioprinting will be discussed focusing on the role of hydrogels and considering both the manufacturing techniques and the applications of these technologies. In particular, the role of cell-laden hydrogels as building blocks for assembling complex 3D tissue-like constructs will be reviewed. Finally, current limitations and future perspective of hydrogel-based bottom-up tissue engineering will be discussed.

1.1 Introduction

Our ability to understand the biological mechanism that underlie many cell-based processes, such as migration, differentiation and force-sensing, is derived from studies performed on two-dimensional (2D), unphysiologically stiff materials like glass and plastic surfaces (fig. 1a). However, cells *in vivo* are likely to operate within a complex and hierarchical environment that contains multiple extracellular matrix (ECM) components, mixed cell populations and complex regulatory signals. Cells cultured in traditional monolayer substrates can differ substantially from those grown in more relevant 3D environment in terms of morphology, cell-cell and cell-matrix interaction, response to pharmaceutical reagents and differentiation pathway. Therefore, culture systems that better mimic the biological milieus are needed to bridge the gap between conventional cultures and complex native *in vivo* environments [1–3]. A range of biomaterials have been developed toward

the introduction of this complexity into cell culture systems, providing ways to control chemical, mechanical, compositional and topographical cues thus more accurately represent features of native tissues. Hydrogels, crosslinked networks that possess high water content, have emerged as the most promising option matrices for cell culture as they recapitulate aspects of the native cellular microenvironment [3–5].

1.2 Hydrogels as extracellular matrix mimic

Hydrogels are three-dimensional networks of hydrophilic homopolimers, copolymers of macromonomers, crosslinked to form insoluble polymer matrices. The three-dimensional structure of the polymer network is stabilized either by chemical cross-linking (covalent bonds) or physical cross-linking (entanglement, crystallites, ionic and hydrogen bonds). A wide range of natural or synthetic polymer compositions and crosslinking techniques have been used to fabricate and functionalize hydrogels with biological and biochemical cues [4–6]. Among their advantages are the possibility to control and modulate the swelling and degradation kinetics, the mechanical and the diffusion properties by regulating the chemistry of the polymeric backbone, its hydrophilicity, the swelling degree and the crosslinking density. Thus, their biological interaction with cells can be tailored depending on the application [6,7].

Hydrogels are by definition capable of binding large quantities of water and possess facile transport of oxygen, nutrients and waste, as well as realistic transport of soluble factors [2]. Therefore, they may promote the cell population to exhibit phenotypes more similar to those found in native tissues than when the cells are grown in monolayer culture (fig. 1b). These ECM-like properties allow cell encapsulation in a highly hydrated, mechanically supportive 3D environment;

making them attractive for regenerative medicine and other biomedical applications [2,3]. Since the formation of many hydrogels can occurs under mild, cytocompatible conditions, they are often used in conjunction with cell micro-encapsulation technologies, which consists in the immobilization of viable cells within a permeable tridimensional construct [8,9].

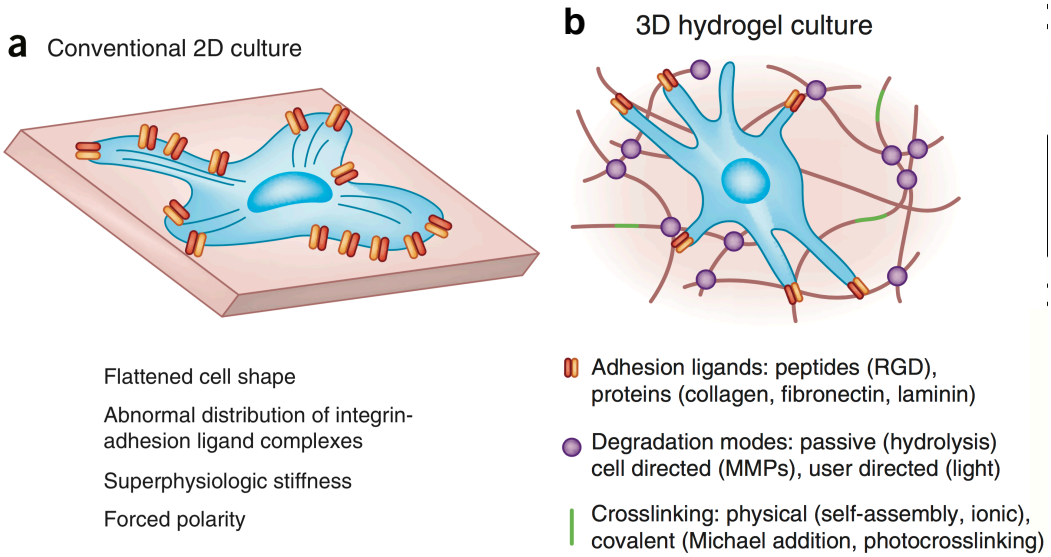

Figure 1. (a) conventional 2D cell culture on unphysiological stiff plastic or glass substrates leads to cells displaying aberrant phenotypes. **(b)** Engineered hydrogels can be used to recapitulate a more realistic 3D microenvironemt to encapsulated cells. Hydrogels design variables are indicated considering the typical physiological cues of the extracellular matrix (ECM). Adapted from [3].

Hydrogels are suitable for a wide range biomedical and pharmaceutical application, for example contact lenses, wound dressing and carrier for drug delivery [4]. Furthermore, due to their unique biocompatibility, excellent diffusion properties, range of constituents and desirable physical characteristic, they have been the material of choice for many applications in tissue engineering. They can

serve as scaffold that provide structural integrity to tissue constructs, control drug and protein delivery to tissue and cultures and serve as barriers between tissue and material surface [4,7,10].

1.3 Definitions and recent developments of tissue engineering

Tissue engineering (TE), a major component of regenerative medicine, aims to functionally replace lost and/or damaged tissues, through the combination of bioactive materials with cells to generate engineered constructs [11–13]. TE aims to overcome the limitations of current treatments based on organ transplantation by generating 'artificial' organs and tissue substitutes that can grow along with the patient [11,14]. This discipline has evolved as an interdisciplinary technology combining principles from the life, material and engineering sciences for the development of biological substitutes that restore, maintain or improve tissue function or a whole organ and for the production or realistic tissue constructs for *in vitro* applications [14,15]. TE has emerged not only for overcoming the limitations of current treatments based on organ transplantation but also for generating tissue-engineered surrogates that could be useful for drug screening, chemical toxicity testing and basic cell biology studies [16,17].

Traditional tissue engineering strategies employ a "top-down" approach, in which cells and growth factors are seeded in or onto biodegradable biomaterials to form constructs that can be immediately implanted or incubated *in vitro* prior to transplantation [17,18]. These materials serve as temporary scaffolds and promote the reorganization of the cells to form a functional tissue [15]. The top down approaches have been successfully used for the regeneration of thin avascular tissue over the past decades but are not yet suitable methods for generating 3D structures with physiological relevant size and a functional organization. In fact, the three-

dimensional constructs that have been generated with these scaffold-based TE approaches are typically based on the random distribution of cells, matrix and bioactive cues since their manufacturing have difficulty recreating the intricate microstructural features of native tissues [17–19].

To address this challenge, 'bottom up' tissue engineering aims to recreate biomimetic structures by designing structural features on the microscale to build modular units that can be used as building blocks to create larger tissues [19]. This approach, termed "biofabrication", relies on different additive manufacturing technology in order to pattern and assemble living and non-living material into bio-engineered 3D structures to replicate the complex nature of native tissue [20–22] (fig. 2a). Biofabrication technology encompasses a broad range of physical, chemical, biological, and/or engineering processes and demand contributions from different disciplines like cell and developmental biology, biomaterial science, and mechanical engineering [20]. The paradigm of bottom up tissue engineering concept that involves biofabrication of a cell-laden construct is reported in fig. 2b [23]. Cells are isolated from the patient and may be cultivated *in vitro* on two-dimensional surfaces for efficient expansion. Subsequently, the cells are combined with various biomaterials, small molecules and/or ECM fractions in order to generate a living scaffold. The scaffolds serve for harnessing the innate abilities of cells to sense their local environment through cell–cell and cell–extracellular matrix contacts and self-assemble into a functioning tissue. Bioreactors can be used to provide optimal conditions during the maturation of the cell constructs [15]. Cell-laden constructs can be used as *in vitro* model to study the interaction between different cells and bioactive molecules and to test drug or therapeutic procedures. Moreover, the biofabricated structures could also lead to functional tissue equivalents and potentially to whole functioning organs [17,18,22].

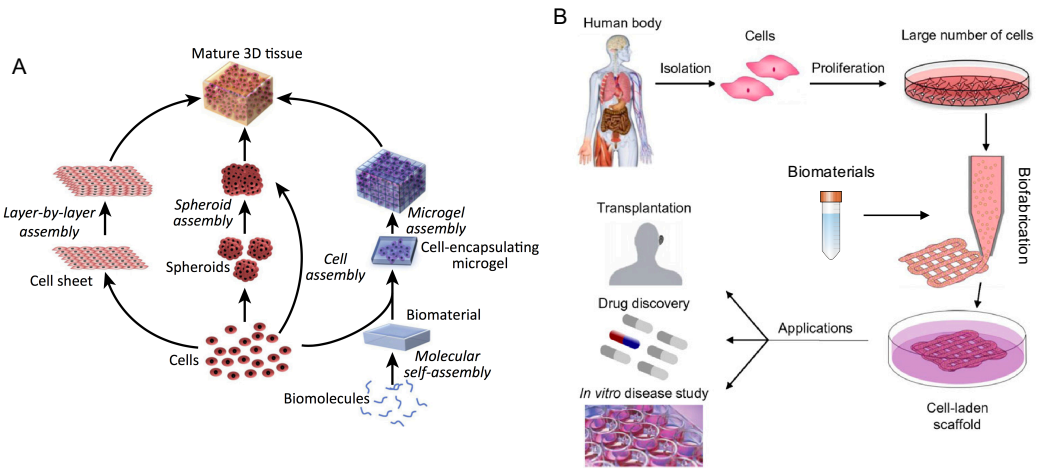

Figure 2. Biofabrication process, techniques, and applications. **(A)** Schematic of multiscale assembly strategies from bottom to top for engineering 3D tissue constructs. The assembly strategies can follow paths starting with biomolecules or cells and can be integrated in the engineering of the final 3D tissue constructs. Moreover, hydrogels can be introduced in the process to support mechanical stress and guide cells in an instructive microenvironment. Adapted from ref. [22]. **(B)** For human therapeutic applications, the typical workflow of biofabrication involves the isolation and expansion of human cells prior to manufacturing the desired cell-laden scaffold. These scaffolds could then ultimately be transplanted as therapeutic devices themselves or used as a testing platform for drug screening and discovery or as an *in vitro* model system for diseases. Adapted from [23].

In order to meet the increasing list of desirable traits of materials for biofabrication and tissue engineering in general, a variety of biomaterials have been developed to mimic specific cell and tissue niches [5,24]. These includes polymers (natural and synthetic), ceramics and composites [24]. In a recently published review, Murphy et al. reported a list of ideal material properties for biofabrication [25]:

- Biocompatibility. Materials should coexist with the endogenous tissue without inducing any undesirable local or systemic responses in the host and should contribute actively and controllably to the biological and functional components of the construct. This include supporting the appropriate cellular functions and facilitating molecular and mechanical signaling.

- Degradation kinetics and byproducts. Degradation rates should match the ability of the cells to replace the materials with their own ECM. Degradation products should be nontoxic, readily metabolized and rapidly cleared from the body. Moreover, materials should demonstrate suitable swelling characteristics without resulting in loss of layer integrity or deformation of the final construct.

- Structural and mechanical properties. Materials should be chosen based on the required mechanical properties of the constructs, as different structural requirements are needed for diverse tissue types.

- Material biomimicry. Engineering of desired structural, functional and dynamic material properties should be based on knowledge of the naturally occurring tissue-specific composition and localization of ECM components in the tissue of interest. The incorporation of ECM components, the addition of surface ligands and the presence of nanoscale features has the potential to affect cell attachment, proliferation, cytoskeletal assembly and differentiation processes.

- Handling and/or printability. Properties that facilitate handling and deposition may include viscosity, gelation methods and rheological properties. The choice of material may be also influenced by its ability to protect cell viability during the extrusion or printing of bioinks, assembling of multi-layered cellularized products, or weaving of fiber-based cell-laden modules.

The polymeric and ceramic materials that have been traditionally processed by additive manufacturing techniques typically require process parameters (e.g., high temperature, solvents, lack of water) that are not compatible with the direct inclusion of cells [24]. Different classes of natural and synthetic hydrogels that gelate in mild conditions are thus gaining increasing interest for fabricating complex 3D cellular microenvironments; they can be tuned for ideal physicochemical properties, degradability and mechanics, and their high water content creates an environment conductive to the encapsulation of cells [24,26].

The modules that serve as building blocks can be created in a number of ways, such as through self-assembled aggregation, creation of cell sheets, direct printing of cells and other supportive biomaterials, and microfabrication of cell-laden hydrogels [17,18]. Commonly used hydrogels modules for cell encapsulation consist in beads [27], fibers [28,29] and films [30]. Once created, these modules can be assembled into larger tissue constructs through a number of methods such as random packing, layer stacking or directed assembly[17,18,26].

1.4 Hydrogels as matrices for cell encapsulation

Hydrogels represent one of the most common scaffolding material in tissue engineering and are used to provide bulk and mechanical constitution to a tissue construct, whether cells and bioactive compounds are adhered to or suspended within the 3D gel framework [9,31]. Cell encapsulation consists in entrapping viable cells within a matrix which should allow cells viability while possibly supporting their growth, organization and metabolic activity [32,33] (fig. 3).

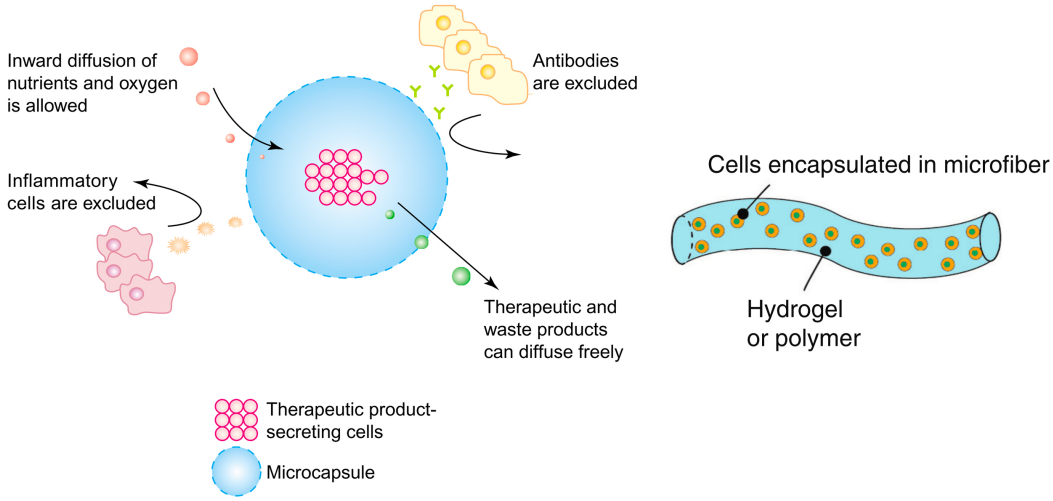

Figure 3. Schematic of the cell encapsulation into hydrogel beads **(left)** (adapted from [33]) or fibers **(right)** (adapted from [34]) This technique consists in enclosing cells and other biologically active materials within the polymeric matrix. The capsule interface allows the bi-directional diffusion of nutrients, oxygen, waste and therapeutic products, but prevents inflammatory cells and antibodies, which might destroy the enclosed cells, from entering the capsule.

Major requirements for the encapsulating material are to allow diffusion of oxygen and nutrients towards the cells. In fact, hydrogels can encapsulate cells during the fabrication process unlike traditional scaffold that are fabricated and seeded with cells in two times [31] (fig. 4). Hydrogels possess many properties which are attractive as stand-alone tissue scaffolds or vehicles to deliver drugs, growth factors or cell therapies: cytocompatibility, tissue mimetic water content, support of cell migration and tissue integration, sustained release of growth factors and controllable physical properties [10,35].

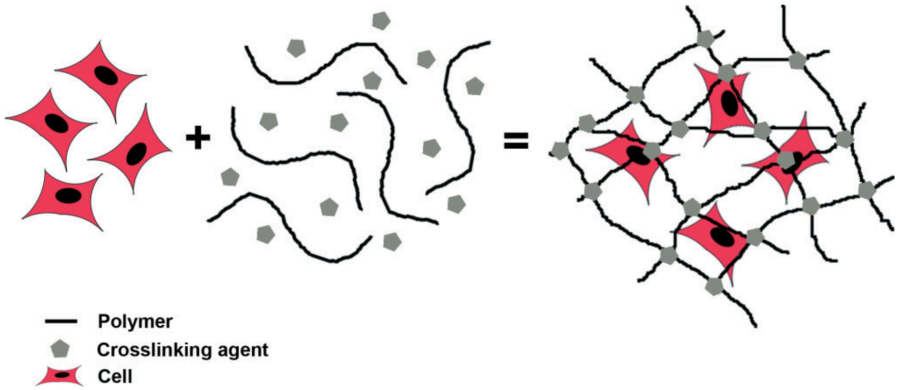

Figure 4. Mechanism of crosslinking of an hydrophilic polymer into a 3D hydrogel. Cells can be encapsulated during gelation if they were suspended in the liquid polymer solution. Adapted from [31].

Hydrogels used in tissue engineering applications are predominantly based on natural derived polymers, including alginate, gelatin, collagen, chitosan, silk fibroin, fibrin and hyaluronic acid, because of their inherent excellent cytocompatibility, low toxicity and susceptibility to enzymatic degradation [7]. Natural hydrogels, derived from polysaccharide or proteins, offer inherent bioactivity except for agarose and alginate and display a chemical and structural resemblance to ECM [36]. Synthetic hydrogels which lack biologic stimuli often require modification to introduce chemical and physical signals for instructive cell and tissue responses [10,37].

Natural and synthetic hydrogels are particularly attractive for biofabrication as artificial ECM to generate physiologically relevant 3D scaffolds for cell and tissue growth. In fact, hydrogels are good candidates for encapsulating cells during their fabrication process: cell-laden hydrogel can serve as building blocks [17,37] or used in conjunction with a set of additive manufacturing techniques that go under the name of bioprinting [25,38]. The principle of bioprinting can be defined as the use of automated 3D robotic technologies in order to place cell-laden materials into

spatially defined structures. The raw materials of bioprinting process, soft biomaterials loaded with living cells, are called 'bioinks' [38,39]. Various key properties including concentration, molecular weight, viscosity, gelation kinetics and stiffness can be selected according to the specific bioink requirements [16,38,39].

Moreover, hydrogels are also suitable to keep cells and fluid separate while allowing diffusion of soluble factors within their structure. This property can be used to encapsulate cells in micron to millimeter size capsules that can serve as delivery vehicles for cell-based therapies [9,32]. These microcapsules can also be engineered to allow for the diffusion of nutrients and removal of metabolites, while prohibiting interaction of encapsulated cells with the immune system, therefore avoiding the rejection of the implant by the host [32,33]. Therefore, encapsulation of cell offers several potential applications as the encapsulated cells can be transplanted within a host where they secrete specific disease treating molecules (e.g. against diabetes [40], anemia [41] or hemophilia [42]).

When cellular adhesion directly to the gel is favored over suspension within the scaffold, incorporation of various active components into the hydrogel structure can dramatically increase the tendency for cellular attachment [7]. For this reason, specific peptide domains have been incorporated into the matrix material for improved cell adhesion, enhanced cell proliferation, or differentiation. For example, ECM proteins bind to soluble growth factors and regulate their distribution, activation and presentation to cells. In fact, cell-ECM interactions are extremely complex in nature, and consequently there is a need for a biomimetic approach to create the native setting for the cells [1,15]. A particular successful strategy to mediate cellular attachment is the inclusion of the RGD (arginine-glycine-aspartic acid) adhesion peptide sequence into the matrix. Cells that have been shown to favorably bind to RGD include fibroblasts, endothelial cells (ECs), smooth muscle cells (SMCs), osteoblasts, and chondrocytes. RGD in hydrogels, which can

be incorporated on the surface or throughout the bulk of the gel, has shown enhanced cellular migration, proliferation, growth and organization in tissue regeneration applications [7].

1.4.1 Methods for cell encapsulation

The entrapment of cells in a hydrogel construct usually starts by suspending cells in a water-based solution of hydrogel precursor, the sol phase. The cell-laden suspension then undergoes a sol gel transition by physical, chemical or biochemical processes. During the entire process, the environmental conditions should not damage the suspended cells being as close as possible to the physiological environment [5,31]. Various methods for encapsulating cells within natural or synthetic-derived microgels have been proposed in the last years. Cells have been encapsulated in microbeads by means of bio-electrospray methods (fig. 5a) [27], with microfluidic-based techniques [43], or by using superhydrophobic surfaces as substrates for crosslinking hydrogel droplets at liquid-air interface (fig. 5b). Moreover, fiber-shaped structures containing cells have been produced using electro-spinning (fig. 5c), extrusion-based methods (wetspinning) (fig. 5d), microfluidic spinning (fig. 5e) or other techniques [29,38]. Other methods to generate cell-laden hydrogel building blocks with specific microarchitecture range from emulsification to photolithography, scanning soft lithography and micromolding [7].

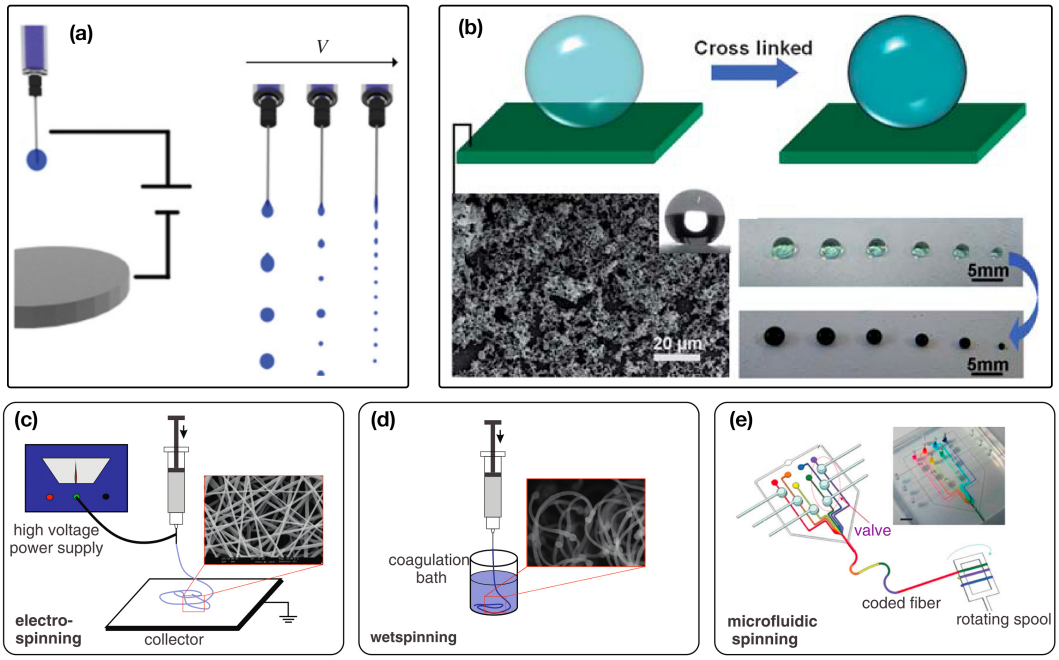

Figure 5. schematic of various methods for manufacturing cell-laden hydrogel modules. **(a)** bio-electrospraying methods permits to create sub-millimeter beads by spraying a polymer solution pumped through a needle connected to a high-voltage generator. Cell-laden droplets of the jet can be collected in a coagulation bath in order to cause hardening (adapted from [5]). **(b)** the principle of preparing hydrogel spheres using a super- hydrophobic substrate (top), a SEM micrograph of a representative superhydrophobic polystyrene substrate (bottom left) and a typical formation process for chitosan hydrogel spheres from the liquid drops on the substrate (bottom right) (adapted from [44]). **(c-e)** various technique for encapsulating cells in fibers for TE (adapted from [29]) **(c)** In electrospinning, an electric field is used to drawn fibers by the flow of a viscoelastic polymer subjected to an applied electric field **(d)** fibers in wetspinning are formed by extruding a pre-gel solution into a coagulation bath by using a syringe needle or micronozzle array; **(e)** microfluidic platforms produce fibers by coaxial flow of a pre-polymer and a crosslinking agent.

1.5 Fabrication strategies for bottom-up tissue engineering

Many different methods for producing 3d culture systems with relevant size have been proposed in the last decade. Bottom-up tissue engineering aims at recreating tissue complexity within engineered constructs, using microfabricated gels as building blocks [7]. Compared with scaffold-based tissue engineering, bottom-up methods allows manipulation of hundreds to thousands of cells per modules [22]. This approach relies on the concept of repeating functional units that are present in native tissues. The building blocks that serve as functional units can be assembled in packed structures having natural tissue like complexity and function according to different techniques. These strategies, ranging from weaving of fiber-like modules [28,29] to layer-by layer overlay of films [17,45,46], are selected according to the tridimensional architecture and composition of the tissue. The hydrogel blocks can range from tens to hundreds of micrometers and typically comprise encapsulated cells within each module [37].

1.5.1 Assembly of cell-laden modules

In a recently published review, Pati and colleagues presented an evolution of the cell-culture models developed in the last decades, starting from 2d cultures to cell cultures on hydrogel membranes, sandwich cultures, to 3D cultures and bioprinting approaches [16] (fig. 7). For all these strategies, hydrogels are the frameworks that allow cell encapsulation in order to create building blocks for subsequent assembling or printing of cell-laden constructs [31,37].

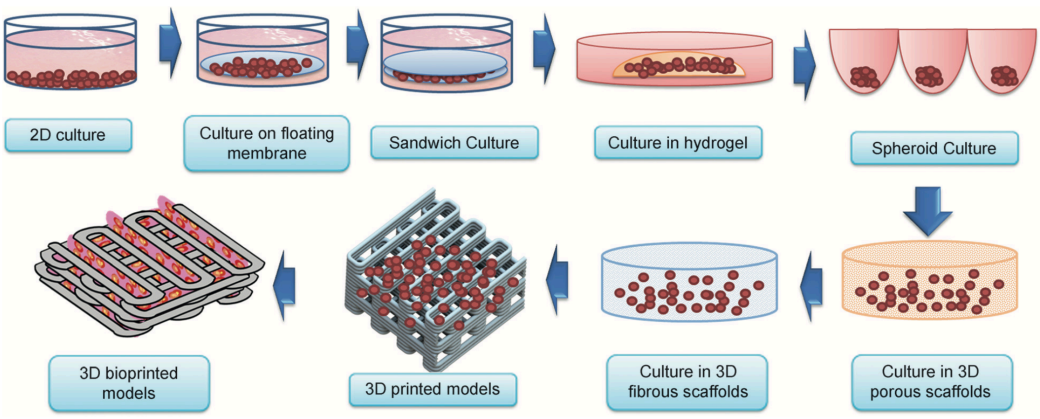

Figure 7. Evolution of cell-culture models. 2D cell cultures have been used for many years and is still being used for simple cell-based assays. Membrane and sandwich cultures were later developed. Hydrogels are usually used to culture encapsulated cells in three dimensions. Spheroid cultures are used as a scaffold-free culture where cell–cell interactions are predominant. 3D scaffolds are produced by various techniques, and cells are subsequently seeded on them. The advent of 3D printing and other additive manufacturing techniques encouraged the fabrication of complex structures in a reproducible manner, with control over their architecture and composition. However, cells are still seeded on the scaffolds after fabrication. 3D bioprinting technology, whereby cell-laden hydrogels can be included in the printing process in the form of bioinks, enables the fabrication of cell-laden constructs. Interestingly, the cellular microenvironment can be modulated with these techniques. To date, 3D bioprinting is the most sophisticated technique to fabricate tissue/organ constructs. Adapted from [16].

In this framework, hydrogel can be used as substrates for the generation of 2D cell sheets or used to encapsulate cells directly during the fabrication process. The first approach allow the subsequent detachment of the cell sheet from the hydrogel substrates and the layer by layer assembly of multiple sheets in order to create a 3D construct [47,48]. The cell sheet-based tissue engineering technology allows

for a scaffold-free sheet of interconnected cells in contact with their natural ECM to be obtained and enables transplanted cell to be engrafted for a long time [47,48]. The formation of layered tissues relies on the use of temperature-responsive hydrogel surfaces (eg. gelatin) or different stimuli that have been utilized to facilitate cell sheet detachment from the culture substrate [49]. In contrast, encapsulating cell within the hydrogel permits the direct manipulation of cell-laden building blocks into designed architectures and spatial organizations [22,50]. Various approaches to assemble microgels into designed architectures and spatial organization have been developed in the last decade. These assembly technologies are based on different techniques and can be classified according to the interaction modes between the microgels and the guiding forces: i) self-assembly, ii) guided assembly and iii) direct assembly [22]. Moreover, different strategies can be combined together in order to increase the level of organization of biological components within an engineered 3d tissue structure. The combination of bioprinting, cell sheet technology, cell encapsulation and micro-, nano-patterning techniques using cells, hydrogels and biochemical cues could be promising to engineered tick tissues that feature a functional histoarchitecture [17,24].

1.5.2 Bioprinting

Bioprinting technique were developed in order to overcome some limitations of cell modules assembling approach, such as the difficulty in generating more complex structures comprising different cell types. Bioprinting is an additive manufacturing technique during which small units of biomaterials and biologics, including living cells, nucleic acids, drug particles, proteins and growth factors are dispensed with micrometer precision to form tissue-like structures [23,25] (fig 6). Using cell printers, hydrogel gelation occurs in situ, thus enabling precise control over spatial and temporal distribution of cells and ECM [38]. The advantages of this process

thus include accurate control of spatial heterogeneity, physical properties, cellular composition and ECM organization, scalability and cost-effectiveness [38,51,52]. The three major bioprinting techniques are based on inkjet, laser-assisted and extrusion methods, each having specific strengths, weaknesses, and limitations [23]. These methods are briefly described in fig. 6.

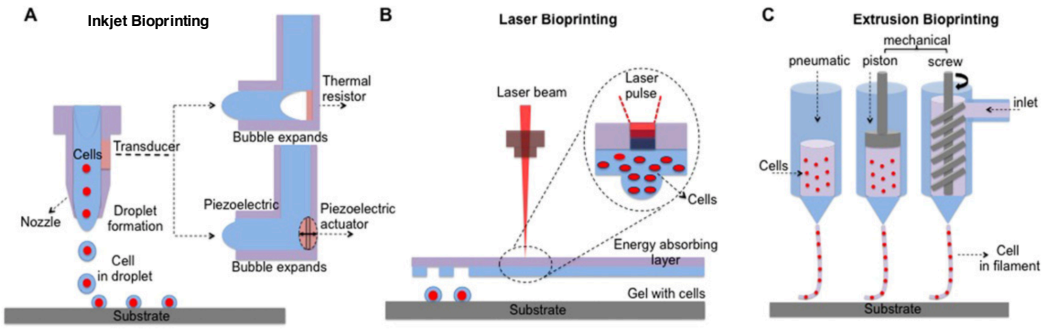

Figure 6. Overview and main components of the most widespread bioprinting approaches. **(A)** Inkjet printers eject small droplets of cells and hydrogel sequentially to build up tissues using thermal or piezoelectric valves to control the inkjet flow. **(B)** Laser-assisted bioprinters use a laser focused on an absorbing layer to generate pressures that propel cell-containing materials onto a collector substrate. **(C)** Extrusion bioprinters use pneumatic or mechanical (piston or screw) dispensing system to continuously extrude a liquid cell–hydrogel solution. Adapted from [38].

In the past 10 years, bioprinting has been widely used in fabrication of living tissues, and bioprinters and bioprinted tissues have gained significant interest in medicine and pharmaceutics [53]. In fact, this technology has a broad utility in various application areas such as tissue engineering and regenerative medicine [54,55], transplantation and clinics [56], drug screening and high-throughput assays [57] and cancer research [53]. Basically, the concept of biofabrication can be divided into three steps [16]:

1) preprocessing for preparation of the building blocks (consisting of cell encapsulated in hydrogel-based modules) or the bio-ink;

2) the processing step, which typically involves the assembly of the microgel modules or the printing of a 3D structure;

3) post-processing, where the fabricated construct is cultured in an incubator or bioreactor to induce maturation and transformation into a functional tissue.

1.6 Applications of hydrogels in tissue engineering

Hydrogels have a central role in regenerative medicine because of their capability to encapsulate cells in an instructive ECM-like environment and to be processed with different techniques in order to obtain 3D microstructured constructs. Tissue manufacture and the application of cell-laden hydrogel constructs have predominantly been discussed from a regenerative medicine perspective. However, the fabrication of tissue-like constructs based on bioprinting or other additive manufacturing techniques can also be beneficial to the fields of drug discovery and testing, and for studying disease processes and developmental biology [9]. In this section, a list of applications is reported. A schematic of different types of hydrogel constructs fabricated with a range of bioprinting and additive manufacturing methods is reported in fig. 8 [39].

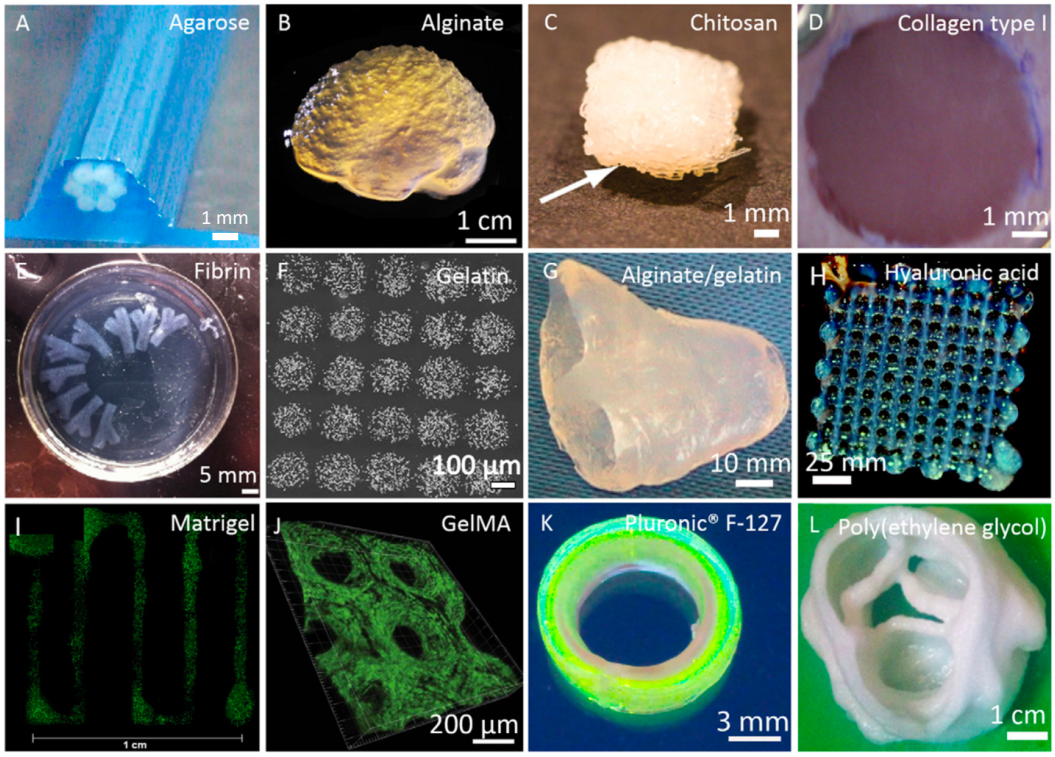

Figure 8. Hydrogel based scaffolds and bioprinted constructs: **(A)** bioprinted agarose filaments [58]; **(B)** 3D printed alginate in brain shape [59] **(C)** chitosan scaffold [60]; **(D)** collagen type I construct for skin tissue regeneration (adapted from [61]); **(E)** fibrin bioprinted tubular scaffolds [59]; **(F)** deposited cells using gelatin bioprinted template [62]; **(G)** 3D 'half-heart' scaffold bioprinted using alginate/gelatin [63]; **(H)** bioprinted hyaluronic acid [64]; **(I)** hepatic carcinoma cell-laden Matrigel graft [57]; **(J)** confocal image of cells in a GelMA (gelatin metacrilate) scaffold [65]; **(K)** bioprinted Pluronic® F- 127 fluorescent tube [66]; **(L)** PEG (Poly(ethylene glycol)) hydrogel bioprinted into an aortic valve construct [67]. Adapted from [39].

1.6.1 Biofabrication for tissue regeneration and regenerative medicine

Different biofabrication approaches have been applied to the development of several types of tissue and organs by using different cell types and different types of

natural or synthetic derived hydrogels. Generated constructs hold promises to create tissue constructs mimicking many tissues and organs such as liver [68], heart [69], bone [70], skin [71], neurons [72], and vascular systems [73]. Fig. 9 demonstrates the scheme of cell encapsulation for tissue engineering applications. Moreover, biofabrication of 3D cell-laden tissue replicates at the microscale represent a powerful tool to study the mechanism of cell aggregate fusion and tissue morphogenesis and can provide a method for high-throughput screening of cell-biomaterial interaction [24].

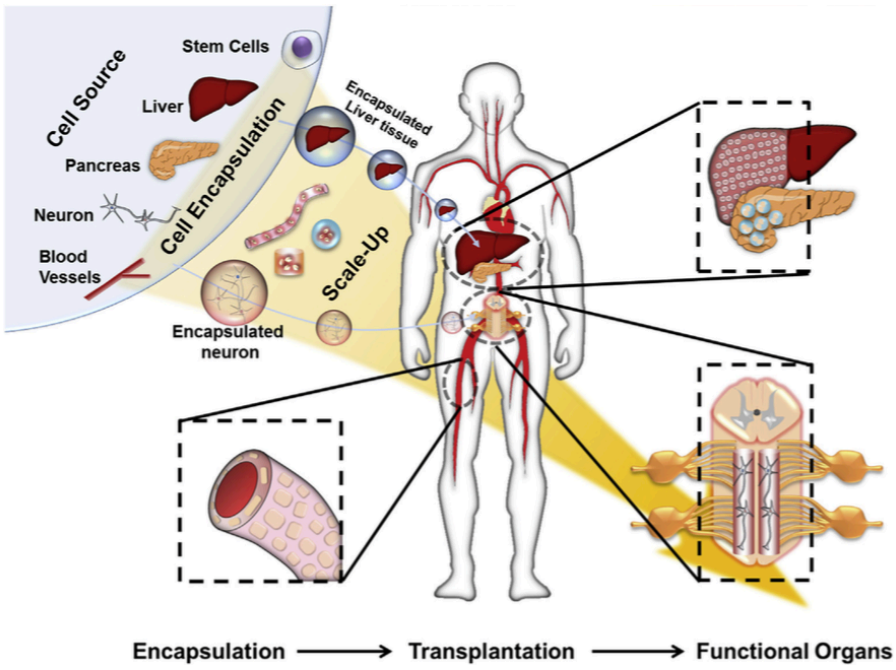

Figure 9. Schematic diagram of cell encapsulation for tissue engineering and cell therapy applications. Different cell types from xeno or allo species or stem cells can be encapsulated and scaled up in order to manufacture functional constructs that are implanted into the body and used to replace or support the function of failed organs. Adapted from [74].

1.6.2 Biofabrication of tissue/organ models for drug discovery and toxicological screening

Improving the ability to predict the efficacy and toxicity of drug candidates earlier in the drug discovery process will speed up the translation of new drugs into clinics [75]. 3D engineered hydrogel matrices allow cell-cell and cell-ECM interactions and microarchitecture similar to native tissue and consequently show a similar response to drug compounds. Allowing rapid identification of potential candidates or substances toxic to human tissues has the potential to reduce the cost and time during the optimization stage of drug development [76]. Hence, biofabricated tissues can provide a valuable step in the development process of drugs by allowing the testing and high-throughput screening of new and promising chemicals on functional human tissue *in vitro* [38,75]. Moreover, the engineering of realistic tissue constructs will help in furthering understanding of tissue physiology and function and lead to the development of refined TE strategies [16,24].

1.6.3 *In vitro* diseases/tumor models

In vitro 3d constructs based on hydrogels laden with human cancer cells have been developed in order to reproduce and mimic the physiological environment of human cancer tissue [16,77]. Advanced in biofabrication offer the opportunity to manufacture complex structures with simulated pathophysiological microenvironment making the disease pathogenesis process studies more relevant *in vitro*. These tumor models could thus be beneficial in cancer research to investigate cancer pathology, growth and metastasis thus avoiding the early stages of clinical trials [24,53,77]. Moreover, maufactured tissue-like constructs offer the opportunity to reproduce accurately 3D *in vitro* microstructures with applications

ranging from cell behavior studies to improving the understanding of brain injuries and neurodegenerative diseases [30].

1.6.4 Hydrogels with drug delivery capabilities.

Hydrogels can also be used as vehicles to deliver drugs, growth factors or cell therapies because they are hydrophilic, biocompatible, and their drug release rate can be controlled and triggered by interactions with biomolecular stimuli. In fact, cells for which a donor shortage exists and that are unable to grow in artificial media, must be provided from xeno- or allo- species [74]. Cell encapsulation based on microscale platforms, in particular beads, fibers and films, permit the diffusion of gas, nutrients, wastes and therapeutic products *in situ* once implanted [78]. Many types of cells, including pancreatic islets cells [79], neurons or neuron-like cells [80], and osteoblast cells that produce human vascular endothelial growth factors (VEGFs) [81] have been successfully encapsulated to achieve certain therapeutic purposes [74].

1.7 Current limitations and future directions

Encapsulation of cell in hydrogel and the creation of functional living tissues in the laboratory holds great promises for different tissue engineering applications. However, several crucial problems deserve attention before these methods may be implemented in clinical applications.

The first issue is related to the material selection which remains a major concern and limitation for generating building blocks or to use as bioink for tissue engineering and regenerative medicine [23]. In fact, one of the major milestones in biofabrication is to manufacture constructs able to mimic the cellular microenvironments from molecular to macroscopic scales in a hierarchical organized manner [38]. Current fabrication and deposition techniques allow

researchers to design and build structures with increasingly complex architectures using hydrogels as building units but many concessions have been made to the detriment of the biological composition of the polymers. In fact, increased polymer concentration, unphysiological mechanical and rheological properties, toxicity of degradation products, non-native cell density and the lack of specific ECM proteins for particular cell types may limit the biological relevance of cell-laden hydrogels [39].

The progress in the field of biofabrication and its translation towards clinical application are hampered by the overall lack of suitable bioinks for the generation of larger 3D constructs that recapitulate the heterocellular organization of the tissue microstructure [37]. Although multiple cell types in hydrogels can migrate and proliferate to some extent, the majority of the currently used bioinks in biofabrication are biomaterials with adherent properties for cell attachment [56]. In particular, the lack of environment for promoting differentiation and growth of stem cells into multiple lineages represent one of the major limitations in currently available hydrogel-based bioinks [82].

The development of unique bioinks, taking into account the required biological competence, the physical requirements dictated by the biofabrication process and the degradation concerns still remains a challenge for polymer chemists and material scientists, as well as the relative toxicity of crosslinking [37]. A solution to this problem could be represented by tunable bioinks with a wide range of material properties, for example new composite mixtures to enhance crosslinking, bioactivity, and other desirable features while maintaining the properties of the base bioinks [23]. In general, highly novel hydrogels should be engineered and developed considering the following requirements, as reported in a recently published review by Ozbolat and colleagues: promotion of cell adhesion, proliferation, aggregation and differentiation toward multiple lineages; exhibition of high mechanical integrity and structural stability without dissolving after gel formation; facilitation

of engraftment with the endogenous tissue without generating immune response; high bioprintability or encapsulation-capacity with rapid solidification and ease of handling during post-processing; and being affordable, abundant and commercially available with appropriate regulatory guidelines for clinical use [56].

Another major concern of current tissue engineering approaches is the inability to adequately vascularize tissues *in vitro* or *in vivo*. Issues of nutrient perfusion and mass transport limitations, especially oxygen diffusion, restrict construct development to smaller than clinically relevant dimensions and limit the ability for *in vivo* integration [73]. Therefore, it becomes organic to expect that bioprinting can provide a viable solution for the vascularization problem and facilitate the clinical translation of tissue engineered constructs. Biofabrication of living tissues and organs at the clinically-relevant volumes vitally depends on the integration of vascular networks. Despite the great progress in biofabrication approaches, building a perusable hierarchical vascular network remains a major challenge. In fact, small-scale manufactured building blocks can survive through diffusion alone, but full-scale organs and larger tissue constructs will require an embedded vasculature system as well as mechanically robust conduits to connect to host arteries and veins [23]. There is much interest in the field as researchers have undertaken a variety of approaches to vascularization, including material functionalization, scaffold design, microfluidic techniques, bioreactor development, endothelial cell seeding, modular assembly, and *in vivo* systems [83]. Biofabrication of living tissues and organs at the clinically-relevant volumes vitally depends on the integration of vascular networks [73].

Although microscale cellular encapsulation approaches enable the precise control over cell size and shape, mass production via cost-effective and labor-efficient methods remains a great challenge. The scale-up of microtechnology-based production systems into biological-relevant size constructs and the

automation for the production of well-controlled encapsulation products represent critical issues. In fact, building blocks preparation for biofabrication application can take several days to weeks due to cell culturing and biomaterial synthesis and this working time may become an issue [23]. These problems may be address by combining large number of microwell-based bioreactors using an automation system. However, in order to translate these methods into a clinical-relevant supply chain, the integration of biofabrication methods with biopreservation strategies is required in order to maintain a stock of partially manufactured constructs ready to be used on-demand. In fact, the long-term storage and transportation of a large stock of building blocks represent a critical issue for the practical use of encapsulated cells in the form of building blocks for biofabrication or as drug-delivery devices [74]. This issue is still under discussion and based on the selected cell source (only autologous or also allogeneic), business model (centralized or decentralized) and manufacturing system (integrated or separated robotic systems) [84].

Biofabrication has become a strong fabrication technique to create complex micro- and macro-scale biomedical systems by assembling or dispensing cell-laden hydrogels. Nevertheless, the manufacturing of functional organs at clinically relevant dimensions is still impossible at the moment because there are several challenges such as but not limited to organization of the heterocellular nature of the tissue microstructure, integration of the vascular network from arteries and veins down to capillaries, incorporation of various cell types to recapitulate complex organ biology, limited structural and mechanical integrity and functionality, and poor long-term storage strategies for biological-relevant constructs [53]. However, recently developed 3D biofabrication techniques provide multiple approaches for biofabrication or assembling of tissue constructs to solve these issues. In particular, the cooperation of advanced technologies that engineer 3D cell micro-

environment, such as microfluidic systems [76,85], biopatterning [86], layer-by-layer assembly [76,87] and biomanufacturing of micro-tissue constructs within scaffolds or scaffold-free environments hold promise to facilitate the fabrication of artificial tissues (fig. 10).

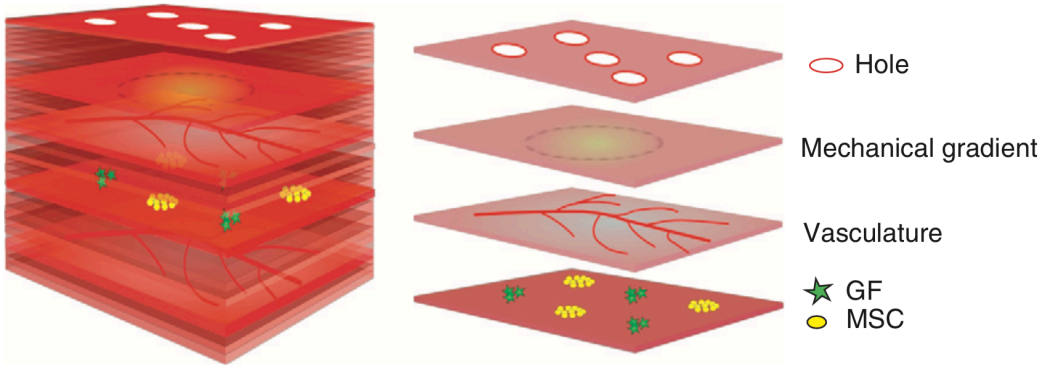

Figure 10. Schematic principle of the layer-by-layer assembly of complex meso- or macroscale tissue constructs. The different layers can be manufactured by using different biofabrication techniques, such as bioprinting or cell microencapsulation, and hydrogels are used in order to provide mechanical integrity and recapitulate the cell-type-specific ECM during the process. These complex tissues feature micropatterns of cells (e.g. mesenchymal stem cells (MSC)), biochemical cues (e.g. growth factors (GF)), physical cues (e.g. stiffness gradients), and defined shapes (e.g. holes). Holes can be processed to favor fluid diffusion through the structure and could also be endothelialized. Adapted from [17].

Although the described techniques are still in their infancy, the integration of cells and biomaterials through multiscale assembly strategies of building blocks or 3D bioprinting technologies offer great potential for the production of realistic tissue and organ models [38,88,89]. Therefore, the interaction and collaboration of researchers from various disciplines are needed to overcome several challenges

before these technologies will improve rapid clinical solutions and advance medical implants [16,23].

Chapter 2.
Alginate Hydrogels as 3D Cell Culture Matrices

A wide variety of hydrogels have been experimented within biofabrication, both for encapsulating cell into building blocks or as bioink for bioprinting applications [56]. Cell-laden hydrogel formulations utilize natural hydrogels such as alginate, agarose, chitosan, collagen, gelatin, fibroin, and hyaluronic acid (HA), as well as synthetic hydrogels such as pluronic (poloxamer) and poly(ethylene glycol) (PEG), or blends of both. Natural hydrogels, derived from polysaccharide or proteins, offer inherent bioactivity, except for agarose and alginate, and display a chemical and structural resemblance to ECM [36,90]. Several reviews papers have been published about hydrogels used for tissue engineering and for detailed information about a wide variety of materials the reader is referred to the paper of Gasperini [5], Ahmed [91], Peppas [6]. Alginate, being the most important material of this work, will be described in detail with respect to its chemical content, crosslinking behavior, biocompatibility, manufacturing capacity and possible modifications in the present chapter.

2.1 Introduction

Sodium alginate, or alginate, is a naturally occurring polysaccharide derived from brown seaweeds. Microbeads obtained by gelation of a sodium alginate solution were used for the first time in the 1980s to encapsulate pancreatic islets and are currently used for encapsulating different cell types and therapeutic agents [92,93]. Alginate is the material of choice for many cell encapsulation applications because

of its proven cytocompatibility, rapid ionic gelation property with divalent cation, hydrophilic nature, and tunable properties. It has been used as a biomaterial in clinic for different applications, such as wound healing, bone graft substitute for spine fusion, and cell therapy [8,93].

2.2 Alginate structure and chemistry

Commercially available alginates can be extracted from algae by using aqueous alkali solutions. After filtration, the alginate is precipitated into a salt with either sodium or calcium chloride and transformed into alginic acid by treatment with diluted HCl. The alginate salt is then transformed into water-soluble sodium alginate powder after a series of purifications and conversions [90,94,95]. A more detailed schematic of the alginate extraction procedure is represented in fig. 11.

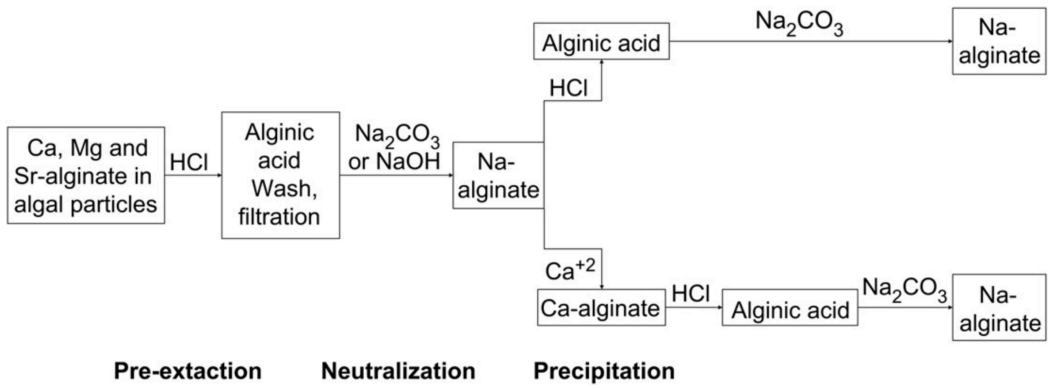

Figure 11. Schematic showing alginate extraction procedure from algae. As a first step in the extraction process, the counterions are removed by proton exchange using 0.1-0.2 M mineral acid. Subsequently, alkali such as sodium carbonate or sodium hydroxide are used to neutralize the insoluble alginic acid to form sodium alginate. In order to remove particulate matter, rigorous separation processes such as sifting, flotation, centrifugation and filtration are then performed. Subsequently,

Sodium alginate is precipitated directly by alcohol, calcium chloride or mineral acids. The product is then dried and milled. Ultrapure and amitogenic alginates that are suitable for biomedical purposes have been produced using more rigorous extraction processes and purification procedures. Adapted from [95].

Alginates are linear polymers consisting of 1,4 linked residues of ß-D-mannuronic acid (M) and α-L-guluronic acid (G) (fig. 12) and, depending on the derivative algae species, polymer segments can be formed by block of consecutive monomers (-GGG- or -MMM-) or by alternative residues (-GMGM-) [96]. The ratio between G and M blocks influences the mechanical properties of the alginate hydrogel as the G block provides structural rigidity to the polymeric structure [5]. In general, gel elasticity, porosity and stability are increased by increasing the molecular weight, G-content G-blocks length [96].

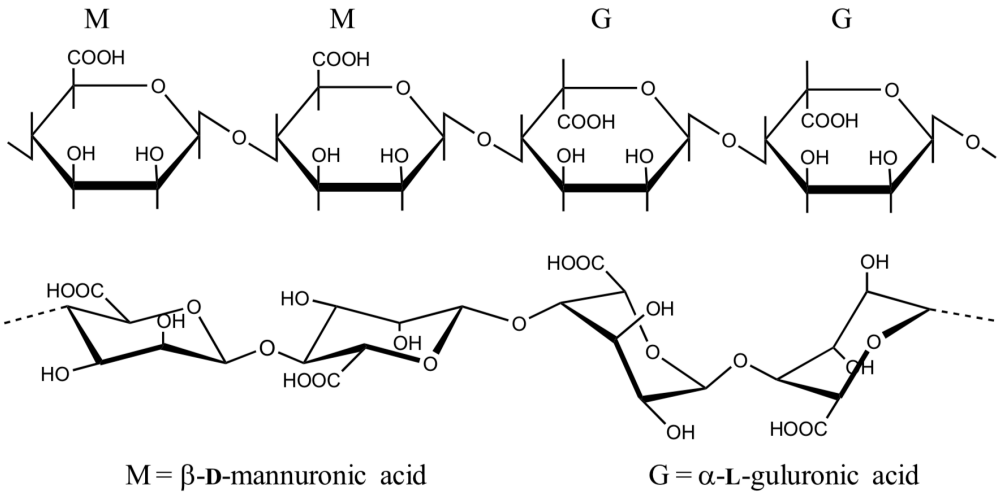

Figure 12. The chemical structure of alginate shown as segment of –MMGG-residues. Adapted from [96].

The alginate hydrogel derives from a water-based solution of sodium alginate. Viscosity of the water solution and solubility of the sodium alginate depend on the solution pH: at physiological condition, alginate is soluble and has an extended random coil conformation and when the pH is lowered, the chains form hydrogen bonds, producing a highly viscous solution. If the solution is too acid, a gelatinous precipitate of alginic acid will forms [96].

2.2.1 Alginate hydrogels

The gelation of sodium alginate solution can occur via two different processes: ionic or covalent cross-linking. The ionic gelation occurs in presence of divalent cations such as Ca_{2+}, $Sr_{2+}$and Ba_{2+}. When they are added to a water-based sodium alginate solution, they bind two adjacent residues allowing the formation of ionic interchain bridges that cause a fast sol-gel transition. The formation of an intermolecular gel network is compatible with the survival of cells that will be evenly distributed throughout the hydrogel if suspended in the alginate solution prior to gelation (fig. 13b) [95,96].

The amount and the type of the gel-forming ions and the gelling conditions, such as temperature, also affect the network structure and permeability. In fact, the alginate gel is characterized by a wide pore size distribution and its porosity is strongly influenced by the nature and concentration of gelling ions [90,96].

Once the gel is formed, it can be dissolved by the exchange of ions with a buffer (e.g. phosphate buffer saline without calcium) or by treatment with a chelating agent for divalent cations such as ethylendiaminetetraacetic acid (EDTA) or sodium citrate. This can be useful to gently release cells entrapped in alginate hydrogels for further downstream processing [96]. On the other side, because these gels can be dissolved due to release of divalent cations into the surrounding media,

a critical drawback of ionically cross-linked alginate gels is the limited long-term stability in physiological condition.

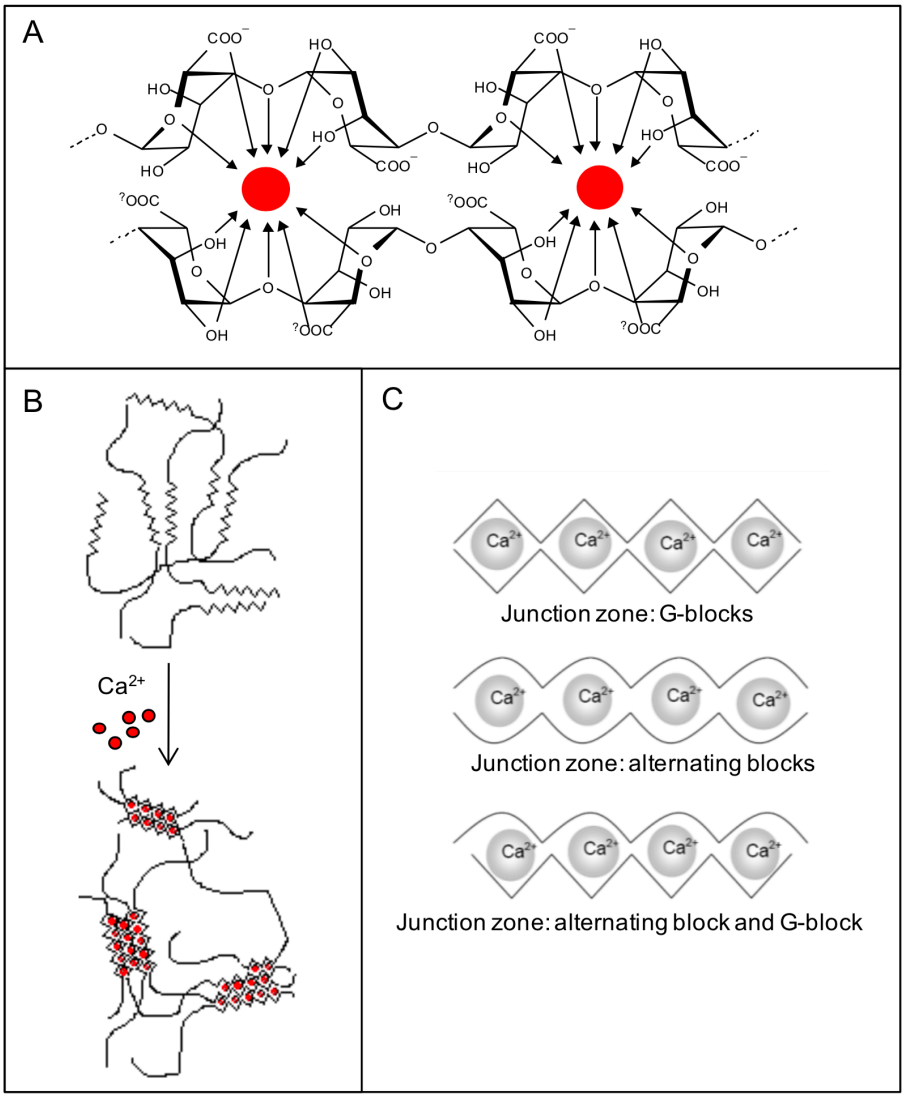

Figure 13. (A) Interaction between gel-forming ion and four resides from two different chain segments. **(B)** Intermolecular network of alginate-polymers in presence of Ca_{2+} ions. **(C)** Gelling ions organized in alternative junction zone. Adapted from [96].

As a less popular alternative to ionic crosslinking, covalently cross-linked hydrogels can be prepared from chemically modified sodium alginate. Different diamines and dihydrazides have been used to covalently crosslink alginate, and photo-crosslinkable hydrogels can be obtained in presence of a photoinitiator and UV light after conjugating methacrylate groups onto the alginate backbone. Covalent crosslinked hydrogels allow better control over the physical properties and provides better chemical stability. However, covalent cross-linking reagents may be toxic and the process is not as easily reversible as in the case of ionic gelation [95,96].

2.3 Therapeutic application of cell-laden alginate hydrogels

Pancreatic islets were the first cells immobilized in calcium alginate matrices by Lim and Sun at the end of the 1970s in order to treat diabetes [92]. From that time, several approaches and adaptations of mammalian cell culture have utilized alginate gels as a model system in biomedical studies and for manufacturing cell therapy constructs [8,78]. Alginate gels can be adapted to serve as either 2d or 3d culture systems, being the latter more relevant from a physiological standpoint. Alginate gels may serve as an ideal blank slate, due to the low protein adsorption and lack of mammalian cell receptors for alginate. The limited inherent cell adhesion and cellular interaction can be an advantage for cell encapsulation applications, but can limit the use of cell-laden constructs for tissue engineering applications [97,98]. Different biochemical modifications can be used to adapt alginate matrix to guide adhesion and function of specific cells and will be discussed later. The use of alginate hydrogels for the realization of scaffolds and cellular constructs as an alternative to cell culture in 2d include the formation of beads, fibers, membranes, meshes, foams and other hydrogel structures that can serve as building blocks

according to the biofabrication paradigm [96,99]. The role of alginate in pharmaceutics and biomedical engineering includes also different applications. Alginate is a commonly used polymer for sustained and localized drug delivery applications, and different binding and gelation mechanism allow to tune the sequence and rate of release [100]. In the form of sponges, hydrogels and electrospun mats, alginate-based wound dressing have been used as substrates for the treatment of acute and chronic wounds, as they offer many advantages including hemostatic capability and gel-forming ability upon adsorption [94].

Encapsulation in alginate hydrogels has shown to be an ease, non-toxic and versatile method for immobilization of cells and many studies describe the use of this technique for treating different diseases comprehending liver failure [101], Parkinson's disease [102], anemia [41], brain tumors [103], cartilage [104] and bone [105] injuries. In this process, living cells are suspended in alginate and the mixed solution is then dripped or extruded into a bath containing calcium chloride or other ions that cause gelation. Since the ionic cross-linking reaction is instantaneous, the cells remain entrapped inside the solid hydrogel matrix. Oxygen and nutrients can diffuse into the gel, and cells products can diffuse outside the matrix. However, the hydrogel represents a barrier to antibodies and immune cells, and implantation studies into animals and diabetic patients have demonstrated long term functionality of alginate hydrogel constructs containing cells [93]. Therefore, cell-laden alginate hydrogel constructs can be implanted into animals or humans and serve as 'biofactory' for the continuous production of proteins or therapeutic agents as, for example, insulin [8,93]. Alginate hydrogels have been also broadly used for the sustained and localized delivery of encapsulated drugs or growth factor by controlled release from the crosslinked matrix. Growth factor can promote or impede cell migration, differentiation and proliferation and they can be combined and delivered from the hydrogel by exploiting different mechanisms, which allows tuning the sequence and

rate of release [98]. As an example, Li and colleagues investigated the release of vascular endothelial growth factor (VEGF), a potent angiogenic molecule, from poly-l-lysine-coated VEGF/alginate microspheres for promoting the vascularization of tissue-engineered bone graft [106].

2.4 Alginate-based encapsulating systems

2.4.1 Alginate microbeads

One of the most studied support for alginate cell encapsulation are microbeads (figure 1), that can be produced through electro hydrodynamic process. In this process, an electrostatic potential is applied to a needle and use to deposit alginate droplets in the coagulation bath where gelation occurs [27]. Cells encapsulated with this technique remain viable inside the beads and are able to proliferate once released from the matrix, as demonstrated in the work of Liaudanskaya et al. [107] (fig. 14).

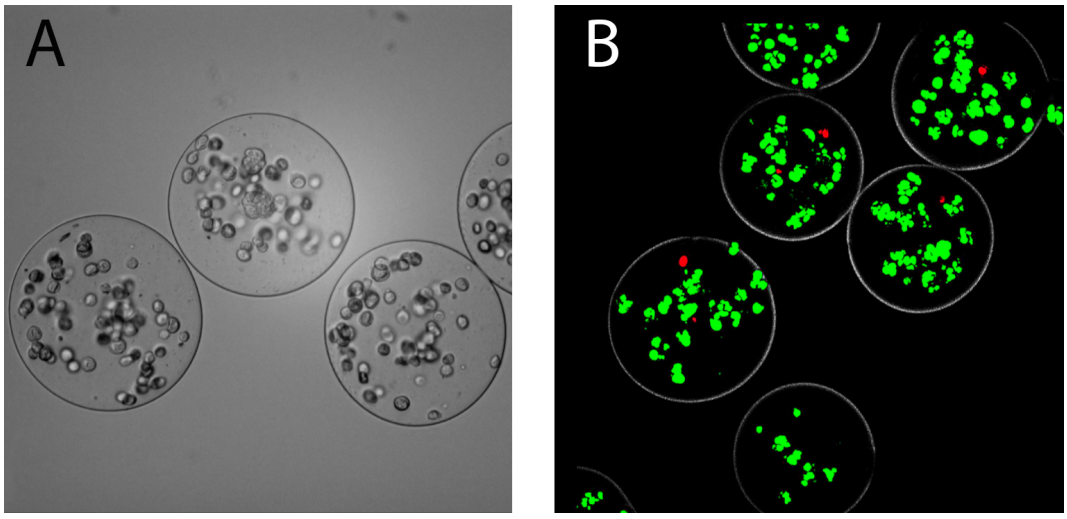

Figure 14. Alginate beads created by means of electro hydrodynamic method. **(A)** Optical microscopy of B50 cells encapsulated in 2% alginate **(B)** Confocal

LIVE/DEAD assay of B50 encapsulated cells. Beads diameter equals to 200 μm. Adapted from [27].

Others techniques that can be used to encapsulate cells in alginate beads include coaxial air or liquid flow [108], the use of micromolding platform [109], microfluidic-based emulsification [110] and the use of superhydrophobic substrates [44]. Alginate has been used for encapsulating pancreatic islets since it provides some advantages over other system. It does not interfere with cellular functions, encapsulation can be done at physiological conditions and it can facilitate the functional survival of the islets when enveloped in microcapsules before long-term tissue culture [40].

2.4.2 Alginate microfibers

Cell-laden microfibers are recognized as another appropriate form of building blocks for assembling cell-laden constructs *in vitro* because many important human tissue and organs are composed of fiber-based or network-like structures [29,34]. Meter long cell-laden fibers can be formed starting from a solution of alginate containing cells using techniques like electro-spinning, wetspinning, microfluidic spinning, interfacial complexation and meltispinning [29,34]. In addition to cell-encapsulating structures, microfibers can also function as support for cell seeding and thus represent a versatile framework [111,112]. The use of cell-laden fibers allows the use of textile technologies for making fabrics and cell-laden structures with precise control over the distribution of different cell types and anisotropic mechanical properties within the constructs. In fact, these fibers can be further assembled by weaving, knitting and reeling into macroscopic cellular structures with various spatial patterns and used as templates for the reconstruction of fiber-shaped functional tissues that mimic muscle fibers, blood vessels or nerve networks

in vivo [29,111]. Alginate is the most frequently used material for manufacturing cell-laden microfibers thanks to its easy handling properties and because the prepolymer solution, the gelation agent and the coagulation bath are all compatible with living cells. Alginate-based microfibers can be easily formed with wetspinning method, extruding the pre-gel solution containing cells into a gelator solution where it continuously polymerizes by using a syringe needle or micronoozle array. As an example, Lee and colleagues reported the successful encapsulation of cells within alginate and alginate-chitosan fibers using a wetspinning microfluidic chip [113]. Nevertheless, since cells cannot adhere on the surface of the alginate hydrogel due to its biological inertia, alginate-based microfibers are typically employed as cell-encapsulating building blocks. In addition, alginate-based microfibers with cell-adhesive materials have been fabricated in order to improve cell adhesion. For example, Onoe et al. developed a double-coaxial laminar flow microfluidic device to create meter-long functional microfibers with a mixture of extracellular matrix proteins and cells as the core and alginate hydrogel as the shell [28] (fig. 15a-c). Akbari and colleagues reported the use of alginate hydrogels containing cells as coatings for synthetic polymer cores in order to create composite living fibers, subsequently assembled using regular textile processes [114] (fig. 15h-i). Alginate microfibers found also application for treating various diseases. In the work of Jue et al., primary pancreatic islets and hepatocytes in the form of hybrid spheroids were encapsulated in collagen-alginate composite microfibers using a microfluidic chip (fig 15d-g). The xenogenic transplantation of these constructs *in vivo* showed great promises for treating end-stage liver diseases [79].

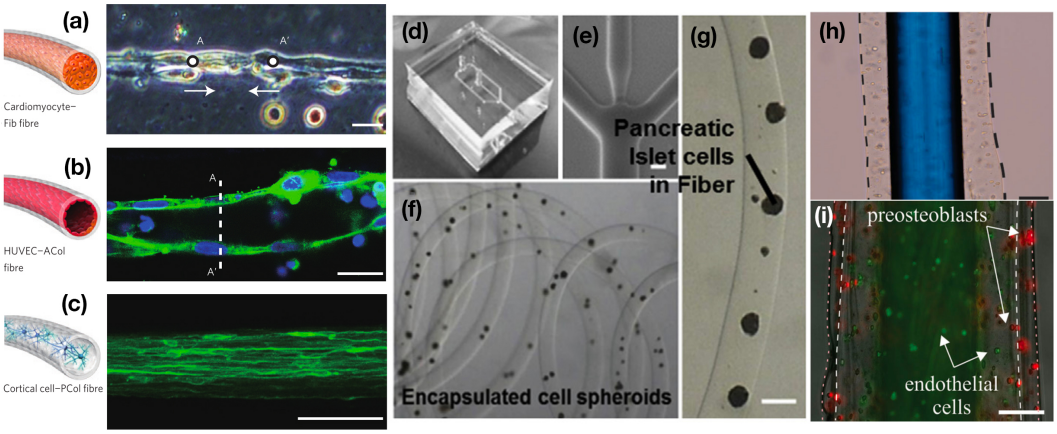

Figure 15. cells encapsulated in alginate-based fibers. **(a-c)** Cell-containing ECM-protein/Ca-alginate core–shell hydrogel microfibers generated with a double coaxial microfluidic device (adapted from [28]) **(d-f)** A PDMS-based microfluidic chip for three-dimensional co-cultured hybrid spheroids composed of primary islets and hepatocytes in alginate microfibers (adapted from [79]) **(h-i)** alginate-coated threads: **(h)** a non-absorbable monofilament suturing thread coated with HEK293 cell-laden hydrogel; **(i)** two-layer coating of endothelial cells (green) and preosteoblasts (red) on a braided suturing thread (adapted from [114]).

2.4.3 Alginate hydrogels as bioinks for bioprinting

Alginate hydrogels are also widely used as a bioink for bioprinting applications, due to their compatibility with cells, fast gelation rate and the ability to control biodegradation (fig. 16). In fact, alginate is reasonably easy to print, as it is easy to process and extrude while protecting the encapsulated cells [96,99]. Moreover, using alginate it is possible to create long-term persistent cell-laden structures, whereas the slow degradation kinetics of the hydrogel can be tuned by oxidation or by modifying the molecular weight distribution of the polymer itself. Alginate hydrogels possess shear thinning properties and, therefore, their viscosity is dependent on the strain rate. The viscosity of alginate is concentration-dependent

and, generally, lower concentrations of alginate are recommended for high cell viability [99,115]. However, low concentration alginate exhibits poor mechanical properties and cannot be used for achieving good resolution in printing applications. Many attempts to optimize the resolution of alginate bioinks have been reported, including optimization of alginate concentration, incorporation of high molecular weight polymers and different hydrogel fabrication methods [52,115].

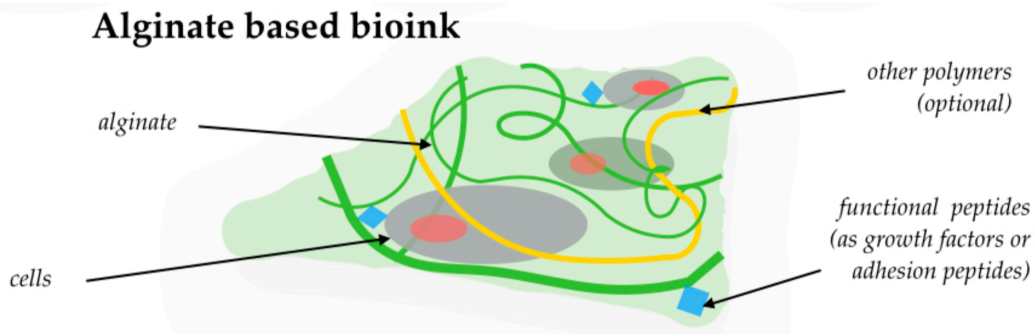

Figure 16. Alginate-based bioink composed of the alginate hydrogel, cells, functional peptides or biomolecules to enhance the biological function of the cells, and other polymers forming the hydrogel to tune specific mechanical or structural properties. Adapted from [99].

Different bioprinting approaches can be used for integrating living cells into three-dimensional alginate hydrogels, and these methods can be classified into three main categories as reported in cap. 1, par. 5. Extrusion-based bioprinting (EBB) performed with the use of a piston or a screw or other pneumatic method; inkjet-based bioprinting (IBB), performed by a piezoelectric actuator or a heater that creates bubbles; laser-assisted bioprinting (LAB), performed by a laser pulse that discharges bioink droplets from a donor slide onto an energy adsorbing layer [51,73]. In case of laser assisted methods, the processes involve high temperature and high energy radiations which make them unsuitable for bioprinting of cell laden

constructs [115]. Therefore, extrusion and inkjet printing are the two major technologies which can be used for printing cell-laden constructs under physiological conditions. Inkjet-based methods have been used for printing 3D cell-laden constructs due to the ability to provide good cell viability (around 90%). On the other side, the employed bioinks must be less viscous in comparison to extrusion printing and cell density also must be lower. For these reasons, the most employed printing solution for alginate-based bioinks relies on the extrusion process, since it provides a platform to print cell-laden constructs efficiently and in a controllable manner compatible with cell survival [115].

In EBB methods, cells are blended with a hydrogel and loaded into sterilized syringes. The cell-laden hydrogel or cell spheroids are then dispensed by air pressure or a motorized plunger through a micronoozle onto the substrate according to a customized design. Different EBB systems have been experimented for printing living cells onto target-specific positions while encapsulating them in alginate hydrogel. In a recently published review, Ozbolat and coauthors reported a summary of these mechanism that are (i) bioplotting, (ii) bioprinting hydrogel with a secondary nozzle using crosslinker deposition or a spraying system, (iii) bioprinting using a coaxial nozzle-assisted system, (iv) bioprinting pre-crosslinked alginate and further crosslinking it thereafter and (v) bioprinting alginate with an aerosol cross-linking process [52]. There are many reports detailing various extrusion-based 3D tissue-printing systems and the parameters requested for an efficient printing, like printing speed, dispensing pressure and movement distance. As an example, Gasperini et al presented a bioprinting technique that exploits the electrohydrodynamic process to create a jet of liquid alginate beads containing cells [116]. The beads were placed at predefined positions and crosslinked on a gelation substrate thus manufacturing a cell laden hydrogel scaffold block-by-block with the aid of a computer deposition system. Tabriz and colleagues developed a new

extrusion-based bioprinting technique to produce complex alginate hydrogel structures by dividing alginate hydrogel cross-linking process into three steps [117]. Each step corresponded to an increase in crosslinking level of the hydrogel. With this technique they were able to successfully print complex 3D constructs in the shape of branched vascular structures (fig. 17).

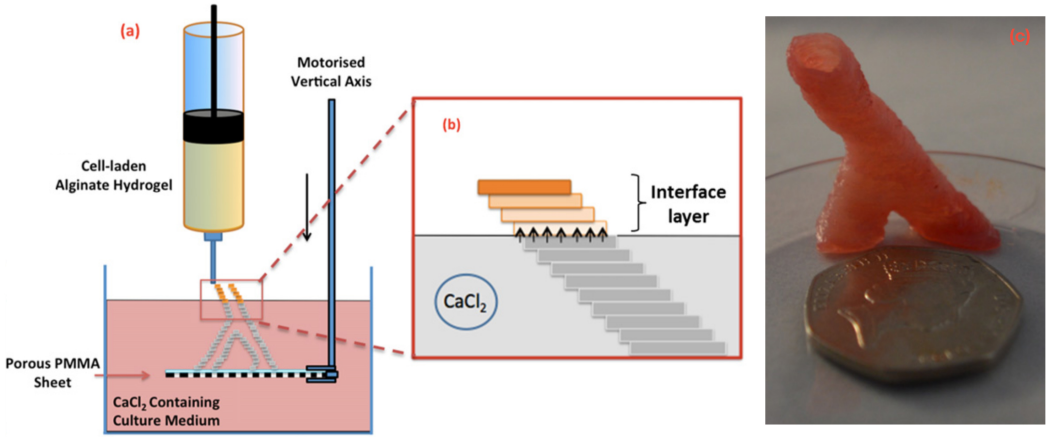

Figure 17. Schematic drawing of an alginate hydrogel 3D printing setup. **(a)** Layers of partially cross-linked alginate hydrogel were printed layer by layer on the porous membrane and at the same time the Z axis was lowered down and the hydrogel were submerged into the CaCl2 bath **(b)** The interface layers: upward diffusion of Ca^{2+} ions into the interface layers which are partially cross-linked above the $CaCl_2$ solution. **(c)** A branched vascular structure. Adapted from [117].

2.5 Modification of alginate hydrogels

Although alginate is extremely cytocompatible, due to its highly hydrophilic nature proteins are minimally adsorbed thus hampering cell attachment on this material. Moreover, despite the intrinsic properties of alginate that make it a favorable material for tissue engineering applications, chemical modifications are often required to promote desirable cellular functions, provide a greater range of

mechanical properties, and facilitate controlled release of encapsulated factors. In order to overcome its limitations, alginate can be modified by covalently grafting extracellular matrix peptides to provide molecule binding sites for cell adhesion, like the RGD (arginine-glycine-aspartate) motif found in collagen or the REDV (arginine-glutamate-aspartate-valine) peptides found in fibronectin [49,81,118]. Another strategy consists in mixing alginate with protein-based cell adhesive components such as collagen [119], gelatin [81], keratin [120] or silk fibroin [121] in order to obtain hybrid hydrogels with improved biocompatibility and enhanced degradation rate. These proteins contain cellular binding motifs, which support cellular attachment in a manner similar to the extra cellular matrix (ECM). Different approaches have been proposed in this regard:

- In their well-known paper from 1999, Rowley and colleagues covalently modified alginate polysaccharides with RGD-containing cell adhesion ligands utilizing aqueous carbodiimide chemistry [118]. Mouse skeletal myoblasts were cultured on the obtained alginate hydrogel surface, where they proliferated and differentiated towards skeletal muscle lineage. The suitability of alginate as an ideal material with which to confer specific cellular interactive properties was thus demonstrated.
- Singh et al. compared the growth of vascular cells on different hydrogels substrates containing alginate (2%, wt/vol) blended with solutions of different proteins (silk fibroin, gelatin, keratin, or elastin at 1%, wt/vol) [122]. The analysis of cell proliferation, metabolic activity and colonization was carried out in 2D and the most promising results were obtained with silk fibroin- and keratin-containing hydrogels, which supported the growth of all types of vascular cells.
- Bocaccini and colleagues published several papers regarding alginate modification for enhancing its biocompatibility by resembling the mechanical,

structural and chemical properties of the native extracellular matrix. In their works, they developed modified alginate hydrogels in which cell adhesive functionality were conferred by blending with gelatin [97], silk fibroin [123] and keratin [120]. They used this hybrid material to fabricate hydrogel films and hydrogel microcapsules. Cells were either seeded onto prefabricated hydrogel substrates (2D) or encapsulated during hydrogel microcapsules formation obtained with pressure-driven extrusion technique (3D). Their results indicated that such novel hybrid hydrogels supported cell attachment, spreading and proliferation and thus represent promising materials for biomedical applications in tissue-engineering and regeneration. As an example, the presence of silk fibroin in the blend makes the gel stiffer compared with pure alginate, and improve the physical-chemical properties in both the geometries of the blend [123]. As far as cell-interaction is concerned, they showed that silk fibroin provides anchorage and a growth-supporting environment for both cells seeded on the films and for cells encapsulated in the microcapsule compared with structure of pure alginate [123]. However, they did not compare the behavior of cells processed with the different hydrogel systems.

- Cell-sheet culture substrates were developed by Yan and coworkers using the ability of calcium alginate hydrogels to be dissolved under mild conditions [49]. The alginate was modified by conjugating the integrin binding peptide sequence RGD to the alginate solution in order to confer cell attachment sites to the hydrogel. The modified alginate hydrogel supported the attachment and growth of fibroblast and human corneal epithelial cells (HCECs) sheets, subsequently detached from the substrate through chelating the calcium using citrate. The cell–cell connections were retained following this release and the cell layers adhered to each other and grew after being stacked.

2.6 Challenges and future directions

A major disadvantage of alginate bioinks is the formation of relatively soft gels at lower concentrations, even after crosslinking. On the other hand, high concentration gels possess high stiffness and low diffusion properties, thus hampering cell proliferation and functionality. Therefore, it is challenging to print multilayered structures which can recapitulate the complexity of tissue-like structures [115]. In this framework, modular approaches would confer the ability to scale up by assembling layer by layer building blocks to create macroscopic tissue constructs.

The size of the hydrogel constructs is another critical parameter for biomedical application of encapsulated cells. The bead, fiber or printed bioinks must be large enough to contain the biological material and larger constructs are also easier to handle during washing or further assembling processes. However, the absence of convection movement within a capsule induces an oxygen- and nutrient-gradient from the surface to the construct resulting in necrosis of the inner cells [124]. In fact, although the nanoscale porosity of alginate gel permits the diffusion of solutes through its network, this process is limited when the size increases. A study published by Gasperini et al. identified the critical diffusion distance of 400 μm for 2% (wt/vol) alginate containing 5 M cells/mL for effective oxygen and nutrient transfer to cells at interior positions [27]. Specific types of geometry can be design in order to balance the critical issues regarding the size of an alginate-based cell culture system.

Chapter 3.
Effect of Cryopreservation on Cell-Laden Hydrogels: Comparison of Different Cryoprotectants

An important issue for the clinical implementation of cell encapsulation and biofabrication techniques is the long-term storage of a large stock of cell/hydrogel building blocks. In this chapter, the impact of cryopreservation on the viability and functionality of cells encapsulated in alginate matrices is presented comparing different cryoprotective agents (CPAs). Human osteosarcoma MG63 cells were encapsulated in sodium alginate fiber constructs with wetspinning method and exposed to different formulations of cryopreservation media, containing dimethyl sulfoxide (DMSO), glycerol, and trehalose. The cell-laden fibers were subsequently slow-cooled down to -80°C and stored in liquid nitrogen. After thawing, viability and death pathway of encapsulated cells were investigated, and metabolic activity and proliferative capacity of cells released from the alginate matrix were evaluated. The viability of MG63 cells encapsulated in alginate matrix ranged from 71%±4% to 85%±2%, depending on the cryoprotective media formulation with no protracted harmful effects from the CPAs. On the other side, cells cryopreserved in encapsulated conditions and released from the hydrogel showed larger metabolic activity and proliferative capacity in tissue culture plate compared to cells cryopreserved in suspension, in particular when DMSO and glycerol were used as CPAs. Results have been correlated with the viscoelastic properties and water content changes of the alginate constructs loaded with the different CPAs.

3.1 Introduction

3.1.1 The principle of cryopreservation

Given recent advantages in the field of biofabrication and bioprinting, the tissue engineering community is becoming increasingly concerned with the problems of bringing manufactured tissue constructs into the clinic and into the market [125]. One major obstacle for the successful clinical and commercial application of emerging cell-based technologies is the development of effective preservation and long-term storage techniques for encapsulated cells. The challenge of maintaining large stock of cell-laden building blocks and bioinks in order to ensure a steady supply will make necessary the creation of banks to meet the unpredictable demand for specific cell-laden constructs in clinical, industrial and scientific research settings [125,126]. Manufacturers and/or distributors thus aim to develop technique that (1) preserve the viability and functionality of encapsulated cells and (2) maintain the integrity of the living constructs or engineered tissue surrogates [127]. Simple preservation techniques, such as *in vitro* culture, hypothermic storage and desiccation have drawbacks including limited shelf-life, high costs, risk of contamination and negative impact on biomaterial integrity. Cryopreservation, an approach based on the principle that chemical and biological processes are effectively arrested at cryogenic temperature, represents a more adequate option that permits the long-term preservation of living cells, tissues and biological samples [125,127,128].

According to cryopreservation principle, the beneficial effect of decreased temperature is used to suppress molecular motion thus arresting metabolic and biochemical reactions. Although temperatures below –80 °C are generally considered sufficient for successful preservation of cells and tissues for periods of time up to 6 months (according to standard protocols), as the storage temperature

is reduced the shelf-life increases dramatically [125]. In fact, a state of "suspended animation" can be achieved below –150 °C as there are very few biologically significant reactions or changes to the physicochemical properties of the system [127]. At –196 °C (the boiling point of liquid nitrogen) the thermal energy is insufficient for any chemical reaction, and the only deterioration that can occur in a biological sample is DNA damage by background radiation and cosmic ray [125]. At liquid nitrogen temperature, the shelf-life of stored cells has been estimated to be of the order of 10^3 years. At the end of the cryopreservation process, cells are thawed and, ideally, resume biological activity [129]. However, experimental findings underlined an apparent contradiction between the concept of preservation and damages occurred to living cells and biological samples due to the cryopreservation process itself [128]. Therefore, an extremely important part of the research in fundamental cryobiology and tissue engineering is to reveal the underlying physical and/or biological mechanisms related to the injury of cells at low temperatures (namely cryoinjury) [128]. The exact mechanism of cryoinjury has long been debated, and the variety of explanations reflects the fact that different cryopreservation protocols affect the cells in different ways [128,130]. According to Pegg, freezing injury has been shown to have two components: direct damage from the ice crystals formation inside the cell; and secondary damage caused by the increase in concentration of solutes as progressively more ice is formed, resulting in dehydration of the cells by osmosis through their semipermeable membranes [131]. Intracellular freezing is generally lethal but can be avoided by sufficiently slow cooling, and under usual conditions osmotic damage dominates (fig. 18). The precise events occurring to cells during freezing, that may be lethal for cell survival, can depend on the cell type, the freezing temperature, the freezing rate, and the nature of the extracellular solutes [128,130].

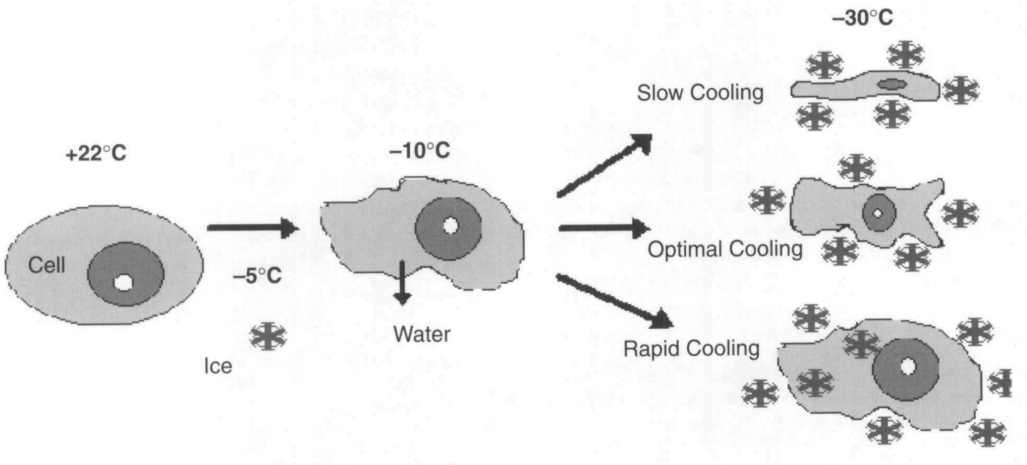

Figure 18. Schematic of the events occurring in cells during freezing. If freezing is too slow, ice formation inside the cells is avoided but cells undergoing slow freezing processes still suffer injuries, due to the severe volume shrinkage and long-term exposure to high-solute concentrations. On the opposite, if cells are cooled too rapidly, intracellular water is not lost fast enough to maintain equilibrium and the cells become increasingly supercooled, thus freezing intracellularly. If cooling rate is optimally balanced, cells lose water rapidly enough to concentrate the intracellular solutes thus avoiding supercooling. As a result, cells dehydrate and do not freeze internally. Adapted from [128].

3.1.2 The role of cryoprotectants

In order to successfully store cells and engineered tissues for extended periods, taking advantage of the protective effects of sub-zero temperatures, damage during freezing and thawing must be minimized [127]. Cryoprotectants agents (CPAs), added during the cryopreservation process, protect cells from cryodamage by decreasing the freezing point at which intracellular ice forms thus minimizing the damage caused by cooling [89,129,130]. CPAs act as osmotic buffers preventing harmful critical electrolyte concentration gradients and stabilize cell membranes by

maintaining macromolecules in their native form [129]. CPAs such as dimethyl sulfoxide (DMSO) and glycerol can penetrate the cell membrane at physiological temperatures, however, their penetration ability rapidly decreases when temperature lowers [125,130,132]. Disaccharides like trehalose, mannitol, and sucrose do not cross the cell membrane and act stabilizing the transmembrane proteins [127]. In some cases, multiple types of cryoprotectants are used in association [133,134]. Nevertheless, CPAs are generally toxic and must be removed by washing protocols after cells thawing [89]. If sufficient cryoprotectant could be introduced to avoid intracellular freezing, osmotic and toxic damage caused by the required high concentrations of cryoprotectant may become critical problems [131]. Therefore, optimization of cryoprotectant agent and concentration for a specific cell type and cooling conditions, as well as understanding the physical and biological factors affecting survival of cells at low temperatures, are required in order to develop effective techniques to protect cellular systems from cryoinjury [127,128,131].

3.1.3 Cryopreservation of engineered tissue constructs

A lack of understanding of the mechanisms responsible for damage of more complex cellular systems – cell aggregates and organized tissues and even organs – has limited the successful cryopreservation of cell aggregates, cell-laden hydrogel modules and engineered tissues used in clinical or industrial applications [127,131]. Critical issues relevant to the application of cryopreservation methods to engineered tissue constructs require knowledge of the individual and combined contributions of the cell and matrix components to the overall response to freezing and thawing [127,129]. There are a number of unique elements that complicate the cryobiology of tissue systems, including heat and mass transfer constraints of these bulk systems, intrinsic differences between isolated and cultured cells, and mechanisms of freezing injury unique to complex cellular systems [131,135]. The

macroscopic size and defined geometry of cell-laden constructs result in restrictions on cooling and warming rates that can lead to spatial variations in cryoprotectant concentration. Moreover, the function of tissue systems depends upon the characteristic cell–cell and cell–matrix interactions that may act as critical targets for or mediators of cryoinjury. Finally, the formation of ice within the nonliving intercellular matrix that contains the living cells can result in excessive dehydration of the surrounding cellular components thus leading to significant injury. The combined effect is an irregular distribution of damage sites within the cell-laden constructs that is also affected by the presence of cryoprotectants and the growth of ice crystal. Therefore, the extension of cryopreservation techniques to structured cellular systems must consider not only the in situ cellular function, but also the effects that matrix structure and composition have on the low-temperature response of the cells [127,135].

Several techniques have been proposed for the cryopreservation of cells encapsulated in different materials, tailored for specific applications such as storage of mesenchymal stromal cells [136], neurospheres [80], and pancreatic substitutes [137]; preservation of tissue-engineered substitutes [138,139]; and assembly of three dimensional constructs containing cells [138,140]. A selection of these works is summarized in tab 1.

Ref.	Cell type / Application	Material	CPAs	Assays
[136]	hMSCs / tissue engineering	alginate microcapsules	DMSO (different amount)	cell viability and metabolism; differentiation pathways
[140,141]	hADSCs / biofabrication, organ manufacturing	gelatin/alginate 3d grid constructs	DMSO, glycerol, dextran-40 (various mixture)	cell viability, proliferation, and metabolism; rheological properties; water content
[139]	hADSCs / cartilage regeneration	k-carrageenan hydrogel discs	DMSO (10% v/v)	cell viability and proliferation; histological analysis; mechanical properties
[133]	CV1 (kidney cell line) / -	Collagen microcapsules	DMSO, ethylene glycol, sucrose (various mixtures)	cell viability; integrity of microcapsules
[142]	HepG2 / transportation of bioengineered products	alginate beads	DMSO (12% v/v), University of Wisconsin Solution (UW) (38% v/v), cholesterol 0.1% wt/vol	Cell viability; protein synthesis; glucose consumption; chemical assessment of alginate (FTIR)
[137]	C2C12 (myoblasts) / insulin-secreting pancreatic substitutes	RGD–modified alginate microcapsules	3M DMSO, 3M 1,2-propanediol, 0.5M sucrose	cell viability and metabolic activity; bead integrity; secretory activity
[143]	hMSCs / regenerative medicine	alginate/gelatin cryogel scaffold	DMSO (10% v/v)	cell viability and metabolism; scanning electron microscopy (SEM) analysis
[134]	keratinocytes / tissue-engineered epidermal graft	chitosan-gelatin membranes	DMSO, trehalose (various mixture)	cell viability and proliferation; secretory activity; mechanical properties

Table 1. Summary of the samples used for the *in vitro* analysis associated with their particular fabrication steps. hMSCs (human mesenchymal stromal cells); hADSCs (human adipose-derived stem cells); mESCs (mouse embryonic stem cells); HepG2 (immortalized hepatocyte cell line). Adapted from [144].

The abovementioned studies examined peculiar properties of the proposed method, focusing on evaluating the viability, proliferation, and differentiation potential of encapsulated cells. Moreover, in certain cases the ability of the materials to withstand the cryopreservation in term of structural integrity and mechanical properties was evaluated [134,138,140]. However, none of these studies has systematically compared the effect of different cryoprotectants.

3.1.4 Aim of the work

In this work, we evaluated the effect of cryopreservation and of different cryoprotectants on the biological recovery of human MG63 osteosarcoma cells encapsulated in alginate filamentous constructs, used as model cells-hydrogel system, made by spinning cells/water alginate solutions onto a gelling bath containing calcium ions [29]. The aim was to optimize the alginate-cryoprotectant formulations and to assess the different ability of DMSO, glycerol, and trehalose to preserve encapsulated cells biological functions after a conventional slow freezing protocol [130,131]. Alginate was selected as matrix because cells can be retrieved by dissolving the encapsulating matrix with the use of chelating agents such as EDTA or sodium citrate [5]. Moreover, alginate does not promote cell adhesion and proliferation due to the absence of biorecognition motifs [96]. In our case, these phenomena could potentially interfere with the response of encapsulated cells that undergoes the cryopreservation process. After thawing, the viability of cells encapsulated in the fibers, and their proliferation and metabolic functions recovery

upon dissolution of the alginate matrix were evaluated. All the results were compared with non-encapsulated cells cryopreserved at the same conditions. The effect of the freezing-thawing on the physical properties of the alginate matrix was evaluated with dynamic rheological tests and by measuring the liquid content of the material before and after freezing. The schematic of the biological experiment is reported in fig. 19.

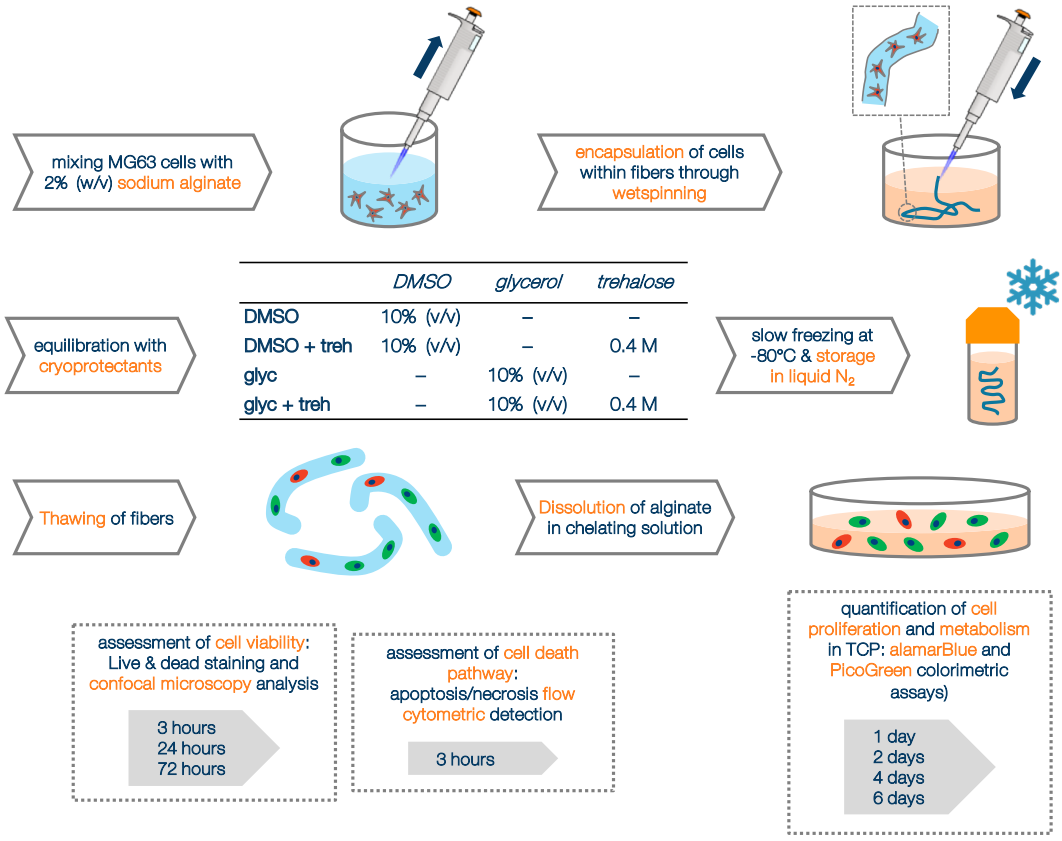

Figure 19. schematic of the biological experiments. MG-63 cell-laden alginate fibers are produced by wetspinning and equilibrated with different formulation of CPAs (containing DMSO, glycerol and trehalose) before slow freezing and storage in liquid nitrogen. After thawing the viability of encapsulated cells is evaluated up to 3 days. A batch of fibers is dissolved in order to release the cells and evaluate the cell viability

and death pathway immediately after thawing. Finally, a batch of released cells is transferred in TCP and cultured up to 6 days in order to evaluate cell recovery in terms of proliferation and metabolic activity.

3.2 Materials and Methods

3.2.1 Materials

The following materials were used: sodium alginate powder derived from brown algae alginic acid, calcium chloride dihydrate, dimethyl sulfoxide (DMSO), glycerol, D-(+)-trehalose dihydrate, sodium citrate dihydrate, 0.05% Triton X-100 (Sigma-Aldrich, USA); Calcein-AM, Propidium Iodide (PI), phosphate buffered saline (PBS), Minimum Essential Media (MEM), 200 mM L-glutamine, 100 mM sodium pyruvate, 100× MEM Non-essential Amino Acids, 100× Antibiotic-Antimycotic solution, 0.05% Trypsin-EDTA solution, Quant-iT PicoGreen dsDNA Assay Kit, alamarBlue Cell Viability Assay (Invitrogen, USA); Fetal Calf Serum, Trypan Blue 0.4% solution (Lonza, Switzerland); MG63 osteosarcoma cell line (ATCC® CRL-1427™) (Istituto Zooprofilattico Sperimentale della Lombardia e dell'Emilia Romagna, Italy); Sonicator (UP400S Heilscher, Germany); Apoptotic/Necrotic Cells Detection Kit (PromoKine, USA).

3.2.2 Hydrogel preparation and sterilization

Alginate powder was dissolved in PBS overnight at room temperature to obtain a 2% wt/vol alginate solution. The crosslinking solution consisted in calcium chloride dihydrate dissolved in distilled water at a concentration of 200 mM. For sterilization, the two solutions were filtered through a 0.22-μm filter before use.

3.2.3 Cell culture and encapsulation

MG63 osteosarcoma cells were thawed and expanded using standard protocols. In particular, cells were expanded in tissue-culture treated flasks as monolayer at 37°C under 5% CO_2 to 85-90% confluence before encapsulation. Culture medium was composed of MEM containing 10% fetal bovine serum (GIBCO), 2mM glutamine, 1 mM sodium pyruvate, 1% non-essential amino acids and 1% Antibiotic Antimycotic solution. At sub-confluence cells were detached from the flask with the Trypsin solution. Subsequently, cells were centrifuged at 1000 rpm for 10 minutes, rinsed in PBS to remove any residues of culture medium and finally dispersed by vortexing inside the buffer. An aliquot of the suspension was used to determine cells concentration using a hemocytometer (Sigma, USA) and Trypan Blue 0.4% as contrasting agent. Cells were centrifuged again and, after removing the supernatant, resuspended in the proper amount of alginate solution to obtain a suspension containing 2×10^6 cells/mL.

400 microns diameter alginate fibers about 5 cm long containing cells were formed by wetspinning [29]. The method involved extruding through a 0.5-20 μL filter tip (Corning, USA) 20 μL of cells/alginate solution onto a Petri dish containing the calcium chloride crosslinking solution. Gelation occurred instantaneously upon contact with the solution containing Ca^{2+} ions. After a few minutes, formed fibers were washed twice with MEM in order to remove residual calcium.

3.2.4 Cryopreservation and thawing

Prior to cryopreservation, cell-laden fibers were incubated at 37°C in 5% CO_2 atmosphere for 30 min in culture medium containing 20% (v/v) FBS with addition

of cryoprotectants (herein referred as cryopreservation media) in the amounts of tab. 2 following indications reported in the literature [134,145].

	DMSO (v/v)	glycerol (v/v)	trehalose (M)
No-CPAs	–	–	–
DMSO	10%	–	–
DMSO+treh	10%	–	0.4
Glycerol	–	10%	–
Glycerol+treh	–	10%	0.4

Table 2. Cryopreservation media composition. The media are prepared by adding the reported compounds to the culture medium.

After incubation, they were moved to cryovials (5 fibers per vial), that were inserted in a commercial cooling box (Cool Cell Freezing Container, Biocision, USA) and cooled from +37 to −80 °C at −1°C /min. The next day, vials were transferred to liquid nitrogen. For *in vitro* evaluations, vials were fast thawed in a water bath at 37°C and immersed in fresh culture medium that was changed after 2 and 4 hours in order to remove CPAs residues from the alginate matrix. Non-encapsulated cells batches were prepared for comparison by using the same procedure. This method is below referred as standard cryopreservation protocol.

3.2.5 *In vitro* evaluation

In vitro evaluations were performed on encapsulated cells (live/dead assays and cell death pathway), on cells released from the alginate matrix and cultured on TCP (proliferation and metabolic activity) and on control batches. The complete scheme of the experiments is reported in fig. 20.

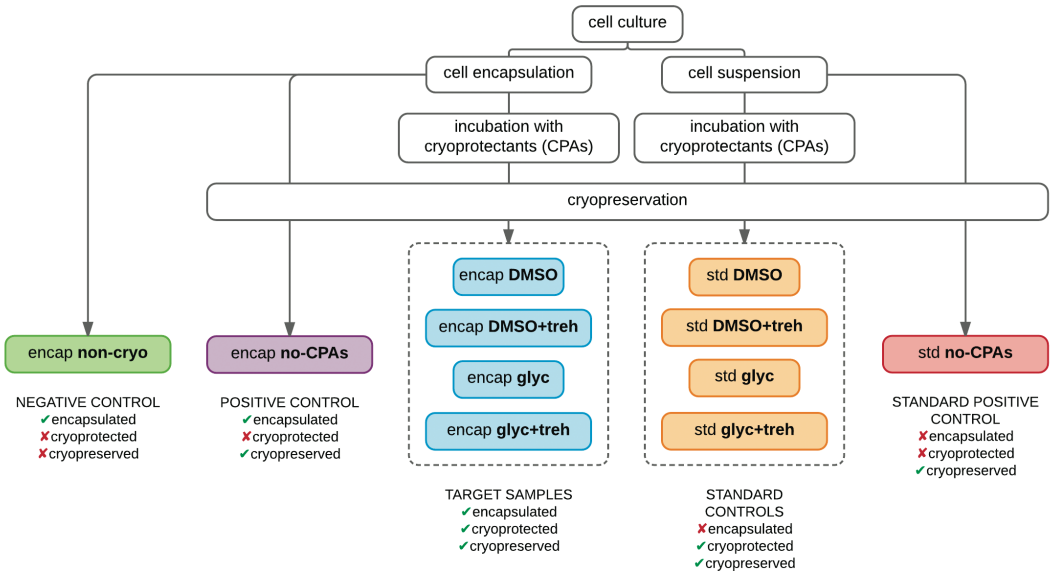

Figure 20. Summary of the samples used for the *in vitro* analysis associated with their particular fabrication steps. Adapted from [144].

For cell release, fibers were incubated in a chelating solution (55 mM trisodium citrate, 10 mM HEPES in PBS) at 37°C for 5 min. After centrifugation at 1000 rpm for 5 min the supernatant was removed, and the precipitate with cells was washed in PBS again to remove any residues of chelating solution. An aliquot of suspension was taken to evaluate the cells concentration using the hemocytometer and Trypan Blue as contrasting agent.

Cells viability and distribution in fibers. Confocal microscopy (Nikon A1, Japan) was used to determine cells viability and distribution in the alginate fibers as prepared (no-CPAs control) and in frozen fibers after thawing, at 3h, 24h and 72h. A standard two-color live/dead assay was performed after incubating the fibers in a PBS solution containing 1 µg/mL calcein AM and 20 µg/mL Propidium Iodide for 30 min at 37°C. Live cells are distinguished by the presence of intracellular esterase activity, determined by the enzymatic conversion of the nonfluorescent cell-

permeant calcein AM to the intensely green fluorescent calcein. Dead cells fluoresce red since their damaged membranes are permeable to the high-affinity fluorescent nucleic acid stain Propidium Iodide. Confocal images were collected along the Z-axis with 10 μm intervals (488 nm wavelength laser and 500 to 550 nm detector for calcein; 560 nm wavelength laser and 570 to 620 nm detector for Propidium Iodide). The viability of encapsulated cells was reported as the ratio of the number of alive cells to the total number of cells in each fluorescent image, automatically counted with the Fiji distribution of image processing software ImageJ [146]. At least 5 fibers were analyzed for each group.

Flow cytometric apoptosis/necrosis detection. Flow cytometry analysis was used to discriminate in control and released cell samples between apoptosis and necrosis pathways, the two essential processes leading to cell death, after staining the cells with an apoptotic/necrotic detection kit (PK-CA707-30017, PromoKine). Cells were incubated for 15 min in the dark in a buffer solution containing Annexin V-FITC and Ethidium Homodimer III. Annexin V labeled with fluorescein (FITC) stains with green fluorescence phosphatidylserines, which are translocated from the inner to the outer surface of the apoptotic cells for phagocytic recognition. Ethidium homodimer III binds to the nucleic acid; it is impermeant to [does not penetrate into] live and early apoptotic cells while staining necrotic and late apoptotic cells with red fluorescence. Subsequently, cells were run at low rates through the FACSCalibur flow cytometer (BD, Singapore) to measure optical transmission, side scattering and emission fluorescence at 530±30 nm and 585±42 nm of at least 10,000 cells, upon excitation at 488 nm. Low green and low red fluorescence was scored as viable (low left quarter), high green and low red fluorescence was scored as early apoptotic (low right quarter), low green and high red fluorescence was scored as late apoptotic/necrotic (upper right quarter), high green and high red fluorescence was scored as late necrotic (upper left quarter) (fig.

21). Standard error was calculated considering the maximum and minimum number of events occurring in each of the four regions by varying the position of the region boundaries.

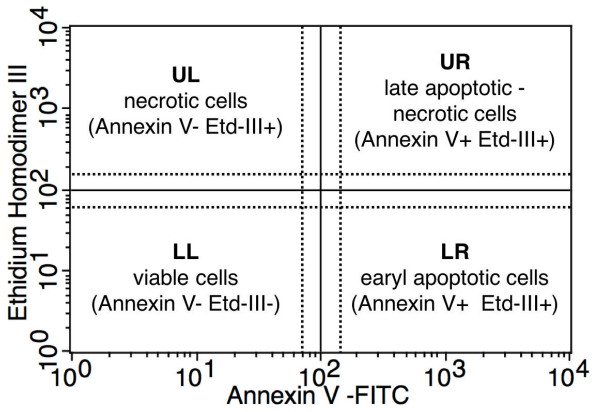

Figure 21. Region classification according to Annexin V and Ethidium Homodimer III intensity after apoptosis/necrosis staining and flow cytometry analysis.

Recovery of cell functionality. Upon thawing, cells were released from the alginate matrix as previously reported and manually counted with a hemocytometer. 2000 cells/cm^2 were then transferred into a TCP (2k cells per well in a 48-well plate) (fig. 22).

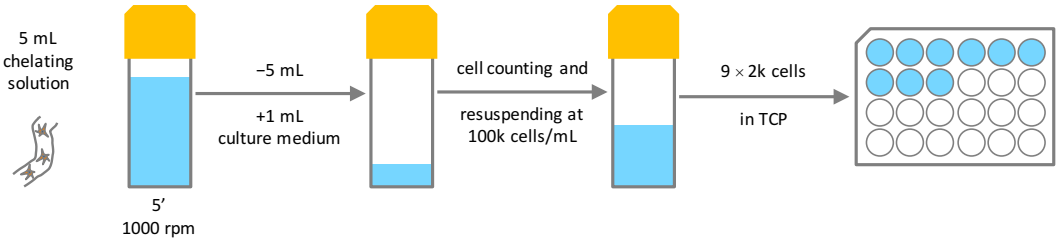

Figure 22. schematic of the method for releasing cells from the alginate matrix after thawing. After dissolving the alginate matrix in a sodium citrate-based chelating solution, released cells are counted and cultured in TCP.

The next day and for 6 days thereafter, the metabolic activity of cells was evaluated with alamarBlue assay, which uses the reducing power of healthy cells to convert resazurin to the fluorescent molecule resorufin, and the proliferation of cells was evaluated with PicoGreen assay, a dsDNA-intercalating fluorophore. At 1, 2, 4 and 6 days, cells were incubated for 2 h with culture medium containing 10% alamarBlue and fluorescence intensity was measured on a plate reader (535±25 nm excitation and 590±20 nm emission; Spark 10M, Tecan, Switzerland). Subsequently, DNA extraction was performed by disrupting the cells membrane with a solution of 0.05% Triton-X in PBS, followed by sonication (UP400S, Hielscher, Germany) for 10 s. PicoGreen was then used for the quantification, measuring the fluorescence intensity of PicoGreen-DNA complex with the plate reader (485±20 nm excitation and 535±25 nm emission). A calibration curve was built up using the DNA standard provided with the assay to correlate fluorescence intensity to DNA concentration. Cells exposed to standard cryopreservation procedure were used as reference. For each test nine replicates were used.

Statistical analysis. Graphpad Prism 7 software was used for statistical analysis. Results are expressed as mean ± standard deviation (SD) and significance was tested using two-way analysis of variance with Tukey's *post hoc* test. A p value of 0.05 was considered significantly different.

3.2.6 Evaluation of material properties

Rheology. Alginate hydrogels were submitted to rheological test before and after freezing by using a parallel-plate rotational rheometer (Discovery HR-2, TA Instruments, USA) with 40 mm diameter plate. The samples were prepared by casting liquid alginate (as described in par. 3.2) onto gelatin molds containing calcium chloride until complete gelation occurred. Alginate discs (diameter 40 mm,

height 2 mm) were then detached from the gelatin substrate and incubated with the different CPAs (as described in par. 3.4) overnight to assure complete diffusion of the CPAs in the alginate matrix. The samples were subsequently cooled to −80°C before transferring into liquid nitrogen and finally thawed at 37°C. After rinsing the sample in DI water to remove the CPA residues, rheological properties were investigated. Frequency sweep experiments were conducted from 0.01 to 10 Hz at a fixed strain and temperature of 2% and 37°C respectively. Storage modulus (G′) and loss modulus (G′′) were measured as a function of frequency. At least 3 samples were evaluated for each condition. As a control, fresh samples were tested after incubation with the CPAs and rinsing in DI water.

Liquid content. The liquid content of the alginate hydrogels before and after freezing was investigated by weighing the samples in the wet and dry state. Alginate discs were fabricated as described in the previous paragraph, incubated in presence of the different CPAs, frozen-thawed and rinsed in DI water overnight to remove any CPA residues. As a control, fresh samples were tested after incubation with the CPAs and rinsing in DI water. Subsequently, the samples were weighted before and after completely drying in an oven at 65°C overnight. The liquid content of the hydrogels was determined by the following equation, where M_{wet} and M_{dry} represent the mass of the samples before and after drying.

$$C_{\%} = \frac{M_{wet} - M_{dry}}{M_{wet}} \times 100$$

At least 5 samples were evaluated for each condition.

3.3 Results

3.3.1 Cells distribution

When injected in the calcium chloride bath, alginate underwent a fast sol-gel transition with the formation of a solid gel fiber. Fibers were left in the crosslinking

solution for about 10 minutes, to allow the diffusion of calcium ions towards the gel core. In fig. 23 a live/dead representation of an alginate fiber containing cells is reported. The mean diameter of the fiber, measured by optical microscopy, is 387±98 μm (n=9), which is compatible with nutrients diffusion in presence of high cell densities [27]. Moreover, cells appear homogeneously distributed inside the fibers.

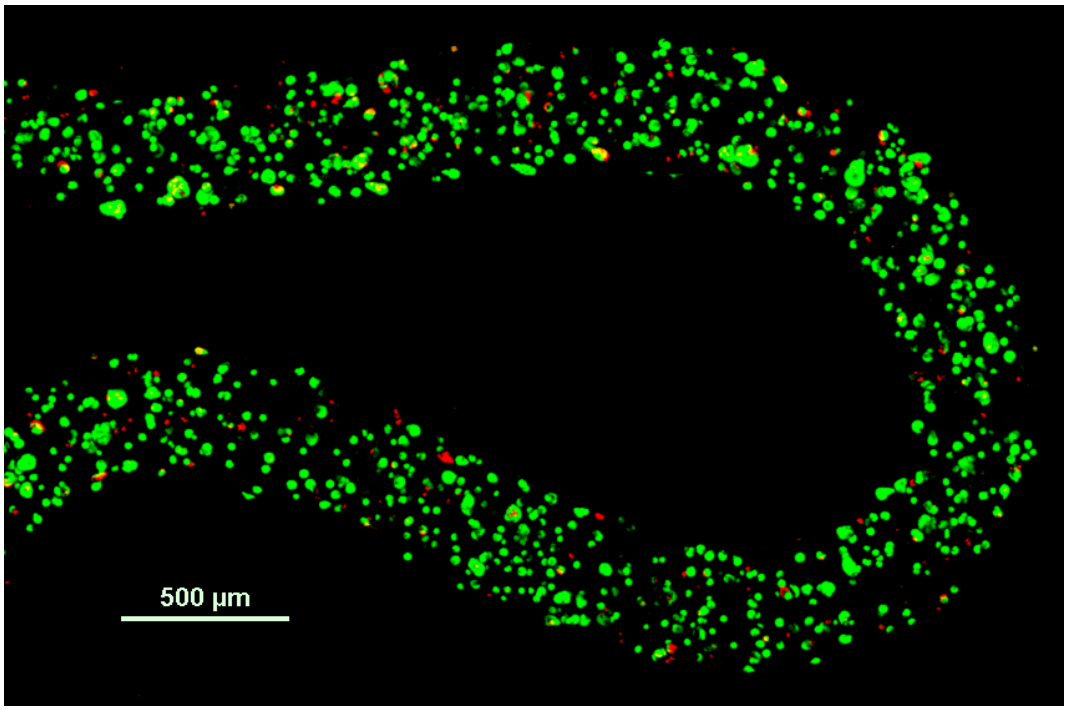

Figure 23. Representative confocal microscopy image of cells encapsulated in a wet-spun alginate fiber stained with live/dead (green/red) fluorescent dyes. Adapted from [144].

3.3.2 Viability of encapsulated cells

The effect of the different cryoprotective formulations on the viability of encapsulated cells was evaluated on all samples after thawing. Visualization of the alginate fibers containing cells by confocal microscopy, after standard Live/Dead

staining, was used to discriminate alive from dead cells (fig. 24 a). Cell viability was evaluated at 3, 24 and 72 hours after thawing. Results were compared with two systems: fibers loaded with cells not frozen (non-cryo) and fibers loaded with cells frozen in absence of cryoprotectant (no-CPAs). Images indicated limited cell death in any of the cryopreserved samples, less than or equal to the non-cryo control. For quantitative analysis, live and dead cells were automatically counted and discriminated using the Object Counter plugin of Fiji software 3 hours after thawing (fig. 24 b). Subsequent time points quantification of cell viability was not performed since Propidium Iodide is not able to stain cells that are dead more than 1-2 days before, not allowing reliable cumulative count of dead cells. A decrease of viable cell number was observed after cryopreservation compared to non-cryo group (viability 91±2%). A higher retention of cell viability was observed for cells cryopreserved with DMSO (85±2%) compared with glycerol (71±4%), DMSO/trehalose (71±2%) and glycerol/trehalose (72±6%).

3.3.3 Apoptosis/necrosis detection after thawing

The effect of the various cryopreservation protocols on the pathway of cell death during freezing were analyzed by flow cytometry (fig. 25 a). Results were compared with non-frozen cells and with cells frozen with standard protocol.

In general, for all cryoprotectants, cell viability was greater than control formulations without any cryoprotectants (no-CPAs controls) (fig. 25 b). We observed a decrease in cell viability for the cryopreserved encapsulated cells compared to the standard cryopreservation protocol both with DMSO (75.0±6.0% vs 60.3±4.6%) or glycerol (80.1±5.0% vs 49.5±2.8%). Furthermore, we observed a decrease of early apoptosis signal and a shift toward late apoptosis/necrosis signal for encapsulated cells. With trehalose, cell viability decreased both for standard

cryopreservation and for cryopreservation after encapsulation (60.3±4.6% vs. 50.1±3.1% for DMSO and 49.5±2.8% vs. 43.7±2.2% for glycerol). This result confirmed the qualitative live/dead confocal analysis evaluations.

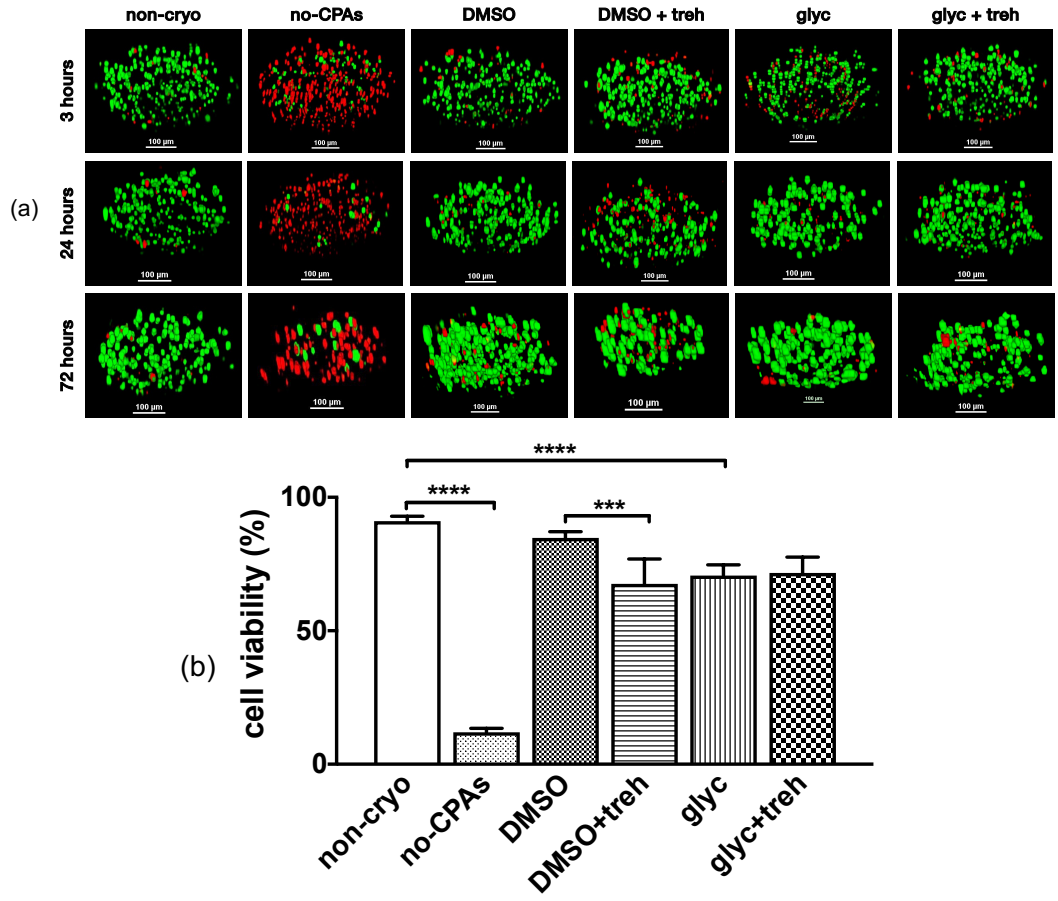

Figure 24. (a) Live/dead analysis with confocal microscopy of MG63 cells encapsulated and frozen in alginate fibers (cross-section) with the different CPAs formulation and at different time points after thawing. All scale bars are 100 µm. (b) cell viability in the fibers analyzed with ImageJ cell counting 3 hours after thawing. Error bars represents mean ± SD (n=5). ***p<0.001 and ****p<0.0001. Adapted from [144].

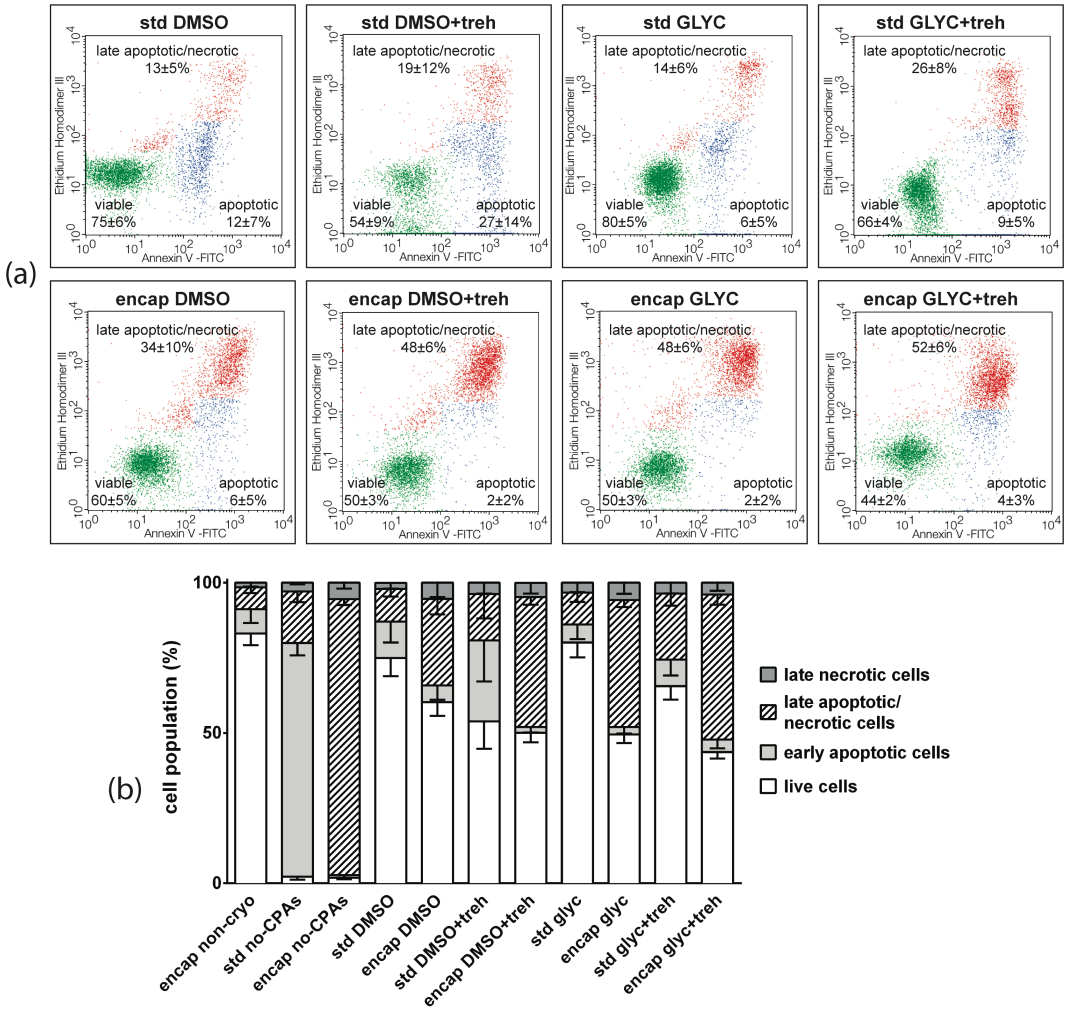

Figure 25. (a) Flow cytometric results of concurrent staining with FITC-Annexin V and Ethidium Homodimer III to detect apoptotic/necrotic cells after thawing (std and encap groups) and dissolution of the alginate matrix (encap groups); (b) corresponding distribution of viable, early apoptotic, late apoptotic and necrotic cells. Error bars represent mean ± SE, calculated on 10^3 gated cells. Adapted from [144].

3.3.4 Cell proliferation and metabolic activity

The results of cell proliferation and metabolic function are reported in fig. 26 and 27 respectively. Upon thawing, cells were released from the alginate matrix using a calcium ions chelating solution and transferred in TCP. The relative fluoresce intensity was normalized to the value at day one for each group. At day two, cells frozen with cryoprotectants showed a comparable DNA content. Considering the effect of encapsulation, at day 4 and 6 we observed a significant increase in cell proliferation in presence of DMSO (increment of 12.5±0.9 fold vs. 15.8±1.8 fold at day 6) and glycerol (16.9±1.4 vs. 18.3±1.3 at day 6). The encapsulated group frozen by using DMSO/trehalose exhibited an increase of cell growth with respect to the DMSO alone (15.8±1.8 vs. 18.6±2.4 at day 6). On the contrary, when glycerol was used, the addition of trehalose led to a significant inhibition of cell proliferation (18.3±1.3 vs. 11.5±1.1 at day 6).

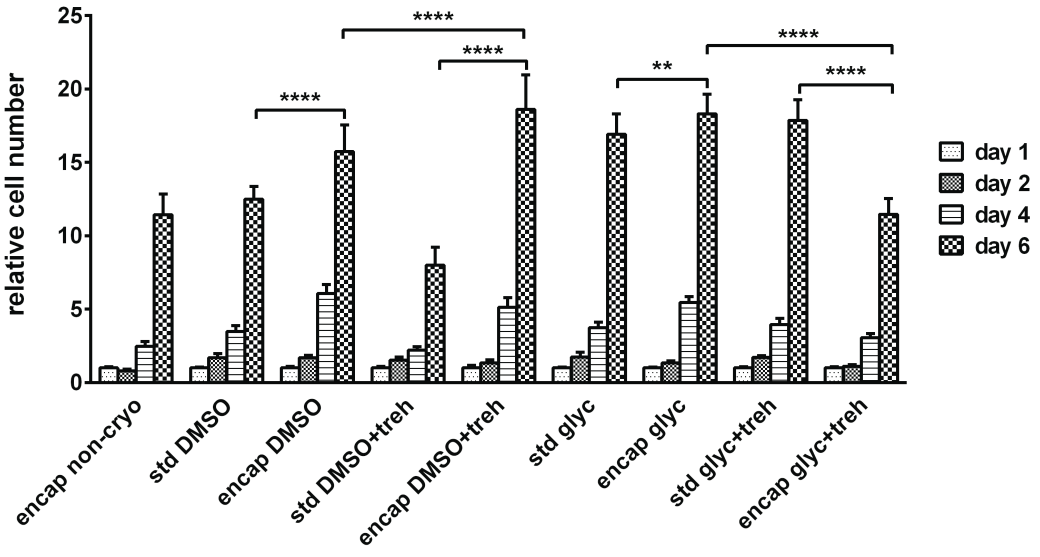

Figure 26. Cell number evaluation at each time point from the various frozen groups after thawing. Std: cell frozen with standard protocol (1M cells/vial in

cryopreservation medium. Encap: cell frozen after encapsulation, following dissolution of the gel. Values are normalized to day 1 for each group. Error bars represent mean ± SD (n=9). **p<0.01 and ****p<0.0001. Adapted from [144].

Cells metabolic activity was determined with the alamarBlue assay and data were normalized to the value at day one for each group. All cryopreserved cells exhibited an increase of metabolic activity from day 1 to 6 and confirmed the trend of cell proliferation signal. Considering the use of a single cryoprotectant, cells frozen after encapsulation exhibited a significantly increased metabolic signal from day 4 onward, both for DMSO (increment of 9.3±0.8 fold vs. 10.3±1.2 fold at day 6) and glycerol (9.9±0.8 vs 14.2±1.2 at day 6). This result matches the cell proliferation profile, and confirms previous results on fibroblasts-like cells cryopreserved in suspension and in a 3D construct [147]. Regarding the effectiveness of the different CPAs for encapsulated cells, glycerol led to higher cell recovery 6 days after thawing. The addition of trehalose during cryopreservation was favorable for the metabolism of cells frozen after encapsulation in presence of DMSO (10.3±1.2 vs 13.1±1.4 at day 6). Overall, encapsulated cell cryopreserved with glycerol led to the best performance in terms of metabolic and proliferative recovery after cryopreservation.

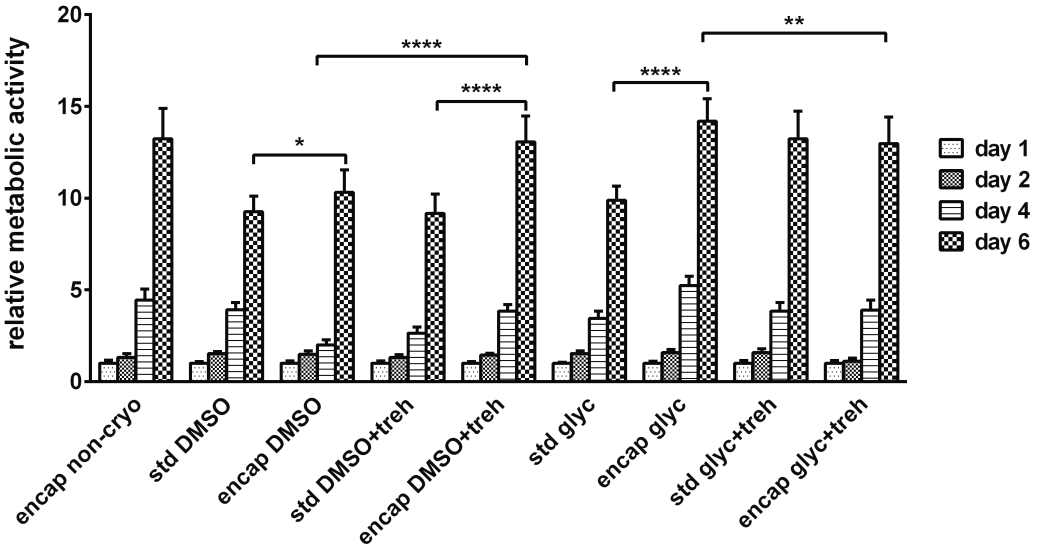

Figure 27. Cell metabolic activity in TCP at each time point from the various frozen groups. Std: cell frozen with standard protocol (1M cells/vial in cryopreservation medium). Encap: cell frozen after encapsulation, following dissolution of the gel. Values are normalized to day 1 for each group. Error bars represent mean ± SD (n=9). *p<0.05, **p<0.01 and ****p<0.0001. Adapted from [144].

3.3.5 Rheological properties

The rheological behavior of the hydrogel was analyzed in order to evaluate the influence of a freezing-thawing cycle on the mechanical properties of alginate. Frequency sweep measurements of alginate samples incubated with the different CPAs before freezing and after thawing were compared. In particular, storage and loss modulus were measured in the linear-viscoelastic limit [148,149] and are shown in fig. 28. A temperature of 37 °C was selected for conducting experiments to mimic *in vitro* conditions. The results showed that each group is in a relatively stable gel state at 37°C (G′>G″ at any frequency) and the cryopreservation with any CPAs formulation only slightly altered the viscoelastic properties of alginate with some

differences when comparing the values of storage and loss modulus before and after freezing-thawing. On the contrary, both the storage (G′) and loss (G″) moduli of samples frozen in absence of any CPAs significantly increased ($p<0.0001$ for G′ and $p<0.001$ for G″ at 1 Hz) with respect to the values detected for the corresponding fresh gels.

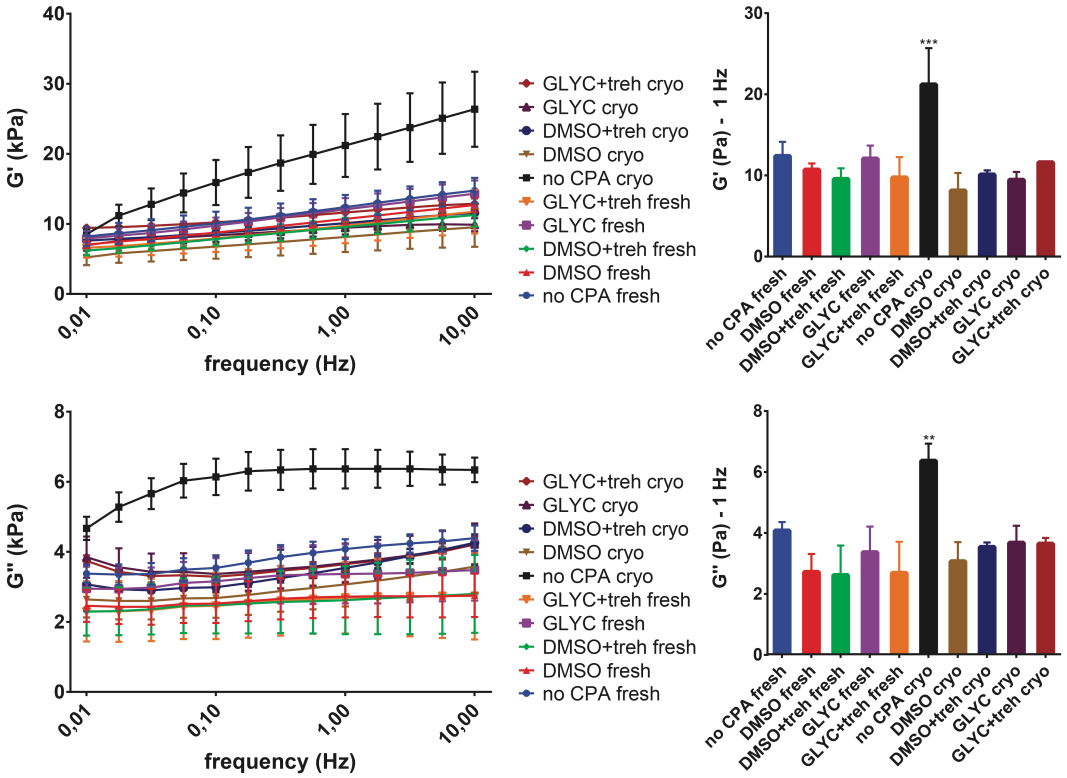

Figure 28. Left: frequency sweep rheological measurements comparing storage modulus (a) and loss modulus (b) of 2% wt alginate samples frozen in presence of the different cryoprotectants. Right: values of G' and G'' at 1 Hz. Error bars represent mean ± SD (n=3). **p<0.01 and ***p<0.001. Confidence levels are referred to the no CPA fresh group. Adapted from [144].

3.3.6 Liquid content

In this study, we evaluated the influence of cryoprotectants and freezing/thawing on the liquid content of alginate hydrogel. After incubating hydrogel samples with the different CPAs, the samples were either rinsed in water or frozen, thawed and rinsed in water before measuring the liquid content. As shown in fig. 29, the equilibrium water content for fresh (non-frozen) hydrogels rinsed in water was not affected by any of the CPAs. On the contrary, we measured an about 2 points % decrease of the water content when the samples were frozen and thawed after incubation without using any CPA as well as a small decrease of the absorbed water for gels treated with glycerol or glycerol/trehalose. The water content decrease of the samples frozen without any CPAs agree with the observed increase of G′ and G″ previously reported.

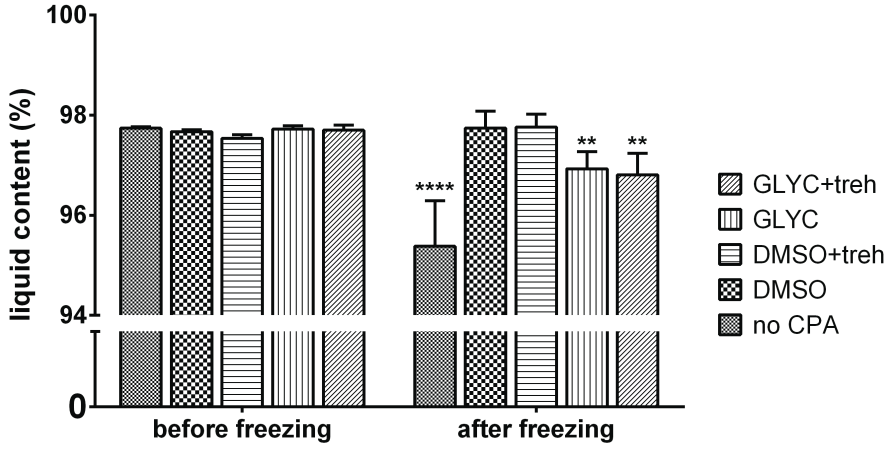

Figure 29. Liquid content study of alginate hydrogels after incubation with the CPAs (before freezing) and after incubation with the CPAs, freezing and thawing (after freezing). Error bars represent mean ± SD (n=5). **p<0.01 and ****p<0.0001. Confidence levels are referred to the relative before freezing counterpart for all the samples after freezing. Adapted from [144].

3.4 Discussion

The issue of preservation and storage of encapsulated cells is an obstacle for translating cell encapsulation to tissue engineering in the form of commercial products [89,127,138]. Cryoprotective agents (CPAs) are added during the freezing process in order to protect cells from cryodamages [131]. DMSO and glycerol, in particular, penetrate cell membrane at physiological temperature and have been extensively used to prevent cell damage during cooling by minimizing intracellular ice formation [125,130]. Furthermore, the addition of trehalose and other disaccharides to these cryoprotectants is known to enhance cell survival during cryopreservation of cell suspension [150] and engineered tissues [133,134].

Many factors may influence cell viability in a cryopreservation system, including fabrication and freezing process, molecule diffusion kinetics in the hydrogel matrix, cell morphology and reorganization of the adhesion sites. Therefore, establishing a cryopreservation protocol for tissue-engineered products cannot disregard an analysis of the interaction between cells, encapsulating biomaterial, cryoprotective agents, freezing method and other conditions that may influence the cellular functionality and demands for an extensive investigation. In this study, we propose a systematic approach for assessing the impact of cryopreservation on engineered tissue, considering the analysis of cell recovery and of the material properties.

In this work, we characterized the influence of cryopreservation on encapsulated cells, comparing the effect of different cryoprotectants on cell response after thawing. For this reason, sodium alginate hydrogel was chosen for encapsulating cells in order to reduce the interaction between cells and their encapsulating matrix. As a model, cells were entrapped in alginate fibers made by wetspinning, which represents a fast and high-throughput encapsulation model [29].

Cell-laden microfibers are easy to prepare, handle and assemble from an engineering standpoint and are appropriate to reconstruct structures with a hierarchical alignment [34]. To validate the cryopreservation technique, MG-63 cell line was chosen as an established human osteosarcoma cell line for bone tissue engineering models with fully genetic characterization [151]. After cell encapsulation, the hydrogel fibers were frozen in presence of different cryopreservation media containing DMSO, glycerol and trehalose, whose effects on cell functionality were compared after thawing.

All CPA formulations successfully prevented the death of encapsulated cells during cryopreservation compared to cells frozen in absence of any cryoprotectants. The estimated post-thaw viability of cells encapsulated and cryopreserved with DMSO was 7% lower than in the non-cryopreserved group and 15% higher than in the group cryopreserved with glycerol, and comparable to the results already published by other groups using the same freezing protocol [136]. The addition of trehalose led to a decrease of cell viability that is larger for the group cryopreserved with DMSO, considering both the encapsulated cells and the control. We also monitored the viability of encapsulated cells up to 3 days after thawing in order to evaluate possible harmful effects of the CPAs that may remain in contact with the cells. In fact, high concentrations of cryoprotective chemicals can be toxic for cells, and toxicity must be reduced by decreasing the time of cell exposure to the cryoprotectants [125]. The analysis of the Live/Dead data excluded protracted detrimental effect of the CPAs since appreciable cell death was not detected after the initial post-thawing observation.

In order to develop methods to mitigate the harmful effect of cryopreservation on encapsulated cells, a detailed study of the possible pathways and mechanism leading to cell death is of primary importance. The exact mechanism leading to apoptosis and necrosis activated during freezing is not well

understood and remains to be studied [152]. Moreover, the death pathway activated in one cell type might not be activated in other cell types. Cell cycle after thawing and releasing from the alginate matrix was compared with non-encapsulated protocol. Flow-cytometric analysis highlighted that both encapsulation in alginate and addition of trehalose reduced the viability of cells after cryopreservation. Besides, we observed a difference in cell-death pathway since the encapsulation led to later stage of apoptosis and necrosis of the cell population. A possible explanation is that the hydrogel acts as barrier that could cause a gradient of the cryoprotectant concentration in the fiber, so leading position dependent damage of cells and subsequent necrosis.

The influence of the different cryoprotective formulation on cell metabolism and proliferation were investigated up to two weeks, since it has been reported that the effectiveness of cryopreservation cannot be reliably determined immediately after thawing [153]. Moreover, a direct correlation between the viability (fig. 5) of a certain cell population and the ability of viable cells in that population to proliferate (fig. 6) and to be metabolically active (fig. 7) was not detected.

Encapsulated cells, thawed and cultured in TCP, showed a larger metabolic activity and proliferative capacity when DMSO and glycerol alone were used as cryoprotectants. Indeed, a previous comparison of fibroblast response to low temperature in suspension and 3D culture indicated a more intense functional expression of stress proteins in 3D constructs [147]. Interestingly, trehalose addition to encapsulated cells had a favorable effect on cell recovery when DMSO was used, and a reverse situation in the case of glycerol. This appears to be contrary to previous studies, which reported how the addition of sugars to cryoprotectants that penetrate cells at physiological temperature leads to a detectable improvement of the results in cryopreservation protocol for both DMSO [134] and glycerol [154]. However, the abovementioned studies used different encapsulation materials and

freezing protocols than those used in the current work, and trehalose has been reported to possess inhibitory effects on proliferation of fibroblast-like cells in certain conditions [155].

In our analysis, we detected an increased number of apoptotic cells corresponding to lower proliferation of the reseeded cells. A possible explanation is that Trypan blue method, that was used to counts the alive cells for the reseeding experiments, doesn't discriminate between vital and early apoptotic cells [156]. Thus, the real viable cells that are able to proliferate are less than those counted with the Trypan Blue exclusion method. Moreover, apoptosis has been reported to be responsible for a low cell recovery rate after cryopreservation [157]. The relationship between the addition of trehalose and apoptosis could be attributed to various reasons and its clarification would require complex and laborious gene expression studies. Moreover, the effect of trehalose must be judged considering its complex interactions with the alginate matrix and DMSO/glycerol, that could affect its diffusion capacity from the medium to the cells. Besides, in our study DMSO better preserved the viability of encapsulated cells compared to glycerol; however, its effect (in absence of trehalose) resulted in increased apoptosis after thawing, corresponding to a diminished proliferation and metabolic capacity. This phenomenon can derive from the different ability of glycerol and DMSO to penetrate the alginate layer and interact with the cell membrane. This evidence highlights the importance of analyzing different cryopreservation protocols for different tissue constructs, in order to find the formulation that best adapt to the chosen cells and materials.

Rheological analysis and liquid content measurement were performed in order to characterize the influence of cryopreservation on the viscoelastic and swelling properties of alginate hydrogel. In fact, these are critical features of hydrogels used in biomaterials and tissue engineering applications, influencing

both tissue morphogenesis and stem cell differentiation. A temperature of 37 °C was selected for conducting the experiments in order to mimic *in vitro* conditions. Based on our results, the values of tan(δ) (higher than 0.2 at any frequency) reveal a clear viscoelastic behavior of the hydrogels. Moreover, it is clear that all the CPAs successfully preserved the viscoelastic properties of alginate after thawing, at the same time preventing the reduction of water content. We hypothesize that, during the freezing process, the presence of the CPAs can influence the growth of ice crystals from the water present in the matrix, thus affecting the conformational changes of the alginate network after thawing [120,158]. In fact, the slow freezing process could generate concentrations fluctuations of the alginate content in solution, and this, thanks to the presence of residues of calcium, could results in a further crosslinking of the gel [159]. Data on the water content (fig. 9) are consistent with the above assumption, as well as the increase of G′ in alginate samples after freezing and the stiffness/frequency relationship (fig. 8). When CPAs are added, ice crystals formation is prevented and concentrations fluctuations are damped. The increase of the matrix rigidity could theoretically negatively impact the cells viability. However, this is a second order effect, being the intracellular ice formation the cause for the cells death.

The collected data demonstrate that cells encapsulated in alginate fibers remained viable after cryopreservation in liquid nitrogen and thawing, hence stocks of cryopreserved cell-laden hydrogel constructs could be thawed when necessary and three-dimensionally assembled [34].

The proposed method can be adopted to compare and select multiple cryopreservation parameters for a given system, including cryopreservation medium formulation, cell density, presence of adhesive motifs in the material and freezing rate. In fact, we evaluated the influence of different parameters on the efficacy of cryopreservation, including the use of different CPAs and the addition

of trehalose to the cryoprotective solution. Moreover, this protocol investigates the impact of encapsulation by comparing the results obtained for entrapped cells with those obtained for suspended cells. This work focused on evaluating the recovery of cells in terms of viability and functionality and the impact of freezing on the rheological properties and water content of the encapsulating hydrogel. The outcome of our research thus offers an approach to investigate the effect of cryopreservation on cell-laden hydrogel constructs, that can be adopted as support for different applications, from biofabrication to cell banking to drug releasing devices.

3.5 Conclusions

In summary, in the present work the possibility to cryopreserve cell-laden alginate fibers in presence of different cryoprotectants formulations was investigated. Encapsulated cells, when cryopreserved in presence of DMSO and glycerol, maintained a viability degree comparable to cells cryopreserved with standard protocols and no protracted harmful effect of the CPAs were observed after thawing. Furthermore, cryopreserved encapsulated cells expressed a faster recovery of functionality, confirming previous works [147]. Overall, we propose a method to produce and store cell-laden hydrogel constructs that can serve as building blocks for subsequent assembly of tissue constructs according to different biofabrication strategies [25,50,160].

Besides, in this paper we present an approach for the evaluation of the effects of cryopreservation on the functionality of cell-laden constructs. In fact, the protocol described herein proposes a method for determining the impact of cryopreservation on cell recovery and material properties after freezing in presence of different cryoprotectants, in short- and mid-term (up to 2 weeks after thawing).

The proposed approach can be adopted for evaluating the effect of other cryopreservation methods on cells encapsulated in specific hydrogel matrices and designed for specific applications. In fact, integration of cryopreservation techniques with cell micro-scale encapsulation introduces a promising approach to the field of tissue engineering and can be adopted as support for bottom-up engineered tissue assembly and cell banking, expansion and release [96,127].

Chapter 4.
Engineering Hydrogels as Building Blocks: Evaluation of Alginate-based Films

4.1 Abstract

The use of hydrogels as building blocks for tissue engineering scaffolding and for the development of three-dimensional cell culture models requires the design of matrices with adequate geometry and physicochemical properties that resemble the native extracellular matrix (ECM). In fact, the composition of the hydrogels must be tuned in order to achieve cell proliferation and functionality inside materials that are compatible with microencapsulation technologies.

In this study, a novel method for encapsulating cells within hydrogel films with micrometer thickness is described. MG63 osteoblast-like cells were encapsulated in alginate films, blended with different proteins (collagen type I, gelatin or silk fibroin) in order to enhance cell attachment, growth and functionality. The best matrix composition for supporting osteoblast cells was selected according to different parameters: cell metabolic (alamarBlue assay) and mitochondrial activity (CCK-8 assay), cell morphology and distribution (F-actin visualization) and vascular endothelial growth factor (VEGF) secretion (ELISA assay).

Addition of proteins to alginate increased cell metabolic (up to 1.62 times for alginate-silk fibroin compared to pure alginate after 14 days) and mitochondrial (up to 1.75 times) activity, provided a suitable anchorage for osteoblast-like cells and enhanced the secretion of VEGF (up to 2.64 times after 72 hours). According to the results obtained in this study, alginate-silk fibroin hybrid hydrogel emerged

as the most promising hydrogel for osteoblasts encapsulation, thus representing a promising biomaterial for soft-tissue regeneration.

The results proved that such novel hybrid hydrogels might find applications as building blocks for assembling complex cell-laden constructs or as support for co-culturing multiple cell populations. Moreover, the proposed alginate-based blends are promising biomaterial to produce osteoblast cells-laden matrices that can support vascularization.

4.2 Introduction

Extracellular matrix (ECM) is a complex tridimensional environment that provides structural support to cells and a regulatory milieu with a variety of important biological functions, including assembling cells into various tissues and organs, regulating growth and cell–cell communication [161]. From a tissue engineering (TE) standpoint, encapsulating cells within modular culture environments and mimicking the complexity of specific cell niches found *in vivo* within hydrogel building blocks is desirable in order to replicate tissue functions *in vitro* [15,161]. The engineering and assembly of tissue-mimicking 3D constructs, considering the intricate and organized nanoscale meshwork of native ECM, is important for tissue regeneration and other important applications of regenerative medicine [3,89]. In fact, the biochemical and biophysical properties of the matrices that surround cells are essential to the functional tissue regeneration since cells can display different phenotypes depending on their microenvironment [162]. A system that can mimic the structural architecture and biological functions of the extracellular matrix (ECM) in 3D should satisfy the following characteristics: have suitable mechanical properties, chemical composition and degradation kinetic,

support cell growth and maintenance, and facilitate nutrient, gas, metabolic waste transport, and signal transduction [2,161].

Moreover, the natural interactions between different cell populations, in turn influenced by the extracellular environment, must be carefully taken into consideration. In fact, the cross-talk between two different cell types through cell signaling, growth factors and cytokines can have a profound effect on cell morphology, gene expression, differentiation and function [163,164]. Co-culture methods – the culture of multiple, distinct cell types within the same environment – are used in tissue engineering and biofabrication to drive tissue formation with the interaction of multiple cell populations or to maintain the potency of stem cells during expansion [165]. As an example, beyond the basic requirements, the hydrogel matrix used to encapsulate cells should also be able to support angiogenesis for an effective regeneration purpose in case of vascularized tissues, such as the bone [164,166]. In fact, the association of vascular endothelial cells (ECs) and bone-forming osteoblasts (OBs) within three-dimensional constructs provide promising means of generating vascular bone tissue-engineered constructs. Therefore, encapsulated cells should express vascular endothelial growth factor (VEGF), the major angiogenic factor involved in physiological and pathological angiogenesis [81,164].

So far two approaches for culturing multi-cellular systems have been proposed: direct co-cultures, which involve direct contact between the different cell populations that are mixed together within the culture environment; indirect co-cultures, which involve the interaction, via soluble factors, between cell types that are physically separated within the culture environment [165,167]. In the latter case, the complex dialogue among cell types within native tissue is recapitulated by signaling factors and cytokines that enrich the culture medium [165]. Cells can be seeded on the scaffold or encapsulated in hydrogels either at the same time, for an homogeneous mix in the construct, or seeded at different times, which is beneficial if the two cell

lines have different proliferation rate [163] (fig. 30). Therefore, the engineering of co-culture strategies for assembling complex multi-cellular constructs represent an important challenge for biofabrication, as these systems better model both physically and biologically the natural tissues. Building blocks must be conceived and designed considering the complex cell-cell and cell-biomaterial interactions, the specific physicochemical characteristic of native tissue and the precise needs of distinct direct or in-direct co-culture techniques [167].

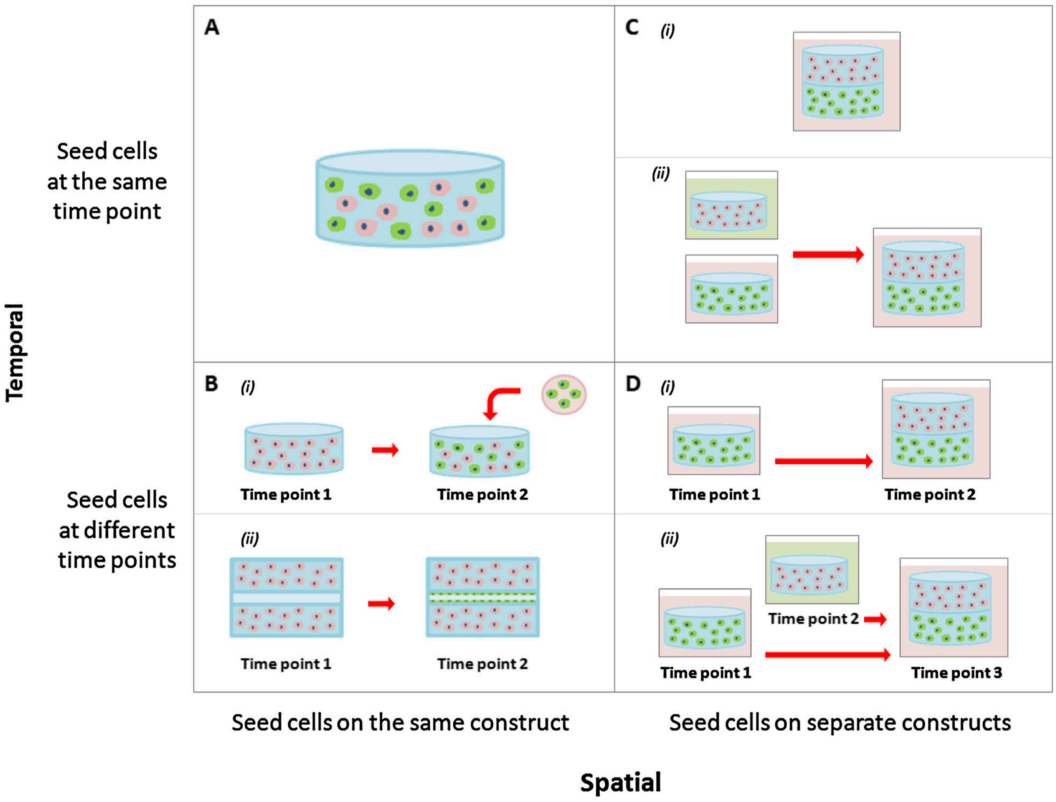

Figure 30. Different cell seeding strategies for co-culture system in tissue engineering. **(A)** Cells seeded together in the same construct at the same time point. **(B)** Cells seeded together in the same construct at different time points. **(C)** Cells seeded in different construct at the time start point and either cultured **(i)** together

or **(ii)** separately. **(D)** Cells seeded in different construct at different time points and either cultured **(i)** together or **(ii)** separately. Adapted from [163].

Designing the cellular microenvironment remains one of the major challenge in tissue engineering, given the complexity of cell-ECM interactions as well as multicellular architectural features and the complex biochemical interactions between different cell types [161]. The choice of the biomaterial is a critical element to enable survival, proliferation and function of the encapsulated cells. Moreover, the encapsulation method must be amenable to fabrication and assembly of complex 3D structures in a manner that does not damage living cells [30]. The research for novel biomaterials has shown the potential of hydrogels to mimic native ECM. Various technologies were developed to manufacture and assemble cell-containing microgels into designed architectures and spatial organizations [89]. Hydrogels are considered an ideal matrix for culturing cells in three dimensions as they possess the capacity of incorporating bioactive molecules, such as growth factors, peptides and extracellular matrix components. In fact, chemical cues and topography of a scaffold are able to influence the proliferation, differentiation and function of the encapsulated cells and hence the quality of the final tissue substitute or tissue model [168]. In particular, the combination of proteins with alginate has proven to effectively modulate the physicochemical and biological properties of the hydrogel. The synergistic effect of multiple cues produces new hydrogels that exhibit a novel structure organization and new properties in order to expand the scope of their application in several areas of tissue engineering [162,169].

Several different technologies have been used to produce cell-laden hydrogel building blocks that mimic specific cell niches; each technique have been tailored to reproduce a certain geometry, chemical cues, stiffness and application. The different hydrogels that can be utilized are limited within the range of techniques

available, based upon their mechanical properties and crosslinking methods [30]. Furthermore, the range of possible geometries and form factors with which it is possible to manufacture building blocks are limited by nutrient perfusion and mass transport limitation issues. In fact, cell growth in 3D and engineered tissue are characterized by the limited diffusion of oxygen, nutrients, metabolites, waste products and signaling molecules, which are continuously produced and consumed by cells to support and maintain their function. 2D monolayer cultures do not mimic these physiologically relevant distributions. The mass transport of oxygen and nutrients is particularly critical because it limits proliferation of encapsulated cells cultures to distances less than a few hundred microns from oxygenated medium or, in living tissues, to similar distance from the nearest capillary [45,83]. Therefore, the encapsulation of cells in hydrogel building blocks with features that exceed 100-200 μm represent a critical barrier for the manufacturing of relevant-size tissue engineered constructs. Different approaches have been proposed to enhance mass transfer of nutrients, oxygen and waste removal in three-dimensional (3D) microenvironment with encapsulated cells. Alginate hydrogels are the materials most widely used for encapsulating cells within building blocks for biofabrication, because of its ability to form matrices which provides an aqueous environment necessary for sustainable cell growth. However, given the limited cell adhesion to alginate, as well as its uncontrolled degradation under physiological conditions, different methods have been proposed in order to functionalize or blend alginate with proteins and other bioactive molecules [169], as widely described in chapter 2. Hybrid hydrogels obtained by combining alginate with various proteins are expected to improve its biocompatibility and enhance cell adhesion to the matrix and functionality of the encapsulated cells. Among naturally occurring proteins, gelatin, collagen and silk fibroin are increasingly used in tissue

engineering applications, as they contain cellular binding motifs which support cellular attachment in a manner similar to ECM [122].

4.2.1 Aim of the work

The aim of this work was to design and characterize an innovative encapsulation method for cells in alginate hydrogel in the shape of films. These films were designed as building blocks for layer-by-layer assembling of hydrogel constructs. MG63 cells were encapsulated exploiting the surface tension of the liquid alginate, subsequently crosslinked in a calcium chloride solution. Hydrogels films are beneficial because their reduced thickness allows nutrients and oxygen to diffuse within the matrix to the encapsulated cells, therefore enabling cells to be cultivated in static conditions. Moreover, hydrogel films can provide a feasible support for either direct or indirect co-cultures systems. Three compounds were evaluated as blending agents to mimic the structural architecture and biological functions of the ECM, thus increasing cell attachment, proliferation and spreading inside the matrix: silk fibroin, collagen type 1, gelatin. The functionality of the cells inside the gel was evaluated in terms of metabolic activity, mitochondrial activity, secretion of vascular endothelial growth factors (VEGFs) and morphology (cytoskeleton/nuclei staining).

Collagen is the most abundant protein in humans, being the main component of the ECM of many tissues, including skin, ligaments, cartilage, tendons and bone. Different classes of collagen exist, the type I being the most abundant and extracted from tissues by enzymatic and acidic treatment. Collagen protein possess a hierarchical structure, and consist of a unique triple helix assembled in a complex supramolecular structure (fig. 31) [5,170].

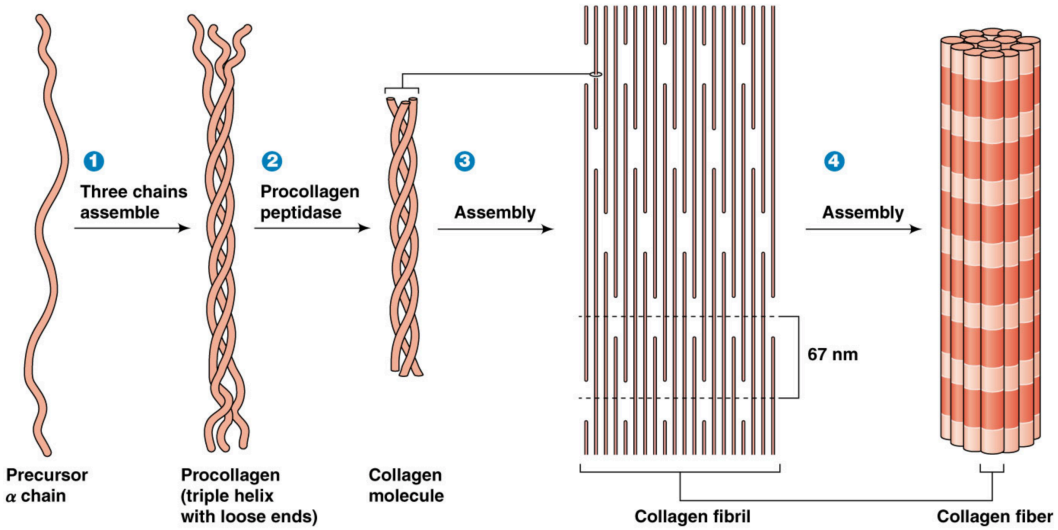

Figure 31. Schematic diagram showing the hierarchical structure of collagen fibers. Three polypeptide strands **(1)** form a right-handed triple helix of collagen **(2)**. These helical molecules furtherly assemble into collagen fibrils **(3)**. Finally, collagen fibrils form as bundles of collagen fibers **(4)**. Adapted from http://www.mun.ca/biology.

Collagen is composed of specific combinations of amino acid sequences that are recognized by cells and can be enzymatically degraded *in vivo*. In particular, the high density of RGD sequences, an important tripeptide for the interaction between a variety of cells and the ECM, facilitate cell adhesion, migration and proliferation when in contact with collagen type I [170]. Because of its biomimetic properties, collagen type I has found many potential applications in tissue engineering, as cell-culture matrix or for the reconstruction of skin, blood vessels, cartilage and bone [5,170].When the liquid solution is neutralized (e.g. with NaOH), collagen self-assemble to form a hydrogel within 30-60 minutes at 37°C. Cells can be encapsulated during the gelation process by mixing them with the neutralized collagen solution and moving the suspension to an incubator [56]. Collagen-based hydrogels are cytocompatible, amenable to cell adhesion without modifications,

and present a native viscoelastic environment to resident cells [3]. Although collagen type I has been used as bioink, it suffers from some important drawbacks including low stiffness, limited long-term stability, slow gelation rate that makes bioprinting of 3D constructs difficult [3,39]. Different collagen-containing hydrogel have been used for biofabrication and cell encapsulation applications and hybrid alginate-collagen blends have been developed to serve as 3D bioprinting bioinks and to incorporate chondrocytes to construct *in vitro* 3D printed cartilage tissue [119].

Gelatin is a soluble protein obtained by partial hydrolysis of collagen. The main sources of gelatin are pig skin, bovine hide, and pork and cattle bones. In order to produce gelatin, the collagen molecules undergo heat and chemical treatments that cleave both covalent and non-covalent bonds thus destabilizing the triple-helix and getting a single-strain water soluble molecule [5]. Gelatin can be dissolved in water by heating the solution above 37°C, as the majority of the polypeptide chain are in a random coil conformation at body temperature. Gelation process (fig. 32) occurs cooling the solution and is based on a coil-to-helix conversion during which the single-strand molecules interact with each other to create helices similar to the collagen triple-helix [171].

Gelatin has been used as a biomaterial because of its biocompatibility, high water-adsorbing ability, non-immunogenicity and degradability [52]. Furthermore, because of its derivation from collagen, gelatin contain cell adhesion motif, which allows cells to recognize and adhere to gelatin-based matrices. As an example, Sarker and colleagues evaluated cell adhesive functionality conferred to alginate hydrogel either by blending or covalently cross-linking with gelatin [97]. The presence of gelatin increased the degree of adhesion, spreading, migration, and proliferation of cell encapsulated in the alginate matrix.

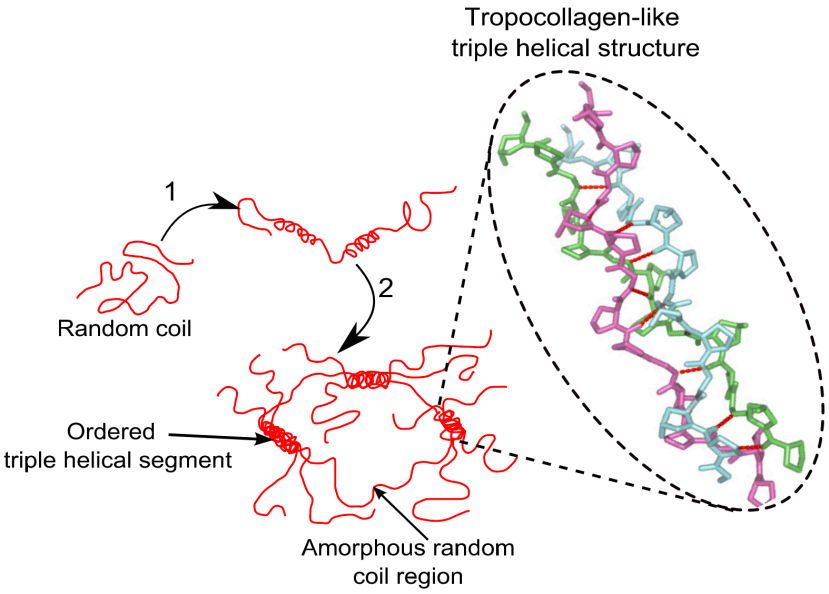

Figure 32. Schematic representation of the gelatin gelation process driven by partial renaturation. When an aqueous gelatin solution is cooled down, the imino acid-rich segments of single-polypeptide chains begin to re-arrange into conformations that are similar to those in the collagen structure (shown in the inset). The 3D network structure is stabilized by lateral inter-chain hydrogen bonding within the helical regions. Adapted from [171].

Silk Fibroin, a fibrous protein derived from *Bombyx mori* cocoons, is characterized by unique mechanical and architectural properties and is thus considered an attractive scaffold material for tissue engineering and cell encapsulation applications [169]. Silks are a class of proteins synthesized by glands of arthropods such as silkworms, spiders, and scorpions. The silk that has been explored more extensively is derived from silkworms (i.e. *Bombyx mori*) [169,172,173]. The larvae *Bombyx mori* uses the silk to prepare to enter the pupal phase enclosing themselves in a cocoon made up of a single silk fiber long around 1.5-2.5 km. The silk fiber is composed of two major protein, silk fibroin (core) and sericin (coating),

a hydrophilic glue-like glycoprotein wrapped around fibroin [173]. Silk fibroin fibers are composed of building blocks of stable anti-parallel β-sheet crystallites held together by hydrogen bond and these hydrophobic domains are linked by small hydrophilic segment, the amorphous domain [173] (fig. 33).

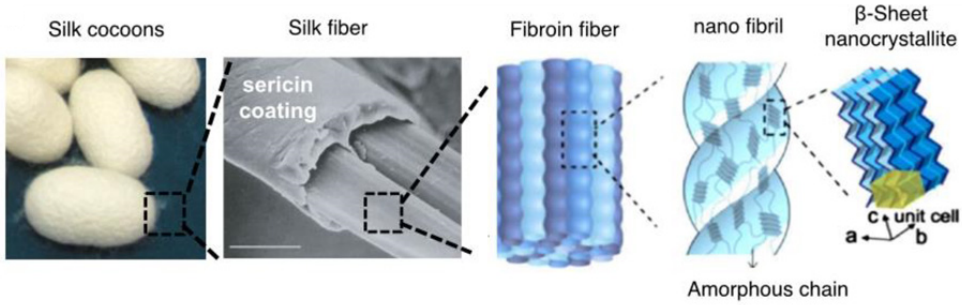

Figure 33. Structure and hierarchical organization of silk fibroin derived from Bombyx Mori. The silk fiber is composed of fibers of fibroin, a structural protein, held together by sericin, adhesive proteins. The fibroin fibers are produced from smaller-diameter nanofibrils made from assembled fibroin proteins. The fibroin proteins fold into a semi-crystalline morphology during spinning, being organized into highly crystalline β sheets and less-ordered domains. Adapted from [174].

Sericin is removed by boiling silk cocoons in alkaline solution (a process called degumming) and the fibroin fibers are dissolved into an aqueous solution that can be further processed into different materials [172]. The silk fibroin water solution is obtained disrupting the β-sheets by dissolution in a high molarity LiBr solution followed by dialysis against water to remove the salts. Li_{2+} and Br_{2+} ions interact with the crystalline region breaking the intermolecular hydrogen bond, which leads to a random coil state. Silk fibroin is water soluble after disruption of the crystalline structure, and forms a transparent solution, forming a gel through the conversion from random coil into β-sheet. The process occurs at lower pH, higher temperatures, and upon mechanical shear, vortexing, exposure to polar

solvents or ultrasonication [173,175]. The gelation rate and the final stiffness are influenced by silk fibroin concentration, pH, temperature, and by parameters with which the fibroin is treated. Cells can be encapsulated during the gel formation, by using mild gelling conditions, such as crosslinking driven by genepin [176].

Silk fibroin is characterized by highly repetitive amino acid sequences that provide to the natural fiber unique mechanical and biological properties [169], in particular the presence of cellular binding motif that could support cellular attachment in a manner similar to the ECM [177]. Due to their excellent biocompatibility and favorable interaction with cells, silk fibroin-based biomaterials have been used for a variety of applications in tissue engineering and biofabrication, including drug delivery, vascular tissue regeneration, wound dressing and bone repair. Silk fibroin sponges can be used as three-dimensional porous scaffold to better mimic the tissue structure and can be formed using salt leaching, gas foaming and freeze-drying methods [173]. Silk fibroin-based scaffolds have been investigated recently to explore their potentials in soft tissue engineering applications such as repairing ligaments, cartilage, primary nerves and skin [121]. Silva and colleagues have reported the development of a hybrid hydrogel by blending alginate and silk fibroin solution in their liquid form and then inducing the gelation of alginate through ionic cross-linking. The combination of the polysaccharide and the protein leads to the formation of a hybrid alginate-based biomaterial, that retains alginate ease of gelation, structural integrity and non-immunogenicity with the addition of biological and adhesive properties of silk fibroin. They used this hybrid hydrogel to fabricate hydrogel substrates and hydrogel microcapsules. The presence of silk fibroin in the blend makes the gel stiffer compared with pure alginate, and improve the cell-adhesive properties of the blend [122,123].

4.3 Materials and Methods

4.3.1 Materials

The following materials were used: *Bombyx mori* silkworm cocoons (purchased from Chul Thai Silk Co., Phetchabun, Thailand); sodium alginate powder derived from brown algae, calcium chloride dihydrate, 0.05% Triton X-100, gelatin from porcine skin, Cell Counting Kit-8 (CCK-8) (Sigma-Aldrich, USA); collagen I from rat tail, VEGF Human ELISA Kit, DAPI (4',6-Diamidino-2-Phenylindole, Dihydrochloride), Alexa Fluor™ 568 Phalloidin (ThermoFisher, USA); phosphate buffered saline (PBS), Minimum Essential Media (MEM), 200 mM L-glutamine, 100 mM sodium pyruvate, 100× MEM Non-essential Amino Acids, 100× Antibiotic-Antimycotic solution, 0.05% Trypsin-EDTA solution; Fetal Calf Serum, Trypan Blue 0.4% solution (Lonza, Switzerland); MG63 osteosarcoma cell line (ATCC® CRL-1427™) (Istituto Zooprofilattico Sperimentale della Lombardia e dell'Emilia Romagna, Italy); Sonicator (UP400S Heilscher, Germany);

4.3.2 Hydrogels preparation and sterilization

Alginate. Alginate powder was dissolved in PBS overnight at room temperature to obtain a 2.5% (wt/vol) alginate solution. The crosslinking solution consisted in calcium chloride dihydrate dissolved in distilled water at a concentration of 200 mM. For sterilization, the two solutions were filtered through a 0.22-μm filter before use.

Silk-fibroin. Silk fibroin was extracted from *Bombyx mori* silkworm cocoons with standard protocol (fig. 34). Initially, silkworm cocoons were cut and cleaned from debris and larvae. In order to remove the sericin content, the cocoons were degummed by immersing them at concentration of 10 g/L in a Na_2CO_3 solution of 1.1 g/L at 98°C for 1h 30min, and then in a Na_2CO_3 solution of 0.4 g/L at 98°C for

1h 30min. The obtained silk fibers were dried at RT for 2 days. Silk fibroin fibers were then dissolved at a concentration of 20 g/100mL in a solution of lithium bromide 9.3 M at 60°C for 4h. The obtained solution was placed in a dialysis cassette with a cellulose membrane (35000 MW), and immersed for 5 days in distilled water at RT. The water was changed at regular intervals of time, three times per day. Subsequently, the cassette was transferred in PBS solution for 24 hours. The resulting solution was then filtered through a 0.22 µm filter under sterile conditions with a syringe. Silk fibroin concentration of the solution was assessed with a spectrophotometer measurement (NanoDrop, nd-1000). The final concentration was finally adjusted to 3% (wt/vol).

Gelatin. Gelatin from porcine skin was dissolved in DI water at 37°C under mild stirring for 1 h to obtain a 3% (wt/vol) gelatin solution. The solution was then autoclaved.

Alginate-based hydrogel precursors were prepared as follows (fig. 35):

- **Alginate-collagen type I blend (ALG-COL)** was obtained by mixing 1 mL sterile collagen I from rat tail with 4 mL sterile alginate solution on ice and adjusting the pH by adding 0.025 µL of NaOH (2% (wt/vol) final concentration of alginate, 0.6% (wt/vol) final concentration of collagen).
- **Alginate-silk fibroin blend (ALG-SF)** was obtained by mixing 1 mL freshly prepared silk-fibroin solution with 4 mL sterile alginate solution (2% (wt/vol) final concentration of alginate, 0.6% (wt/vol) final concentration of silk fibroin).
- **Alginate-gelatin blend (ALG-GEL)** was obtained by mixing 1 mL of freshly prepared gelatin solution with 4 mL sterile alginate solution at 37°C (2%

(wt/vol) final concentration of alginate, 0.6% (wt/vol) final concentration of gelatin).

- **Alginate (ALG)** was obtained by mixing 1 mL of PBS with 4 mL sterile alginate solution (2% (wt/vol) final concentration of alginate).

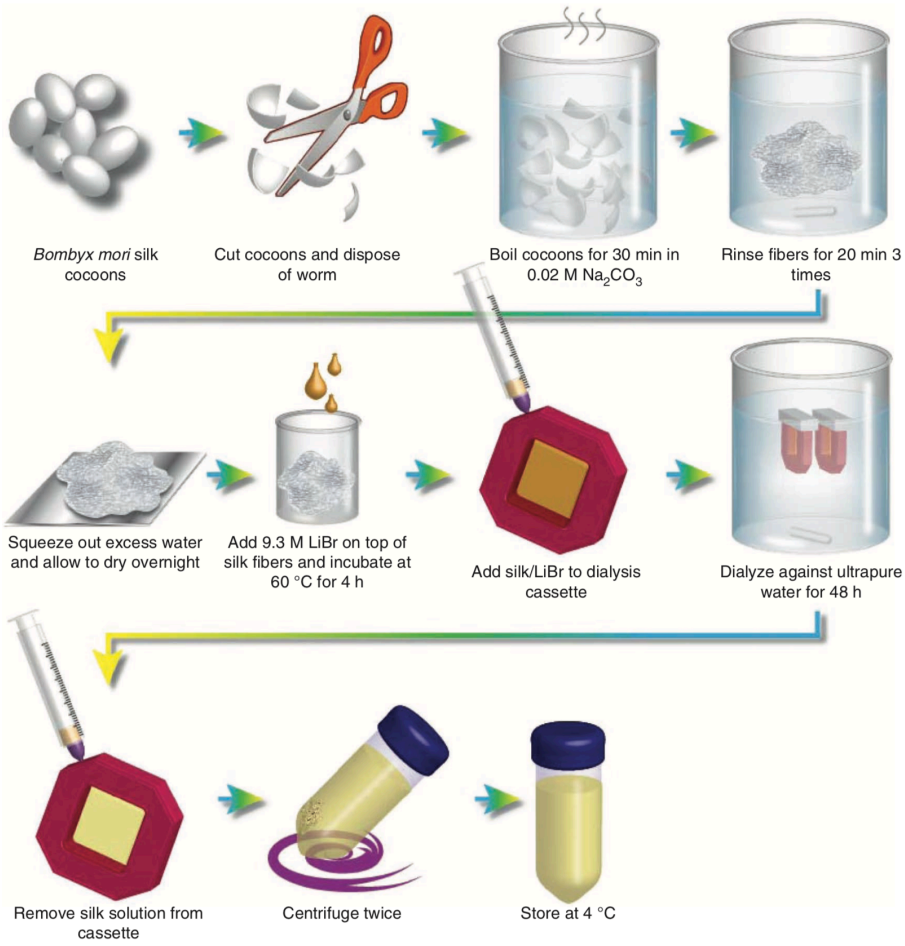

Figure 34. Schematic of the silk fibroin extraction procedure. Going from the raw material (cocoons) to the final aqueous-based solution took 10 days. Note that some steps have been modified to adapt to experimental needs. Adapted from [172].

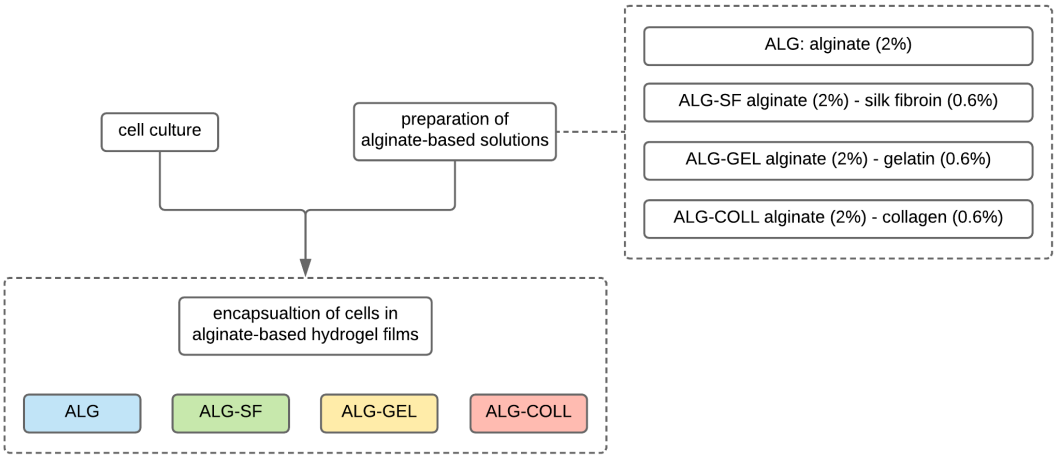

Figure 35. Summary of the produced samples and the different materials that were used.

4.3.3 Cell culture and encapsulation

MG63 osteosarcoma cells were thawed and expanded using standard protocols. In particular, cells were expanded in tissue-culture treated flasks as monolayer at 37°C under 5% CO_2 to 85-90% confluence before encapsulation. Culture medium was composed of MEM containing 10% fetal bovine serum (GIBCO), 2mM glutamine, 1 mM sodium pyruvate, 1% non-essential amino acids and 1% Antibiotic Antimycotic solution. At sub-confluence cells were detached from the flask with the Trypsin solution. Subsequently, cells were centrifuged at 1000 rpm for 10 minutes, rinsed in PBS to remove any residues of culture medium and finally dispersed by vortexing inside the buffer. An aliquot of the suspension was used to determine cells concentration using a hemocytometer (Sigma, USA) and Trypan Blue 0.4% as contrasting agent. Cells were centrifuged again and, after removing the supernatant, resuspended in the proper amount of alginate-based solution to obtain a suspension containing 4×10^6 cells/mL.

Cells were encapsulated in alginate films through a single-step process under a laminar-flow hood (fig. 36). A stainless-steel ring with inner diameter 10 mm was autoclaved, immersed in ethanol and rinsed in DI water. The ring was then immersed in one of the alginate-based solution containing cells and immediately extracted and immersed in the crosslinking solution containing calcium ions for about 10 seconds, causing the cell entrapment into the already gelled thin disk. The film was then detached from the metal ring with the aid of metal autoclaved tweezers and transferred to a TCP. After few minutes, crosslinking solution was discharged and fresh medium was added in each well to cover the films. The samples were then incubated at 37 °C with 5 % CO_2.

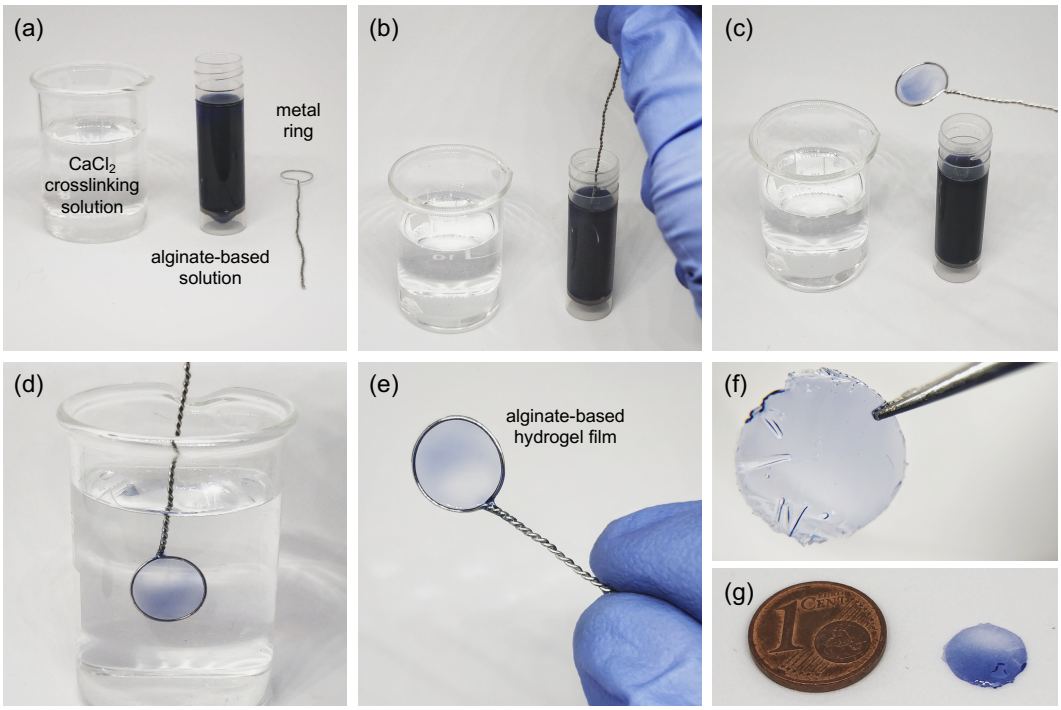

Figure 36. Formation of the alginate-based films containing cells. A representative alginate-based solution has been stained blue **(a)**. A stainless-steel ring is immersed in the alginate blend solution **(b)** and, when extracted, a film is formed inside the

ring due to surface tension **(c)**. The ring is then immersed in the crosslinking solution containing calcium ions **(d)** for 10 second and, when extracted, the film gelates inside the ring **(e)**. The film is finally removed from the ring with the aid of tweezers **(f)**. Representative image of the dimensions of the film **(g)**.

4.3.4 *In vitro* evaluation

In vitro evaluations were performed on encapsulated cells up to 14 days. During this time, the alginate-based hydrogel films containing cells were cultured in 48 well-plates. The complete scheme of the experiments is reported in fig. 37.

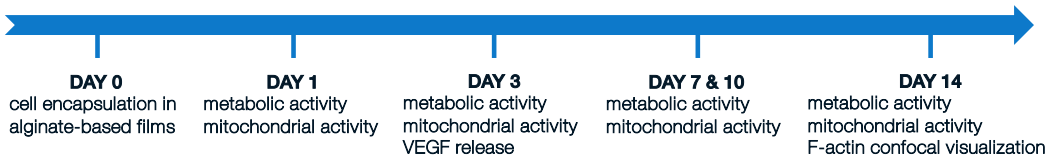

Figure 37. Schematic of the performed assays and relative time points.

Cells metabolic activity. At different time points after cell encapsulation (1, 3, 7, 10 and 14 days), the metabolic activity of the encapsulated cells was evaluated with alamarBlue assay, which uses the reducing power of healthy cells to convert resazurin to the fluorescent molecule resorufin. The alginate-based films containing cells were incubated for 2 h in the dark with culture medium containing 10% alamarBlue. Subsequently, 100 L of supernatant from each sample was transferred into a well of a 96 well-plate and fluorescence intensity was measured in triplicate on a plate reader (535±25 nm excitation and 590±20 nm emission; Spark 10M, Tecan, Switzerland).

Cells mitochondrial activity. At different time points after cell encapsulation (1, 3, 7, 10 and 14 days), the mitochondrial activity of the encapsulated cells was evaluated with Cell Counting Kit-8 (CCK-8) through the enzymatic conversion of

tetrazolium salt. The water-soluble tetrazolium salt, WST-8, is bioreduced by cellular dehydrogenases to an orange-color formazan product that is soluble in tissue culture medium. The amount of the formazan dye, generated by the activities of dehydrogenases in cells, is directly proportional to the number of living cells. At the different time points, culture media were completely removed from the samples and freshly prepared culture medium containing 10 % (v/v) CCK-8 assay kit was added, followed by incubation for 2 h in the dark. Subsequently, 3x100 μL of supernatant from each sample was transferred into a 96 well-plate absorbance measurement at 450 nm with a microplate reader (Spark 10M, Tecan, Switzerland)

VEGF release. Vascular endothelial growth factor (VEGF) secretion from the encapsulated cells was measured by performing a quantitative solid-phase sandwich Enzyme-Linked Immunosorbent Assay (Human VEGF ELISA Kit) using the culture medium as substrate. 24 and 72 h after cell encapsulation, the culture medium was collected and stored up to −20°C before assaying according to manufacturer's instructions. Subsequently, the total VEGF secreted in the first 3 days from the cells encapsulated in the different alginate-based hydrogel film was evaluated with the ELISA method. This assay requires a compatible antibody pair that recognize different antigenic targets (epitopes) on the same antigen. The first antibody, VEGF-165 called capturing antibody, was coated on a plate and used to immobilize the VEGF upon binding during incubation with the sample. Free proteins were removed by a washing step and then a biotinylated detecting antibody was added to bind to a second epitope-binding site on the VEGF. After washing away unbound biotinylated antibody, horseradish peroxidase (HRP)-conjugated streptavidin was pipetted to the wells. The wells were washed again, a Tetramethylbenzidine (TMB) substrate solution was added to the wells and colorimetric signal developed in proportion to the amount of target protein bound. The Stop Solution changed the color from blue to yellow, and the optical density of

each well was determined using a microplate reader (Spark 10M, Tecan, Switzerland) at 450 nm test wavelength (550nm used as reference). A calibration curve was built up using the VEGF standard provided with the assay to correlate absorbance intensity to VEGF concentration. For each test nine replicates were used.

Evaluation of cell morphology and distribution. After 14 days of culture, cell distribution was evaluated by staining the samples with Alexa Fluor™ 568 Phalloidin and DAPI (4',6-diamidino-2-phenylindole), which selectively binds to cytoskeleton F-actin and nuclei respectively. The alginate-based films containing cells were washed twice with PBS and then fixed in 4% paraformaldehyde (PFA) for 20min at room temperature. After washing twice with PBS, the samples were stored at 4°C overnight. Subsequently, cell membranes were permeabilized with Triton X-100 (Sigma-Aldrich, USA) solution (0.2 % in PBS) for 30 min and then washed twice in PBS. For the staining, a solution of DAPI (300 nM in PBS) and Alexa Fluor™ 568 Phalloidin (5 µL of stock solution for each sample) was added to the samples and stored for 30 minutes at room temperature in the dark. The samples were then washed twice with PBS and the images were acquired through a confocal microscope (Nikon A1, Japan). The cytoskeletons fluoresce red since Alexa Fluor™ 568-conjugated Phalloidin selectively label F-actin. DAPI binds strongly to A-T rich regions in DNA, thus staining blue the cell nuclei. Confocal images were collected along the Z-axis with 10 µm intervals (405 nm excitation, 460/10 emission for DAPI; 560 nm excitation and 595/25 emission for Alexa Fluor™ 568 Phalloidin).

Statistical analysis. Graphpad Prism 7 software was used for statistical analysis. Results are expressed as mean ± standard deviation (SD) and significance was tested using two-way analysis of variance with Tukey's *range* test. A p value of 0.05 was considered significantly different.

4.4 Results and discussion

Cell-compatibility of materials used for encapsulating cells critically affects the subsequent fate of biofabricated and assembled constructs. Therefore, soft materials that support cell attachment, proliferation, and function are needed for cell encapsulation in novel applications for regenerative medicine applications. Pure alginate hydrogel has been proved to be a suitable material for micro-encapsulation, as it provides an aqueous environment necessary for nutrients and metabolites exchange. However, it does not promote cell adhesion and often does not support cell proliferation and metabolic function. Modification of the hydrogel composition by adding different molecules such as native protein components or peptide sequences is thus expected to improve biocompatibility of alginate-based matrices. In fact, incorporation of cell-adhesion ligands enables cell-matrix interactions and leads to an increased cell functionality and matrix remodeling [81,122]. The most widely investigated method for alginate modification has been the incorporation of bioactive molecules, such as gelatin and RGD (Arg-Gly-Asp) sequence, into oxidized alginate. However, the chemical modification process involves several steps, being relatively expensive and time consuming.

In this work, we present an innovative method to fabricate alginate-based hydrogel films containing cells by exploiting the surface tension of liquid alginate. This strategy could enable culturing multiple cell types in different films, controlling the molecular distribution of the bioactive molecules within the matrix, and the subsequent stack of the films in order to obtain ticker constructs. The films can be used as feasible support for assembling constructs containing multiple type of cells, since the specific geometry of the films is suitable for 3D/3D co-culture and for hybrid 2D/3D co-culture. Furthermore, the multi-cellular system can be spatially and temporally modulated, in order to cultivate cells directly in the same

construct or indirectly by enabling the solely interaction via soluble factors. Ultimately, this strategy can be useful to study the interaction between different cell types as well as to manufacture complex tissue models in order to test drugs and therapeutics. As an example, a functional 3D layered model could be beneficial to probe multi-layered neural circuits, enabling a better understanding of traumatic brain injuries (TBI) as well as performing preliminary evaluation of new therapeutic treatments[30]. As an example, the engineering of functional skin requires stratified skin cellular structures that are crucial for the regeneration of cell-to-cell and cell-to-extracellular matrix interactions. Therefore, three-dimensional (3D) organotypic reconstruction of multiple skin layers has been suggested for skin repair and to model progresses of skin diseases or damages [46]. Moreover, hydrogel-based constructs in the shape of film are beneficial as cardiac patch [178] and as support for cell-sheets technique [179].

MG63 cells, an established osteoblast-like cell line for bone tissue engineering models with fully genetic characterization, were encapsulated in the films [151]. In order to support proliferation and functionality of the encapsulated cells, different nature derived proteins were incorporated during hydrogels formation. The experimental campaign focused on the evaluation of the effect of the different hydrogels, in order to identify the best formulation in terms of cell proliferation, metabolic activity, adhesion and functionality. In particular, as osteoblast have been widely used in combination with endothelial cells for bone tissue engineering applications, the secretion of VEGFs was investigated [81].

When immersed in the alginate-based solution containing cells, a thin film formed within the metal ring due to surface tension. Upon immersing the ring in the crosslinking solution containing calcium ions, the solution gelled thus entrapping the cells inside the film. Cells appeared homogeneously distributed inside the films. The mean thickness of the films, measured by optical microscopy,

is 248±13 μm (n=9), which is compatible with nutrients diffusion in presence of high cell densities [27]. In fact, according to the *in vitro* measurements in 3D spheroids, reported by Gasperini *et al*. an oxygen diffusion limit of 250 μm was observed experimentally, indicating that the encapsulated cell behavior was unlikely influenced by hypoxia and the differences between pure alginate and alginate/protein hydrogel films resulted from the presence of the proteins [27]. Importantly, a single hydrogel film containing cells is sufficiently strong mechanically that it can be easily manipulated and stacked into multiple-layer constructs to generate 3D cultures. Therefore, it is possible to assemble 3D cultures of cells controlling the properties of the construct at the μm length scale.

4.4.1 Cell metabolic activity

Quantitative assessment of the metabolic activity of MG63 cells encapsulated in alginate-based hydrogel films over 14 days of incubation is shown in figure 38. The absolute values show a growth trend of cell metabolic activity during all the 14 days of the experiment (fig. 38 a). At each time point the cells of the ALG-SF group are those that exert the greatest metabolic activity, followed by those of the ALG-GEL, ALG-COL and ALG group. Observing the normalized data compared to the samples containing only alginate (fig. 38 b), it is highlighted that one day after cell encapsulation there is the maximum difference between the groups (increment of 282±22 % for ALG-SF, 239±13 % for ALG-GEL, 149±19 % for ALG-COL). By increasing the incubation period, the difference between the groups tends to decrease, and in fact at day 14 all the samples containing proteins in the gel have a comparable cellular metabolic activity value. However, a statically significant difference with respect to samples containing only alginate persists (increment of 162±11 % for ALG-SF, 154±3 % for ALG-GEL, 151±2 % for ALG-COL).

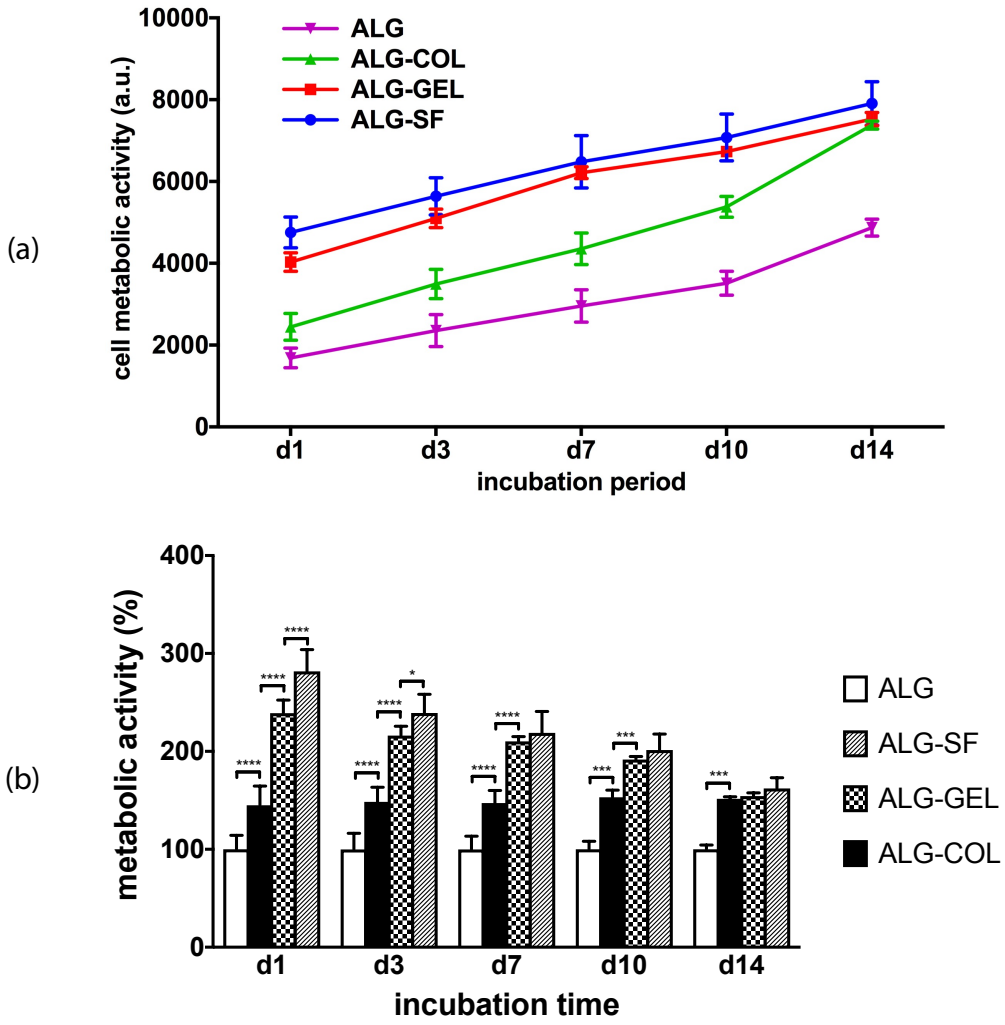

Figure 38. Metabolic activity of MG63 cells after 1, 3, 7, 10 and 14 days of incubation, encapsulated in alginate (ALG), alginate-collagen (ALG-COL), alginate-gelatin (ALG-GEL), alginate-silk fibroin (ALG-SF). **(a)** Total values **(b)** Fold change relative of pure alginate (ALG) values. Error bars represent standard deviation (n = 7). *p < 0.05, ***p < 0.001 and ****p < 0.0001.

This behavior can be explained by the formation of cell-matrix contacts in the hydrogel film in presence of proteins, leading to more functional cells immediately after encapsulation. However, since the proteins had not been covalently linked to

the polysaccharide matrix, part of the bioactive molecules is released from the gel during incubation, thus justifying the reduction of the difference between the groups in the long term. Moreover, since the different proteins have different diffusive capacities within the hydrogel matrix, the functionality of the cells can be explained in quantitative terms as well as for the different effect that the bioactive molecules have in establishing cell-matrix contacts.

4.4.2 Cell mitochondrial activity

Quantitative assessment of the mitochondrial activity of MG63 cells encapsulated in alginate-based hydrogel films over 14 days of incubation is shown in figure 39. Mitochondrial activity is an important aspect of normal cellular function, playing an important role in cell proliferation, apoptosis or cell death and hence in regulation of the cellular functions [123]. The absolute values show a growth trend of cell metabolic activity during all the 14 days of the experiment (fig. 39 a), and these results are in accordance with the above described results of the metabolic activity. In fact, at each time point the cells of the ALG-SF group are those that exert the greatest metabolic activity, followed by those of the ALG-GEL, ALG-COL and ALG group. According to the normalized data compared to the samples containing only alginate (fig. 39 b), the maximum difference between the groups was detected one day after cell encapsulation (increment of 331±69 % for ALG-SF, 252±38 % for ALG-GEL, 112±15 % for ALG-COL). After 14 days of incubation, the mitochondrial activity of cells immobilized in presence of proteins was significantly higher compared to those grown in the pure alginate constructs (increment of 175±10 % for ALG-SF, 161±6 % for ALG-GEL, 120±10 % for ALG-COL).

(a)

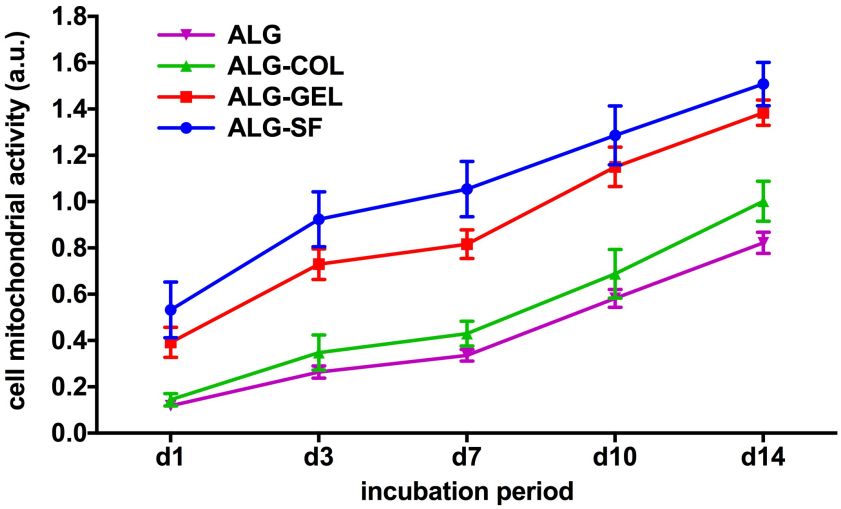

(b)

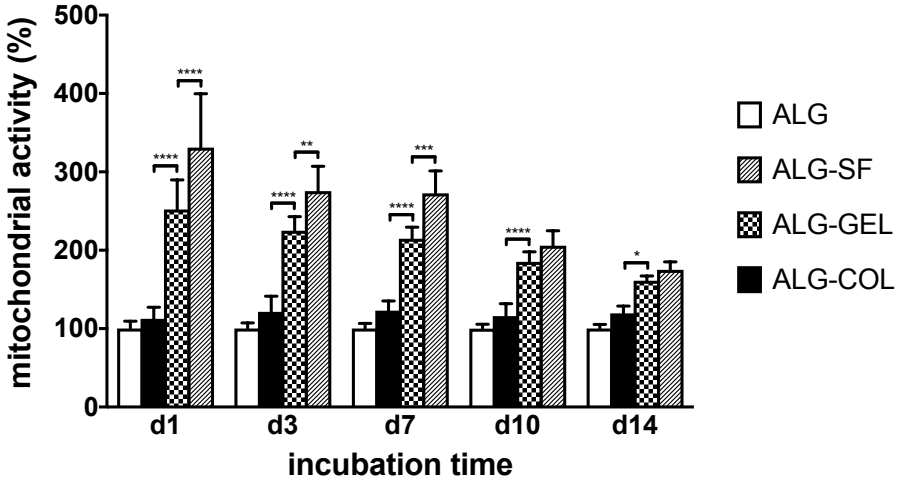

Figure 39. Mitochondrial activity of MG63 cells after 1, 3, 7, 10 and 14 days of incubation, encapsulated in alginate (ALG), alginate-collagen (ALG-COL), alginate-gelatin (ALG-GEL), alginate-silk fibroin (ALG-SF). **(a)** Total values **(b)** Fold change relative of pure alginate (ALG) values. Error bars represent mean ± SD (n = 7). *$p < 0.05$, **$p < 0.01$, ***$p < 0.001$ and ****$p < 0.0001$.

4.4.3 VEGF release

In figure 40, the VEGFs release from MG-63 cells encapsulated in alginate-based hydrogel after 72 h of cultivation is shown. Numerous studies have demonstrated the critical role of vascularization in successful tissue integration during bone fracture repair. VEGF is well known as an effective endothelial cell-specific stimulus, that can regulate endothelial tube assembly through a local paracrine effect. It is constitutively expressed by osteoblast and osteoblast-like cells (e.g. MG63), thus playing a fundamental role in cell-to-cell communication between osteogenic and endothelial lineages during the vascularization process of bone-tissue engineered constructs [73,164,180]. The release of VEGF from immobilized cells in soft matrices should correlate with the observed increased in the angiogenic potential of such constructs [181,182]. The amount of expressed VEGF in cells immobilized in a hydrogel constructs could depend on the chemical composition of the matrix as well as on the micro-environmental conditions (cell density, diffusion of oxygen and nutrients, presence and concentration of other regulating factors in the culture medium) [81]. According to the present study, enhanced VEGF secretion from osteoblast-like cells was measured in the cell culture medium from alginate-protein matrices over 3 days of cultivation compared with pure alginate films. In particular, significantly higher VEGF secretion was measured in the cell culture medium from cells encapsulated in presence of silk fibroin and gelatin (increment of 264±44 % for ALG-SF, 246±33 % for ALG-GEL, 160±18 % for ALG-COL).

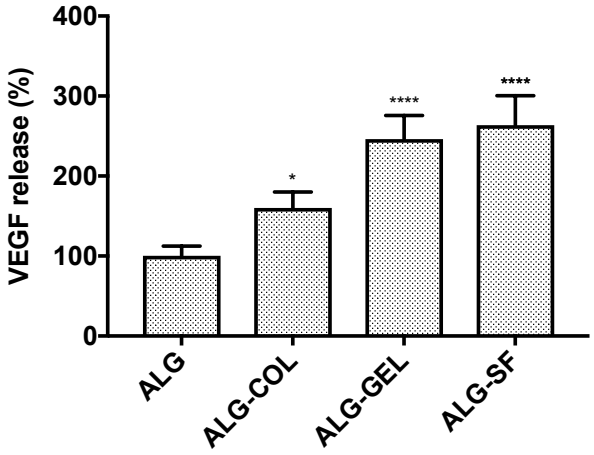

Figure 40. Vascular endothelial growth factor released from MG-63 cells immobilized in alginate-based hydrogel films after 72 h of incubation: alginate (ALG), alginate-collagen (ALG-COL), alginate-gelatin (ALG-GEL), alginate-silk fibroin (ALG-SF). Fold change relative of pure alginate (ALG) values *$p<0.05$, ****$p<0.0001$ compared with ALG.

These results confirm those that emerged from the analysis of cell metabolic and mitochondrial activity, and the observed VEGF release profile can be explained by the increased activity of the cells, triggered by the presence of cell-matrix adhesion sites. In fact, other studies have shown a direct correlation between cell viability and metabolic activity with an increased secretion of VEGF from osteoblast like-cells, as for example Grigore *et al.* who evaluated the used of alginate-gelatin and alginate-RGD matrices to encapsulate MG63 cells [81].

4.4.4 Cell morphology and distribution

The morphology of MG63 cells entrapped in alginate-based hydrogel films was studied by fluorescent staining with Alexa Fluor™ 568 Phalloidin and DAPI, 14 days after encapsulation. Cell distribution in 3D was examined using confocal

microscopy and the resulted images are reported in fig. 41. Cells were found to be uniformly distributed through the whole film in all four hydrogel formulation films. We observed that cells entrapped in pure alginate hydrogel maintained a spherical morphology. Even cell clusters, which identify cell proliferation sites, were seen to be spherical, in accordance to our expectations considering the poor adhesion-capacity of alginate. The addition of collagen to the alginate did not provide any improvement in the cell-proliferation capacity of the hydrogel, confirming the result of cell mitochondrial activity. However, alginate-collagen promoted the protrusion of small actin filaments in the surrounding matrix, even if cells maintained their spherical shape. Cells encapsulated in alginate-gelatin and alginate-silk fibroin displayed multiple elongated protrusion and even formation of cell-cell contact over distance of 100 μm. Significantly more cells were found in these films, thus suggesting that SF and gelatin can provide a proliferation-supporting environment for osteoblast-like cells. These findings are in accordance to the cell mitochondrial activity data, showing that both cell–material and cell–cell contacts lead to increased cell viability. Cells immobilized in presence of gelatin formed compact aggregates while, on the contrary, cells encapsulated in presence of silk fibroin tend to form randomly shaped clusters and cell chains.

These results suggest that silk fibroin can provide a suitable anchorage and a growth-supporting environment for these osteoblast-like cells, as the initial attachment of cells promotes cell survival and plays a role in regulation of cell function and signaling [81,97]. Nevertheless, it is worth mentioning that the elongation of the cell clusters observed in the hydrogel formulations containing proteins is not a sign of strong cell–matrix adhesion. By contrast, different groups observed that the cross-linking of alginate with proteins or bioactive peptide sequences facilitated a better cell adhesion, as they noticed better cell spreading and migration in comparison to the alginate-proteins blends [97].

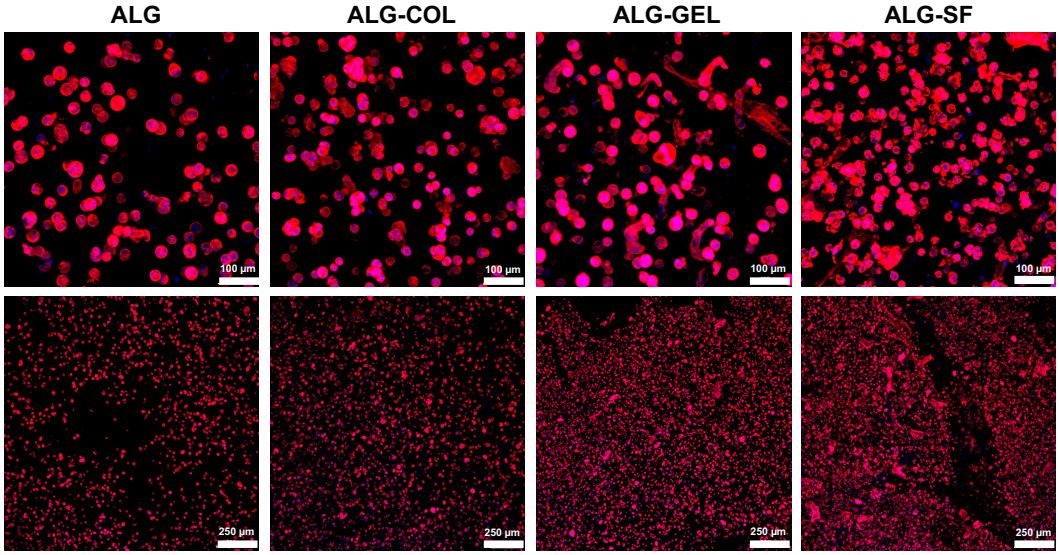

Figure 41. Confocal microscopy of MG-63 cells immobilized in alginate-based hydrogel films after 14 days of incubation: alginate (ALG), alginate-collagen (ALG-COL), alginate-gelatin (ALG-GEL), alginate-silk fibroin (ALG-SF). Cells were stained for the F-actin cytoskeleton with Alexa Fluor™ 568 Phalloidin (red) and nuclei with DAPI (blue). All scale bars are 100 µm **(top images)** or 250 µL **(bottom images)**.

Gathering these results, it is possible to conclude that alginate-silk fibroin blend presents superior MG63 cell compatibility compared to pure alginate and alginate blended with collagen. After 14 days of incubation, the behavior in terms of metabolic and mitochondrial activity was comparable with cells encapsulated in alginate-gelatin gel, but in the case of silk fibroin cells presented more randomly shaped clusters thus suggesting the presence of an environment more favorable to cell adhesion. Interestingly, the release of VEGF from cells encapsulated in ALG-SF within the first 3 days of incubation suggests that this matrix, in combination with osteoblast or osteoblast-like cells, may provide a support for vascular tissue regeneration applications. In fact, VEGFs are well known as a regulatory signal for

endothelial tube assembly. In future studies, endothelial cells could be used in combination with osteoblast cells in order to validate the use of alginate-based films as matrices that support vascularization. Further studies will be necessary to evaluate the cell–cell and cell–material interactions of the endothelial cells after film formation process, as well as the mechanical stability and behavior of such constructs. Alternative interesting applications include cell delivery and 3D models for cell culture and drug screening. Furthermore, the proposed geometry can serve as support for manufacturing cell-sheet in order to facilitate handling and assembly procedure [17].

Several challenges should be addressed before hydrogel film-based tissue constructs can be used in biofabrication approaches for regenerative medicine. Different methods to manipulate and stack multiple films must be evaluated, as well as the use of bioreactors in order to support a biologically active environment within multiple-layered constructs. The physico-mechanical properties of the films should also be determined to understand the *in vitro* degradation mechanism. Moreover, the mechanical properties of hydrogels itself should be improved by, for example, the creation of nanocomposites with nanoscale inorganic fillers. In addition, the degradation of cross-linked materials should be adapted to the in-situ formation of ECM. The adoption of these materials for biofabrication procedures – for example, cell printing processes – to create hierarchically and intra-complex porous architectures for tissue mimicking constructs, should be further investigated.

4.5 Future Directions

Future work will focus on the integration of the proposed matrices, containing osteoblast-like cells (OBs), with endothelial cells (ECs) in order to develop vascularized constructs.

Initially, Human Umbilical Vein Endothelial Cells (HUVECs) will be used as cell line model for endothelial cells. Different cell seeding strategies for the two cell populations will be evaluated, ranging from seeding the cells together in the same film to developing hybrid 2d-3d matrices (one cell line encapsulated within the film and the other seeded on top of it). In fact, MG63 cell-laden films should act as a biological substrate for HUVECs adhesion and promote their proliferation and organization in capillary-like networks, due to the release of proangiogenic factors. The ability of the two cell lines to cross-talk by paracrine signaling and cell-to-cell contacts will be characterized. As an example, ELISA assay and gene expression PCR will be used to assess the expression and release of paracrine molecules that can trigger the expression of gene markers for the bone tissue and for neo-angiogenesis processes.

Subsequently, multiple alginate-based hydrogel building blocks containing ECs and OBs will be stacked layer-by-layer to generate pre-vascularized constructs that can serve for bone tissue engineering or as a bone unit model. In this framework, the ability of different films to self-assemble and the ability of cells to migrate within the assembled constructs will be evaluated. Finally, assembled constructs might be moved to a perfusion bioreactor in order to ensure the oxygen supply and physical cues to the cells during the initial phases of tissue maturation.

The composition of the alginate-based hydrogel matrix, the cell seeding strategy and the parameters for cultivating cell-laden films and the assembled constructs will be tuned and adapted according to the obtained results.

4.6 Conclusions

In the present study, an innovative method to manufacture micrometer-thickness films containing living cells has been proposed. This technique potentially enables the biofabrication of multiple-layer constructs composed of different layers, each of them designed to maximize the compatibility with the encapsulated cell type. Moreover, the proposed geometry can be adapted as support for manufacturing constructs containing multiple cell types according to different direct and indirect methods. Potentially, this technique can be used to biofabricate clinically-relevant sized soft tissue models with complex and multi-cellular structures. In order to improve cell behavior, the current study has proposed the use of alginate blended with protein solutions (collagen, gelatin, silk fibroin) for cell microencapsulation.

The results of our comparative analysis demonstrated that overall best compatibility with osteoblast-like MG63 cells was observed for silk fibroin-containing alginate hydrogel, which promoted cell attachment, growth, and functionality. In particular, the incorporation of silk fibroin within the matrix promoted the secretion of VEGFs from the encapsulated cells. The proposed hybrid hydrogel thus represents a promising candidate for supporting the fabrication of vascularized cell-laden hydrogel constructs. Further studies will investigate the use of other material combinations and their applicability as soft matrices for more complex biofabrication approaches and different areas of tissue engineering.

References

[1] B. M. Baker and C. S. Chen, "Deconstructing the third dimension – how 3D culture microenvironments alter cellular cues" *J. Cell Sci.*, vol. 125, no. 13, pp. 3015–3024, 2012.

[2] M. W. Tibbitt and K. S. Anseth, "Hydrogels as extracellular matrix mimics for 3D cell culture" *Biotechnol. Bioeng.*, vol. 103, no. 4, pp. 655–63, Jul. 2009.

[3] S. R. Caliari and J. A. Burdick, "A practical guide to hydrogels for cell culture" *Nat. Methods*, vol. 13, no. 5, pp. 405–414, Apr. 2016.

[4] A. S. Hoffman, "Hydrogels for biomedical applications" *Adv. Drug Deliv. Rev.*, vol. 64, pp. 18–23, Dec. 2012.

[5] L. Gasperini, J. F. Mano, and R. L. Reis, "Natural polymers for the microencapsulation of cells" *J. R. Soc. Interface*, vol. 11, no. 100, pp. 20140817–20140817, Sep. 2014.

[6] N. a. Peppas, J. Z. Hilt, A. Khademhosseini, and R. Langer, "Hydrogels in biology and medicine: from molecular principles to bionanotechnology" *Adv. Mater.*, vol. 18, no. 11, pp. 1345–1360, Jun. 2006.

[7] B. V Slaughter, S. S. Khurshid, O. Z. Fisher, A. Khademhosseini, and N. a Peppas, "Hydrogels in regenerative medicine" *Adv. Mater.*, vol. 21, no. 32–33, pp. 3307–29, Sep. 2009.

[8] G. D. Nicodemus and S. J. Bryant, "Cell encapsulation in biodegradable hydrogels for tissue engineering applications" *Tissue Eng. Part B. Rev.*, vol. 14, no. 2, pp. 149–65, Jun. 2008.

[9] H. Zimmermann, F. Ehrhart, D. zimmermann, K. Müller, A. Katsen-Globa, M. Behringer, P.J. Feilen, P. Gessner, G. Zimmermann, S.G. Shirley, M.M.

Weber, J. Metze and U. Zimmermann, "Hydrogel-based encapsulation of biological, functional tissue: Fundamentals, technologies and applications" *Appl. Phys. A Mater. Sci. Process.*, vol. 89, no. 4, pp. 909–922, 2007.

[10] J. A. Hunt, R. Chen, T. van Veen, and N. Bryan, "Hydrogels for tissue engineering and regenerative medicine" *J. Mater. Chem. B*, vol. 2, no. 33, pp. 5319–5338, 2014.

[11] A. Atala, "Engineering tissues, organs and cells" *J. Tissue Eng. Regen. Med.*, vol. 1, no. 2, pp. 83–96, Mar. 2007.

[12] A. Khademhosseini and R. Langer, "Microengineered hydrogels for tissue engineering" *Biomaterials*, vol. 28, no. 34, pp. 5087–92, Dec. 2007.

[13] R. Langer and J. Vacanti, "Tissue engineering" *Science (80-.).*, vol. 260, no. 5110, pp. 920–926, May 1993.

[14] A. Atala, "Engineering organs" *Curr. Opin. Biotechnol.*, vol. 20, no. 5, pp. 575–92, Oct. 2009.

[15] T. Dvir, B. P. Timko, D. S. Kohane, and R. Langer, "Nanotechnological strategies for engineering complex tissues" *Nat. Nanotechnol.*, vol. 6, no. 1, pp. 13–22, Jan. 2011.

[16] F. Pati, J. Gantelius, and H. A. Svahn, "3D Bioprinting of tissue/organ models" *Angew. Chemie Int. Ed.*, vol. 55, no. 15, pp. 4650–4665, Apr. 2016.

[17] B. Guillotin and F. Guillemot, "Cell patterning technologies for organotypic tissue fabrication" *Trends Biotechnol.*, vol. 29, no. 4, pp. 183–190, Apr. 2011.

[18] J. Nichol and A. Khademhosseini, "Modular tissue engineering: engineering biological tissues from the bottom up" *Soft Matter*, vol. 5, no. 7, p. 1312, Jan. 2009.

[19] D. L. Elbert, "Bottom-up tissue engineering" *Curr. Opin. Biotechnol.*, vol. 22, no. 5, pp. 674–680, 2011.

[20] V. Mironov, T. Trusk, V. Kasyanov, and S. Little, "Biofabrication: a 21st

century manufacturing paradigm" *Biofabrication*, vol. 1, no. 2, p. 22001, Jun. 2009.

[21] C. J. Ferris, K. G. Gilmore, G. G. Wallace, and M. In het Panhuis, "Biofabrication: an overview of the approaches used for printing of living cells" *Appl. Microbiol. Biotechnol.*, vol. 97, no. 10, pp. 4243–58, May 2013.

[22] S. Guven, P. Chen, F. Inci, S. Tasoglu, B. Erkmen, and U. Demirci, "Multiscale assembly for tissue engineering and regenerative medicine" *Trends Biotechnol.*, vol. 33, no. 5, pp. 269–279, May 2015.

[23] C. Mandrycky, Z. Wang, K. Kim, and D.-H. Kim, "3D bioprinting for engineering complex tissues" *Biotechnol. Adv.*, vol. 34, no. 4, pp. 422–434, Jul. 2016.

[24] F. P. W. Melchels, M. a N. Domingos, T. J. Klein, J. Malda, P. J. Bartolo, and D. W. Hutmacher, "Additive manufacturing of tissues and organs" *Prog. Polym. Sci.*, vol. 37, no. 8, pp. 1079–1104, 2012.

[25] S. V Murphy and A. Atala, "3D bioprinting of tissues and organs" *Nat. Biotechnol.*, vol. 32, no. 8, pp. 773–785, Aug. 2014.

[26] P. Bajaj, R. M. Schweller, A. Khademhosseini, J. L. West, and R. Bashir, "3D biofabrication strategies for tissue engineering and regenerative medicine" *Annu. Rev. Biomed. Eng.*, vol. 16, no. 1, pp. 247–276, Jul. 2014.

[27] L. Gasperini, D. Maniglio, and C. Migliaresi, "Microencapsulation of cells in alginate through an electrohydrodynamic process" *J. Bioact. Compat. Polym.*, vol. 28, no. 5, pp. 413–425, Aug. 2013.

[28] H. Onoe, T. Okitsu, A. Itou, M. Kato-Negishi, R. Gojo, D. Kiriya, K. Sato, S. Miura, S. Iwanaga, K. Kuribayashi-Shigetomi, Y. T. Matsunaga, Y. Shimoyama and S. Takeuchi, "Metre-long cell-laden microfibres exhibit tissue morphologies and functions" *Nat. Mater.*, vol. 12, no. 6, pp. 584–90, 2013.

[29] A. Tamayol, M. Akbari, N. Annabi, A. Paul, A. Khademhosseini, and D. Juncker, "Fiber-based tissue engineering: progress, challenges, and opportunities" *Biotechnol. Adv.*, vol. 31, no. 5, pp. 669–687, Sep. 2013.

[30] R. Lozano, L. Stevens, B. C. Thompson, K. J. Gilmore, R. Gorkin III, E. M. Stewart, M. in het Panhuis, M. Romero-Ortega and G G. Wallace, "3D printing of layered brain-like structures using peptide modified gellan gum substrates" *Biomaterials*, vol. 67, pp. 264–273, Oct. 2015.

[31] R. Gauvin, R. Parenteau-Bareil, M. R. Dokmeci, W. D. Merryman, and A. Khademhosseini, "Hydrogels and microtechnologies for engineering the cellular microenvironment" *Wiley Interdiscip. Rev. Nanomedicine Nanobiotechnology*, vol. 4, no. 3, pp. 235–246, May 2012.

[32] H. Uludag, P. De Vos, and P. A. Tresco, "Technology of mammalian cell encapsulation" *Adv. Drug Deliv. Rev.*, vol. 42, no. 1–2, pp. 29–64, 2000.

[33] G. Orive, R. M. Hernández, A. R. Gascón, R. Calafiore, T. M.S. Chang, P. De Vos, G. Hortelano, D. Hunkeler, I. Lacík, A.M. J. Shapiro and J. L. Pedraz, "Cell encapsulation: promise and progress" *Nat. Med.*, vol. 9, no. 1, pp. 104–7, Jan. 2003.

[34] H. Onoe and S. Takeuchi, "Cell-laden microfibers for bottom-up tissue engineering" *Drug Discov. Today*, vol. 20, no. 2, pp. 236–246, Feb. 2015.

[35] N. C. Hunt and L. M. Grover, "Cell encapsulation using biopolymer gels for regenerative medicine" *Biotechnol. Lett.*, vol. 32, no. 6, pp. 733–742, Jun. 2010.

[36] S. Ji and M. Guvendiren, "Recent advances in bioink design for 3D bioprinting of tissues and organs" *Front. Bioeng. Biotechnol.*, vol. 5, no. April, pp. 1–8, Apr. 2017.

[37] J. Malda, J. Visser, F. P. Melchels , T. Jüngst , W. E. Hennink , W. J. A. Dhert, J. Groll and D. W. Hutmacher., "25th anniversary article: engineering

hydrogels for biofabrication" *Adv. Mater.*, vol. 25, no. 36, pp. 5011–5028, Sep. 2013.

[38] A. Arslan-Yildiz, R. El Assal, P. Chen, S. Guven, F. Inci, and U. Demirci, "Towards artificial tissue models: past, present, and future of 3D bioprinting" *Biofabrication*, vol. 8, no. 1, p. 14103, Mar. 2016.

[39] M. Hospodiuk, M. Dey, D. Sosnoski, and I. T. Ozbolat, "The bioink: A comprehensive review on bioprintable materials" *Biotechnol. Adv.*, vol. 35, no. 2, pp. 217–239, Mar. 2017.

[40] P. de Vos, M. M. Faas, B. Strand, and R. Calafiore, "Alginate-based microcapsules for immunoisolation of pancreatic islets" *Biomaterials*, vol. 27, no. 32, pp. 5603–5617, Nov. 2006.

[41] A. Murua, G. Orive, R. M. Hernández, and J. L. Pedraz, "Xenogeneic transplantation of erythropoietin-secreting cells immobilized in microcapsules using transient immunosuppression" *J. Control. Release*, vol. 137, no. 3, pp. 174–8, Aug. 2009.

[42] B. Sayyar, M. Dodd, J. Wen, S. Ma, L. Marquez-Curtis, A. Janowska-Wieczorek and G Hortelano, "Encapsulation of factor IX-engineered mesenchymal stem cells in fibrinogen-alginate microcapsules enhances their viability and transgene secretion" *J. Tissue Eng.*, vol. 3, no. 1, p. 2041731412462018, Dec. 2012.

[43] C. Colosi, S. R. Shin, V. Manoharan, S. Massa, M. Costantini, A. Barbetta, M. R. Dokmeci, M. Dentini and A. Khademhosseini, "Microfluidic bioprinting of heterogeneous 3D tissue constructs using low-viscosity bioink" *Adv. Mater.*, vol. 28, no. 4, pp. 677–684, Jan. 2016.

[44] W. Song, A. C. Lima, and J. F. Mano, "Bioinspired methodology to fabricate hydrogel spheres for multi-applications using superhydrophobic substrates" *Soft Matter*, vol. 6, no. 23, p. 5868, 2010.

[45] R. Derda, A. Laromainea, A. Mammotoc, S. K. Y. Tanga, T. Mammotoc, D. E. Ingberb and G. M. Whitesidesa, "Paper-supported 3D cell culture for tissue-based bioassays" *Proc. Natl. Acad. Sci.*, vol. 106, no. 44, pp. 18457–18462, Nov. 2009.

[46] W. Lee, W. Lee, J. C. Debasitis, V. K. Lee, J.-H. Lee, K. Fischer, K. Edminster, J.-K. Parkb, S.-S. Yooa, "Multi-layered culture of human skin fibroblasts and keratinocytes through three-dimensional freeform fabrication" *Biomaterials*, vol. 30, no. 8, pp. 1587–1595, 2009.

[47] I. E. Hannachi, M. Yamato, and T. Okano, "Cell sheet technology and cell patterning for biofabrication" *Biofabrication*, vol. 1, no. 2, p. 22002, Jun. 2009.

[48] K. Matsuura, R. Utoh, K. Nagase, and T. Okano, "Cell sheet approach for tissue engineering and regenerative medicine" *J. Control. Release*, vol. 190, pp. 228–239, Sep. 2014.

[49] J. Yan, F. Chen, and B. G. Amsden, "Cell sheets prepared via gel-sol transition of calcium RGD-alginate" *Acta Biomater.*, vol. 30, pp. 277–284, 2016.

[50] S. Tasoglu, U. A. Gurkan, S. Wang, and U. Demirci, "Manipulating biological agents and cells in micro-scale volumes for applications in medicine" *Chem. Soc. Rev.*, vol. 42, no. 13, p. 5788, Jul. 2013.

[51] K. Hölzl, S. Lin, L. Tytgat, S. Van Vlierberghe, L. Gu, and A. Ovsianikov, "Bioink properties before, during and after 3D bioprinting" *Biofabrication*, vol. 8, no. 3, p. 32002, Sep. 2016.

[52] I. T. Ozbolat and M. Hospodiuk, "Current advances and future perspectives in extrusion-based bioprinting" *Biomaterials*, vol. 76, pp. 321–343, 2016.

[53] I. T. Ozbolat, W. Peng, and V. Ozbolat, "Application areas of 3D bioprinting" *Drug Discov. Today*, vol. 21, no. 8, pp. 1257–1271, 2016.

[54] K. Jakab, C. Norotte, F. Marga, K. Murphy, G. Vunjak-Novakovic, and G. Forgacs, "Tissue engineering by self-assembly and bio-printing of living cells" *Biofabrication*, vol. 2, no. 2, p. 22001, Jun. 2010.

[55] L. Moroni, J. R. De Wijn, and C. A. Van Blitterswijk, "3D fiber-deposited scaffolds for tissue engineering: Influence of pores geometry and architecture on dynamic mechanical properties" *Biomaterials*, vol. 27, no. 7, pp. 974–985, 2006.

[56] I. T. Ozbolat, "Bioprinting scale-up tissue and organ constructs for transplantation" *Trends Biotechnol.*, vol. 33, no. 7, pp. 395–400, Jul. 2015.

[57] J. E. Snyder, Q. Hamid, C. Wang, R. Chang, K. Emami, H. Wu and W. Sun, "Bioprinting cell-laden matrigel for radioprotection study of liver by pro-drug conversion in a dual-tissue microfluidic chip" *Biofabrication*, vol. 3, no. 3, p. 34112, Sep. 2011.

[58] C. Norotte, F. Marga, L. Niklason, and G. Forgacs, "Scaffold-free vascular tissue engineering using bioprinting" *Biomaterials*, vol. 30, no. 30, pp. 5910–5917, Oct. 2009.

[59] T. J. Hinton, Q. Jallerat, R. N. Palchesko, J. H. Park, M. S. Grodzicki, H.-J. Shue, M. H. Ramadan, A. R. Hudson and A. W. Feinberg, "Three-dimensional printing of complex biological structures by freeform reversible embedding of suspended hydrogels" *Sci. Adv.*, vol. 1, no. 9, pp. e1500758–e1500758, Oct. 2015.

[60] K. Ye, R. Felimban, K. Traianedes, S. E. Moulton, G. G. Wallace, J. Chung, A. Quigley, P. F. M. Choong and D. E. Myers, "Chondrogenesis of infrapatellar fat pad derived adipose stem cells in 3D printed chitosan scaffold" *PLoS One*, vol. 9, no. 6, p. e99410, Jun. 2014.

[61] S. Michael, H. Sorg, C.-T. Peck, L. Koch, A. Deiwick, B. Chichkov, P. M. Vogt and K. Reimers "Tissue engineered skin substitutes created by laser-assisted

bioprinting form skin-like structures in the dorsal skin fold chamber in mice" *PLoS One*, vol. 8, no. 3, p. e57741, Mar. 2013.

[62] N. A. Raof, N. R. Schiele, Y. Xie, D. B. Chrisey, and D. T. Corr, "The maintenance of pluripotency following laser direct-write of mouse embryonic stem cells" *Biomaterials*, vol. 32, no. 7, pp. 1802–1808, Mar. 2011.

[63] T. Xu, C. Baicu, M. Aho, M. Zile, and T. Boland, "Fabrication and characterization of bio-engineered cardiac pseudo tissues" *Biofabrication*, vol. 1, no. 3, p. 35001, Sep. 2009.

[64] L. Pescosolido, W. Schuurman, J. Malda, P. Matricardi, F. Alhaique, T. Coviello, P. R van Weeren, W. J. A. Dhert, W. E. Hennink and T. Vermonden "Hyaluronic acid and dextran-based semi-IPN hydrogels as biomaterials for bioprinting" *Biomacromolecules*, vol. 12, no. 5, pp. 1831–1838, May 2011.

[65] R. Gauvin, Y.-C. Chen, J. W. Leed, P. Somand, P. Zorlutuna, J. W. Nichol, H. Bae, S. Chend and Ali Khademhosseini "Microfabrication of complex porous tissue engineering scaffolds using 3D projection stereolithography" *Biomaterials*, vol. 33, no. 15, pp. 3824–3834, May 2012.

[66] M. Müller, J. Becher, M. Schnabelrauch, and M. Zenobi-Wong, "Nanostructured pluronic hydrogels as bioinks for 3D bioprinting" *Biofabrication*, vol. 7, no. 3, p. 35006, Aug. 2015.

[67] L. A. Hockaday, K. H. Kang, N. W. Colangelo, P. Y. C. Cheung, B. Duan, E. Malone, J. Wu, L. N. Girardi, L. J. Bonassar, H. Lipson, C. C. Chu and J. T. Butcher, "Rapid 3D printing of anatomically accurate and mechanically heterogeneous aortic valve hydrogel scaffolds" *Biofabrication*, vol. 4, no. 3, p. 35005, Sep. 2012.

[68] R. Chang, K. Emami, H. Wu, and W. Sun, "Biofabrication of a three-dimensional liver micro-organ as an *in vitro* drug metabolism model" *Biofabrication*, vol. 2, no. 4, p. 45004, Dec. 2010.

[69] H. F. Lu, M. F. Leong, T. C. Lim, Y. P. Chua, J. K. Lim, C. Du and A. C. A. Wan, "Engineering a functional three-dimensional human cardiac tissue model for drug toxicity screening" *Biofabrication*, vol. 9, no. 2, 2017.

[70] D. Tang, R. S. Tare, L. Y. Yang, D. F. Williams, K. L. Ou, and R. O. C. Oreffo, "Biofabrication of bone tissue: approaches, challenges and translation for bone regeneration" *Biomaterials*, vol. 83. pp. 363–382, 2016.

[71] N. Cubo, M. Garcia, J. F. del Cañizo, D. Velasco, and J. L. Jorcano, "3D bioprinting of functional human skin: production and *in vivo* analysis" *Biofabrication*, vol. 9, no. 1, p. 15006, 2016.

[72] M. a Lancaster, M. Renner, C. A. Martin, D. Wenzel, L. S. Bicknell, M. E. Hurles, T. Homfray, J. M. Penninger, A. P. Jackson and J. A. Knoblich "Cerebral organoids model human brain development and microcephaly" *Nature*, vol. 501, no. 7467, pp. 373–9, Sep. 2013.

[73] P. Datta, B. Ayan, and I. T. Ozbolat, "Bioprinting for vascular and vascularized tissue biofabrication" *Acta Biomater.*, vol. 51, pp. 1–20, Mar. 2017.

[74] A. Kang, J. Park, J. Ju, G. S. Jeong, and S.-H. Lee, "Cell encapsulation via microtechnologies" *Biomaterials*, vol. 35, no. 9, pp. 2651–2663, Mar. 2014.

[75] W. Peng, D. Unutmaz, and I. T. Ozbolat, "Bioprinting towards physiologically relevant tissue models for pharmaceutics" *Trends Biotechnol.*, vol. 34, no. 9, pp. 722–732, Sep. 2016.

[76] R. Chang, K. Emami, H. Wu, and W. Sun, "Biofabrication of a three-dimensional liver micro-organ as an *in vitro* drug metabolism model" *Biofabrication*, vol. 2, no. 4, p. 45004, Dec. 2010.

[77] C. Wang, Z. Tang, Y. Zhao, R. Yao, L. Li, and W. Sun, "Three-dimensional *in vitro* cancer models: a short review" *Biofabrication*, vol. 6, no. 2, p. 22001, Apr. 2014.

[78] G. Orive, E. Santos, J. L. Pedraz, and R. M. Hernández, "Application of cell encapsulation for controlled delivery of biological therapeutics" *Adv. Drug Deliv. Rev.*, vol. 67–68, pp. 3–14, Apr. 2014.

[79] Y. Jun *et al.*, "3D co-culturing model of primary pancreatic islets and hepatocytes in hybrid spheroid to overcome pancreatic cell shortage" *Biomaterials*, vol. 34, no. 15, pp. 3784–3794, May 2013.

[80] R. Malpique *et al.*, "Alginate encapsulation as a novel strategy for the cryopreservation of neurospheres" *Tissue Eng. Part C Methods*, vol. 16, no. 5, pp. 965–977, Oct. 2010.

[81] A. Grigore, B. Sarker, B. Fabry, A. R. Boccaccini, and R. Detsch, "Behavior of encapsulated MG-63 cells in RGD and gelatine-modified alginate hydrogels" *Tissue Eng. Part A*, vol. 20, no. 15–16, pp. 2140–50, 2014.

[82] S. Tasoglu and U. Demirci, "Bioprinting for stem cell research" *Trends Biotechnol.*, vol. 31, no. 1, pp. 10–19, Jan. 2013.

[83] M. Lovett, K. Lee, A. Edwards, and D. L. Kaplan, "Vascularization strategies for tissue engineering" *Tissue Eng. Part B Rev.*, vol. 15, no. 3, pp. 353–370, Sep. 2009.

[84] R. a. Rezende, F.D.A.S. Pereiraa, V. Kasyanovb, D.T. Kemmoku, I. Maia, J.V.L. da Silvaa and V. Mironova, "Scalable biofabrication of tissue Spheroids for organ printing" *Procedia CIRP*, vol. 5, pp. 276–281, Jan. 2013.

[85] M. a. Daniele, D. a. Boyd, A. a. Adams, and F. S. Ligler, "Microfluidic strategies for design and assembly of microfibers and nanofibers with tissue engineering and regenerative medicine applications" *Adv. Healthc. Mater.*, vol. 4, no. 1, pp. 11–28, 2015.

[86] U. A. Gurkan, R. El Assal, S. E. Yildiz, Y. Sung, A. J. Trachtenberg, W. P. Kuo, and U. Demirci, "Engineering anisotropic biomimetic fibrocartilage microenvironment by bioprinting mesenchymal stem cells in nanoliter gel

droplets" *Mol. Pharm.*, vol. 11, no. 7, pp. 2151–2159, Jul. 2014.

[87] S. Moon, S. K. Hasan, Y. S. Song, F. Xu, H. O. Keles, F. Manzur, S. Mikkilineni, J. W. Hong, J. Nagatomi, E. Haeggstrom, A. Khademhosseini, and U. Demirci, "Layer by layer three-dimensional tissue epitaxy by cell-laden hydrogel droplets" *Tissue Eng. Part C Methods*, vol. 16, no. 1, pp. 157–166, Feb. 2010.

[88] F. Pati, J. Jang, D. Ha, S. W. Kim, J. Rhie, J. Shim, D. Kim and D.Cho, "Printing three-dimensional tissue analogues with decellularized extracellular matrix bioink" *Nat. Commun.*, vol. 5, p. 3935, 2014.

[89] S. Guven and U. Demirci, "Integrating nanoscale technologies with cryogenics: a step towards improved biopreservation" *Nanomedicine*, vol. 7, no. 12, pp. 1787–1789, Dec. 2012.

[90] M. Rinaudo, "Main properties and current applications of some polysaccharides as biomaterials" *Polym. Int.*, vol. 57, no. 3, pp. 397–430, Mar. 2008.

[91] E. M. Ahmed, "Hydrogel: preparation, characterization, and applications: a review" *J. Adv. Res.*, vol. 6, no. 2, pp. 105–121, 2015.

[92] F. Lim and A. Sun, "Microencapsulated islets as bioartificial endocrine pancreas" *Science (80-.).*, vol. 210, no. 4472, pp. 908–910, Nov. 1980.

[93] H. Zimmermann, S. G. Shirley, and U. Zimmermann, "Alginate-based encapsulation of cells: past, present, and future" *Curr. Diab. Rep.*, vol. 7, no. 4, pp. 314–20, Aug. 2007.

[94] K. Y. Lee and D. J. Mooney, "Alginate: properties and biomedical applications" *Prog. Polym. Sci.*, vol. 37, no. 1, pp. 106–126, Jan. 2012.

[95] S. N. Pawar and K. J. Edgar, "Alginate derivatization: a review of chemistry, properties and applications" *Biomaterials*, vol. 33, no. 11, pp. 3279–3305, Apr. 2012.

[96] T. Andersen, P. Auk-Emblem, and M. Dornish, "3D cell culture in alginate hydrogels" *Microarrays*, vol. 4, no. 2, pp. 133–161, 2015.

[97] B. Sarker, J. Rompf, R. Silva, N. Langb, R. Detscha, J. Kaschtac, B. Fabryb and A. R. Boccaccini "Alginate-based hydrogels with improved adhesive properties for cell encapsulation" *Int. J. Biol. Macromol.*, vol. 78, pp. 72–78, Jul. 2015.

[98] A. D. Augst, H. J. Kong, and D. J. Mooney, "Alginate hydrogels as biomaterials" *Macromol. Biosci.*, vol. 6, no. 8, pp. 623–33, Aug. 2006.

[99] E. Axpe and M. Oyen, "Applications of alginate-based bioinks in 3D bioprinting" *Int. J. Mol. Sci.*, vol. 17, no. 12, p. 1976, Nov. 2016.

[100] J. Sun and H. Tan, "Alginate-based biomaterials for regenerative medicine applications" *Materials (Basel).*, vol. 6, no. 4, pp. 1285–1309, Mar. 2013.

[101] S. Jitraruch, A. Dhawan, R. D. Hughes, C. Filippi, D. Soong, C. Philippeos, S. C. Lehec, N. D. Heaton, M. S. Longhi and R. R. Mitry., "Alginate microencapsulated hepatocytes optimised for transplantation in acute liver failure" *PLoS One*, vol. 9, no. 12, p. e113609, Dec. 2014.

[102] S. V. Bhujbal, P. de Vos, and S. P. Niclou, "Synthesis of alginate-curcumin nanocomposite and its protective role in transgenic Drosophila model of Parkinson's disease" *Adv. Drug Deliv. Rev.*, vol. 67–68, pp. 142–153, Apr. 2014.

[103] S. V. Bhujbal, P. de Vos, and S. P. Niclou, "Drug and cell encapsulation: Alternative delivery options for the treatment of malignant brain tumors" *Advanced Drug Delivery Reviews*, vol. 67–68. pp. 142–153, Apr-2014.

[104] D. Nguyen, D. A. Hägg, A. Forsman, J. Ekholm, P. Nimkingratana, C. Brantsing, T. Kalogeropoulos, S. Zaunz, S. Concaro, M. Brittberg, A. Lindahl, P. Gatenholm, A. Enejder and S. Simonsson, "Cartilage tissue engineering by the 3D bioprinting of iPS cells in a nanocellulose/alginate bioink" *Sci. Rep.*,

vol. 7, no. 1, p. 658, Dec. 2017.

[105] J. Venkatesan, R. Nithya, P. N. Sudha, and S. K. Kim, "Role of alginate in bone tissue engineering" *Adv. Food Nutr. Res.*, vol. 73, pp. 45–57, 2014.

[106] Q. Li, T. Hou, J. Zhao, and J. Xu, "Vascular endothelial growth factor release from alginate microspheres under simulated physiological Ccmpressive loading and the effect on human vascular endothelial cells" *Tissue Eng. Part A*, vol. 17, no. 13–14, pp. 1777–1785, Jul. 2011.

[107] V. Liaudanskaya, L. Gasperini, D. Maniglio, A. Motta, and C. Migliaresi, "Assessing the impact of electrohydrodynamic jetting on encapsulated cell viability, proliferation, and ability to self-assemble in three-dimensional structures" *Tissue Eng. Part C Methods*, vol. 21, no. 6, pp. 631–638, Jun. 2015.

[108] C. Barron and J.-Q. He, "Alginate-based microcapsules generated with the coaxial electrospray method for clinical application" *J. Biomater. Sci. Polym. Ed.*, vol. 28, no. 13, pp. 1245–1255, Sep. 2017.

[109] B. R. Lee, J. W. Hwang, Y. Y. Choi, S. F. Wonga, Y. H. Hwang, D. Y. Lee and S. Lee, "*In situ* formation and collagen-alginate composite encapsulation of pancreatic islet spheroids" *Biomaterials*, vol. 33, no. 3, pp. 837–45, Jan. 2012.

[110] L. Liu, F. Wu, X. Ju, R. Xie, W. Wang, C. H. Niu and L. Chu, "Preparation of monodisperse calcium alginate microcapsules via internal gelation in microfluidic-generated double emulsions" *J. Colloid Interface Sci.*, vol. 404, pp. 85–90, Aug. 2013.

[111] H. Onoe, R. Gojo, Y. Tsuda, D. Kiriya, and S. Takeuchi, "Core-shell gel wires for the construction of large area heterogeneous structures with biomaterials" *Proc. IEEE Int. Conf. Micro Electro Mech. Syst.*, pp. 248–251, 2010.

[112] S. Takeuchi, "Cell-laden hydrogel beads, fibers and plates for 3D tissue construction" *Solid-State Sensors, 2013 Transducers & Eurosensors XXVII:*

The 17th International Conference on Solid-State Sensors, Actuators and Microsystems (TRANSDUCERS & EUROSENSORS XXVII), no. June, pp. 1515–1518, 2013.

[113] B. R. Lee, K. H. Lee, E. Kang, D. S. Kim, and S. H. Lee, "Microfluidic wet spinning of chitosan-alginate microfibers and encapsulation of HepG2 cells in fibers" *Biomicrofluidics*, vol. 5, no. 2, pp. 1–9, 2011.

[114] M. Akbari, A. Tamayol, V. Laforte, N. Annabi, A. H. Najafabadi and A. Khademhosseini and D. Juncker, "Composite living fibers for creating tissue constructs using textile techniques" *Adv. Funct. Mater.*, vol. 24, no. 26, pp. 4060–4067, 2014.

[115] A. Panwar and L. Tan, "Current status of bioinks for micro-extrusion-based 3D bioprinting" *Molecules*, vol. 21, no. 6, p. 685, May 2016.

[116] L. Gasperini and D. Maniglio, "An electrohydrodynamic bioprinter for alginate hydrogels containing living cells," *Tissue Engineering Part C: Methods*, vol 21, no. 2, pp. 123-132, 2015

[117] A. G. Tabriz, M. A. Hermida, N. R. Leslie, and W. Shu, "Three-dimensional bioprinting of complex cell laden alginate hydrogel structures" *Biofabrication*, vol. 7, no. 4, p. 45012, 2015.

[118] J. a Rowley, G. Madlambayan, and D. J. Mooney, "Alginate hydrogels as synthetic extracellular matrix materials" *Biomaterials*, vol. 20, no. 1, pp. 45–53, Jan. 1999.

[119] X. Yang, Z. Lu, H. Wu, W. Li, L. Zheng, and J. Zhao, "Collagen-alginate as bioink for three-dimensional (3D) cell printing based cartilage tissue engineering" *Mater. Sci. Eng. C*, vol. 83, no. June 2017, pp. 195–201, Feb. 2018.

[120] R. Silva, R. Singhb, B. Sarkera, D. G. Papageorgiou, J. A. Juhasza, J A. Roetherd, I. Cicha, J. Kaschtad, D. W. Schubertd, K. Chrissafisc, R.Detscha

and A. R. Boccaccini., "Hybrid hydrogels based on keratin and alginate for tissue engineering" *J. Mater. Chem. B*, vol. 2, no. 33, pp. 5441–5451, 2014.

[121] Y. Wang, X. Wang, J. Shi, R. Zhu, J. Zhang, Z. Zhang, D. Ma, Y. Hou, F. Lin, J. Yang and M. Mizuno, "A biomimetic silk fibroin/sodium alginate composite scaffold for soft tissue engineering" *Sci. Rep.*, vol. 6, no. 1, p. 39477, Dec. 2016.

[122] R. Singh, B. Sarker, R. Silva, R. Detsch, B. Dietel, C. Alexiou, A. R. Boccaccini and I. Cicha, "Evaluation of hydrogel matrices for vessel bioplotting: vascular cell growth and viability" *J. Biomed. Mater. Res. Part A*, vol. 104, no. 3, pp. 577–585, Mar. 2016.

[123] R. Silva, R. Singh, B. Sarker, D. G. Papageorgiou, J. A. Juhasz, J. A Roether, I. Cicha, J. Kaschta, D. W. Schubert, K. Chrissafis, R. Detsch and A. R. Boccaccini, "Soft-matrices based on silk fibroin and alginate for tissue engineering" *Int. J. Biol. Macromol.*, vol. 93, pp. 1420–1431, Dec. 2016.

[124] E. C. Novosel, C. Kleinhans, and P. J. Kluger, "Vascularization is the key challenge in tissue engineering" *Adv. Drug Deliv. Rev.*, vol. 63, no. 4–5, pp. 300–311, Apr. 2011.

[125] J. O. M. Karlsson and M. Toner, "Long-term storage of tissues by cryopreservation: critical issues" *Biomaterials*, vol. 17, no. 3, pp. 243–256, 1996.

[126] L. G. Griffith and G. Naughton, "Tissue engineering - Current challenges and expanding opportunities" *Science*, vol. 295, no. 5557, pp. 1009–1014, 08-Feb-2002.

[127] J. P. Acker, "Biopreservation of cells and engineered tissues" in *Tissue Engineering II*, vol. 103, no. October 2005, Springer Berlin Heidelberg, 2006, pp. 157–187.

[128] D. Gao and A. K. Critser, "Mechanisms of cryoinjury in living cells" vol. 4,

no. 4, pp. 187–196, 2000.

[129] X. Zhang, P. N. Catalano, U. A. Gurkan, I. Khimji, and U. Demirci, "Emerging technologies in medical applications of minimum volume vitrification" *Nanomedicine*, vol. 6, no. 6, pp. 1115–1129, Aug. 2011.

[130] H. T. Meryman, "Cryopreservation of living cells: principles and practice" *Transfusion*, vol. 47, no. 5, pp. 935–945, May 2007.

[131] D. E. Pegg, "The history and principles of cryopreservation" in *Health Affairs*, vol. 12, no. suppl 1, 2007, pp. 39–57.

[132] L. E. McGann, "Optimal temperature ranges for control of cooling rate" *Cryobiology*, vol. 16, no. 3, pp. 211–216, Jun. 1979.

[133] B. C. Heng, H. Yu, and S. C. Ng, "Strategies for the cryopreservation of microencapsulated cells" *Biotechnol. Bioeng.*, vol. 85, no. 2, pp. 202–213, Jan. 2004.

[134] F. Chen, W. Zhang, W. Wua, Y. Jin, L. Cenb, J. D. Kretlowd, W. Gaoe, Z. Dai, J. Wang, G. Zhou, W. Liu, L. Cui and Y. Cao, "Cryopreservation of tissue-engineered epithelial sheets in trehalose" *Biomaterials*, vol. 32, no. 33, pp. 8426–8435, 2011.

[135] T. H. Jang, S. C. Park, J. H. Yanga, J. Y. Kima, J. H. Seoka, U. S. Parka, C. W. Choi, S. R. Lee and J. Hanb, "Cryopreservation and its clinical applications" *Integr. Med. Res.*, vol. 6, no. 1, pp. 12–18, Mar. 2017.

[136] A. I. Pravdyuk, Y. A. Petrenko, B. J. Fuller, and A. Y. Petrenko, "Cryopreservation of alginate encapsulated mesenchymal stromal cells" *Cryobiology*, vol. 66, no. 3, pp. 215–222, Jun. 2013.

[137] H. F. Ahmad and A. Sambanis, "Cryopreservation effects on recombinant myoblasts encapsulated in adhesive alginate hydrogels" *Acta Biomater.*, vol. 9, no. 6, pp. 6814–22, 2013.

[138] P. F. Costa, A. F. Dias, R. L. Reis, and M. E. Gomes, "Cryopreservation of

cell/scaffold tissue-engineered constructs" *Tissue Eng. Part C Methods*, vol. 18, no. 11, pp. 852–858, 2012.

[139] E. G. Popa *et al.*, "Cryopreservation of cell laden natural origin hydrogels for cartilage regeneration strategies" *Soft Matter*, vol. 9, no. 3, pp. 875–885, 2013.

[140] X. Wang and H. Xu, "Incorporation of DMSO and dextran-40 into a gelatin/alginate hydrogel for controlled assembled cell cryopreservation" *Cryobiology*, vol. 61, no. 3, pp. 345–351, Dec. 2010.

[141] Xiaohong Wang, K.-S. Paloheimo, Huirong Xu, and Chang Liu, "Cryopreservation of cell/hydrogel constructs based on a new cell-assembling technique" *J. Bioact. Compat. Polym.*, vol. 25, no. 6, pp. 634–653, Nov. 2010.

[142] P. Kilbride, J. Gonzalez-Molina, N. Maurmann, J. M. da Silva, S. Gibbons, C. Selden, B. Fuller and J. Morris, "Impact of storage at −80°C on encapsulated liver spheroids after liquid nitrogen storage" *Biores. Open Access*, vol. 5, no. 1, pp. 146–154, Jun. 2016.

[143] A. Katsen-Globa, I, Meiser, Y, A. Petrenko, R. V. Ivanov, V. I. Lozinsky, H. Zimmermann, A. Yu. Petrenko, "Towards ready-to-use 3-D scaffolds for regenerative medicine: adhesion-based cryopreservation of human mesenchymal stem cells attached and spread within alginate–gelatin cryogel scaffolds" *J. Mater. Sci. Mater. Med.*, vol. 25, no. 3, pp. 857–871, Mar. 2014.

[144] N. Cagol, W. Bonani, D. Maniglio, C. Migliaresi, and A. Motta, "Effect of cryopreservation on cell-laden hydrogels: comparison of different cryoprotectants" *Tissue Eng. Part C Methods*, vol. 24, no. 1, pp. 20–31, Jan. 2018.

[145] H. Huang, J. K. Choi, W. Rao, S. Zhao, P. Agarwal, G. Zhao and X. He, "Alginate hydrogel microencapsulation inhibits devitrification and enables large-volume low-CPA cell vitrification" *Adv. Funct. Mater.*, vol. 25, no. 44,

pp. 6839–6850, Nov. 2015.

[146] J. Schindelin, I. Arganda-Carreras, E. Frise, V. Kaynig, M. Longair, T. Pietzsch, S. Preibisch, C. Rueden, S. Saalfeld, B. Schmid, J. Tinevez, D. James White, V. Hartenstein, K. Eliceiri, P. Tomancak and A. Cardona, "Fiji: an open-source platform for biological-image analysis" *Nat. Methods*, vol. 9, no. 7, pp. 676–682, Jun. 2012.

[147] K. Liu, Y. Yang, and J. Mansbridge, "Comparison of the stress response to cryopreservation in monolayer and three-dimensional human fibroblast cultures: stress proteins, MAP kinases, and growth factor gene expression" *Tissue Eng.*, vol. 6, no. 5, pp. 539–554, Oct. 2000.

[148] J. M. Zuidema, C. J. Rivet, R. J. Gilbert, and F. A. Morrison, "A protocol for rheological characterization of hydrogels for tissue engineering strategies" *J. Biomed. Mater. Res. - Part B Appl. Biomater.*, vol. 102, no. 5, pp. 1063–1073, 2014.

[149] H. Li, S. Liu, and L. Li, "Rheological study on 3D printability of alginate hydrogel and effect of graphene oxide" pp. 10–12, 2016.

[150] A. Eroglu, M. J. Russo, R. Bieganski, A. Fowler, S. Cheley, H. Bayley and M. Toner, "Intracellular trehalose improves the survival of cryopreserved mammalian cells" *Nat. Biotechnol.*, vol. 18, no. 2, pp. 163–167, Feb. 2000.

[151] E. M. Czekanska, M. J. Stoddart, J. R. Ralphs, R. G. Richards, and J. S. Hayes, "A phenotypic comparison of osteoblast cell lines versus human primary osteoblasts for biomaterials testing" *J. Biomed. Mater. Res. - Part A*, vol. 102, no. 8, pp. 2636–2643, 2014.

[152] A. Bissoyi, B. Nayak, K. Pramanik, and S. K. Sarangi, "Targeting cryopreservation-induced cell death: a review" *Biopreserv. Biobank.*, vol. 12, no. 1, pp. 23–34, 2014.

[153] Y. Naaldijk, A. Friedrich-Stöckigt, S. Sethe, and A. Stolzing, "Comparison of

different cooling rates for fibroblast and keratinocyte cryopreservation" *J. Tissue Eng. Regen. Med.*, vol. 10, no. 10, pp. E354–E364, Oct. 2016.

[154] T. E. Honadel and G. J. Killian, "Cryopreservation of murine embryos with trehalose and glycerol" *Cryobiology*, vol. 25, no. 4, pp. 331–337, Aug. 1988.

[155] K. Takeuchi, M. Nakazawa, Y. Ebina, K. Sato, T. Metoki, Y. Miyagawa and T. Ito, "Inhibitory effects of trehalose on fibroblast proliferation and implications for ocular surgery" *Exp. Eye Res.*, vol. 91, no. 5, pp. 567–577, Nov. 2010.

[156] S. W. Perry, L. G. Epstein, and H. A. Gelbard, "Simultaneous in situ detection of apoptosis and necrosis in monolayer cultures by TUNEL and trypan blue staining" *Biotechniques*, vol. 22, no. 6, p. 1102—1106, 1997.

[157] X. Xu, S. Cowley, C. J. Flaim, W. James, L. Seymour, and Z. Cui, "The roles of apoptotic pathways in the low recovery rate after cryopreservation of dissociated human embryonic stem cells" *Biotechnol. Prog.*, vol. 26, no. 3, pp. 827–837, Jan. 2010.

[158] M. Ribeiro, M. A. de Moraes, M. M. Beppu, F. J. Monteiro, and M. P. Ferraz, "The role of dialysis and freezing on structural conformation, thermal properties and morphology of silk fibroin hydrogels" *Biomatter*, vol. 4, no. 1, p. e28536, Jan. 2014.

[159] G. Levy and T. W. Schwarz, "The role of residual calcium in the viscosity changes of sodium alginate solutions" *J. Am. Pharm. Assoc. (Scientific ed.)*, vol. 47, no. 6, pp. 455–457, Jun. 1958.

[160] S. Tasoglu, C. H. Yu, V. Liaudanskaya, S. Guven, C. Migliaresi, and U. Demirci, "Magnetic levitational assembly for living material fabrication" *Adv. Healthc. Mater.*, vol. 4, no. 10, pp. 1469–1476, Jul. 2015.

[161] H. Geckil, F. Xu, X. Zhang, S. Moon, and U. Demirci, "Engineering hydrogels as extracellular matrix mimics" *Nanomedicine*, vol. 5, no. 3, pp. 469–484,

Apr. 2010.

[162] X. Jia and K. L. Kiick, "Hybrid multicomponent hydrogels for tissue engineering" *Macromol. Biosci.*, vol. 9, no. 2, pp. 140–156, Feb. 2009.

[163] J. Baldwin, M. Antille, U. Bonda, E. M. De-Juan-Pardo, K. Khosrotehrani S. Ivanovski, E. B. Petcu and D. W. Hutmacher, "*In vitro* pre-vascularisation of tissue-engineered constructs A co-culture perspective" *Vasc. Cell*, vol. 6, no. 1, p. 13, 2014.

[164] M. Grellier, L. Bordenave, and J. Amédée, "Cell-to-cell communication between osteogenic and endothelial lineages: implications for tissue engineering" *Trends Biotechnol.*, vol. 27, no. 10, pp. 562–571, 2009.

[165] N. K. Paschos, W. E. Brown, R. Eswaramoorthy, J. C. Hu, and K. A. Athanasiou, "Advances in tissue engineering through stem cell-based co-culture" *J. Tissue Eng. Regen. Med.*, vol. 9, no. 5, pp. 488–503, May 2015.

[166] J. K. Gandhi, E. C. Opara, and E. M. Brey, "Alginate-based strategies for therapeutic vascularization" *Ther. Deliv.*, vol. 4, no. 3, pp. 327–341, Mar. 2013.

[167] K. G. Battiston, J. W. C. Cheung, D. Jain, and J. P. Santerre, "Biomaterials in co-culture systems: Towards optimizing tissue integration and cell signaling within scaffolds" *Biomaterials*, vol. 35, no. 15, pp. 4465–4476, May 2014.

[168] F. Zhu, Y. Chen, S. Yang, Q. Wang, F. Liang, X. Qu and Z. Hu, "Surface patterned hydrogel film as a flexible scaffold for 2D and 3D cell co-culture" *RSC Adv.*, vol. 6, no. 66, pp. 61185–61189, 2016.

[169] R. Silva, B. Fabry, and A. R. Boccaccini, "Fibrous protein-based hydrogels for cell encapsulation" *Biomaterials*, vol. 35, no. 25, pp. 6727–6738, Aug. 2014.

[170] K. Lee and D. Mooney, "Hydrogels for tissue engineering," *Chem. Rev.*, vol. 101, no. 7, 2001.

[171] M. Roussenova, J. Enrione, P. Diaz-Calderon, A. J. Taylor, J. Ubbink, and M.

A. Alam, "A nanostructural investigation of glassy gelatin oligomers: molecular organization and interactions with low molecular weight diluents" *New J. Phys.*, vol. 14, no. 3, p. 35016, Mar. 2012.

[172] D. N. Rockwood, R. C. Preda, T. Yücel, X. Wang, M. L. Lovett, and D. L. Kaplan, "Materials fabrication from *Bombyx mori* silk fibroin" *Nat. Protoc.*, vol. 6, no. 10, pp. 1612–1631, Sep. 2011.

[173] Y. Qi, H. Wang, K. Wei, Y. Yang, R. Zheng, I. S. Kim and K. Zhang, "A review of structure construction of silk fibroin biomaterials from single structures to multi-level structures" *Int. J. Mol. Sci.*, vol. 18, no. 3, 2017.

[174] R. Freeman, J. Boekhoven, M. B. Dickerson, R. R. Naik, and S. I. Stupp, "Biopolymers and supramolecular polymers as biomaterials for biomedical applications" *MRS Bull.*, vol. 40, no. 12, pp. 1089–1101, Dec. 2015.

[175] A. Matsumoto, J. Chen, A. L. Collette, U. Kim, G. H. Altman, P. Cebe and D. L. Kaplan, "Mechanisms of silk fibroin sol−gel transitions, *J. Phys. Chem. B*, vol. 110, no. 43, pp. 21630–21638, Nov. 2006.

[176] W. Sun, T. Incitti, C. Migliaresi, A. Quattrone, S. Casarosa, and A. Motta, "Genipin-crosslinked gelatin-silk fibroin hydrogels for modulating the behaviour of pluripotent cells" *J. Tissue Eng. Regen. Med.*, vol. 10, no. 10, pp. 876–887, Oct. 2016.

[177] H. Yamada, Y. Igarashi, Y. Takasu, H. Saito, and K. Tsubouchi, "Identification of fibroin-derived peptides enhancing the proliferation of cultured human skin fibroblasts" *Biomaterials*, vol. 25, no. 3, pp. 467–472, 2004.

[178] E. Rosellini, C. Cristallini, N. Barbani, G. Vozzi, and P. Giusti, "Preparation and characterization of alginate/gelatin blend films for cardiac tissue engineering" *J. Biomed. Mater. Res. - Part A*, vol. 91, no. 2, pp. 447–453, Nov. 2009.

[179] K. Sakaguchi, T. Shimizu, S. Horaguchi, H. Sekine, M. Yamato, M. Umezu and T. Okano, "*In vitro* engineering of vascularized tissue surrogates" *Sci. Rep.*, vol. 3, p. 1316, 2013.

[180] K. Kyriakidou *et al.*, "Dynamic co-seeding of osteoblast and endothelial cells on 3D polycaprolactone scaffolds for enhanced bone tissue engineering" *J. Bioact. Compat. Polym.*, vol. 23, no. 3, pp. 227–243, 2008.

[181] H. Keshaw, A. Forbes, and R. M. Day, "Release of angiogenic growth factors from cells encapsulated in alginate beads with bioactive glass" *Biomaterials*, vol. 26, no. 19, pp. 4171–4179, Jul. 2005.

[182] N. C. Hunt, R. M. Shelton, D. J. Henderson, and L. M. Grover, "Calcium-alginate hydrogel-encapsulated fibroblasts provide sustained release of vascular endothelial growth factor" *Tissue Eng. Part A*, vol. 19, no. 7–8, pp. 905–914, Apr. 2013.

Scientific production

- **Cagol N**, Bonani W, Maniglio D, Migliaresi C, Motta A. (2018) Effect of cryopreservation on cell-laden hydrogels: comparison of different cryoprotectants. *Tissue Engineering: Part C*, **24**, 20-31

- Parisi L, Zomer Volpato F, **Cagol N**, Siciliano M, Migliaresi C, Motta A, Sala R. (2016) An innovative protocol for schwann cells extracellular matrix proteins extraction. *Journal of Biomedical Materials Research Part A*, **104**, 3175–3180

- **Cagol N**, Bonani W, Maniglio D, Migliaresi C, Motta A. Review on cell encapsulation methods and material. Manuscript *in preparation*

Participation to Congresses, Schools and Workshops

Congresses

- TERMIS (Tissue Engineering and Regenerative Medicine) European Meeting 2014 (Genova; June 10th-13th)
- **11th International Symposium on Frontiers in Biomedical Polymers** (Riva del Garda; July 8th-11th 2015) – oral presentation: Cryopreservation of Cells Encapsulated in Hydrogel: Evaluation of recovery after Thawing
- **Biofabrication 2016 International Conference** (Winston Salem – NC – USA; Oct. 29th-31st 2016) – poster: Cryopreservation of cell-laden hydrogel constructs
- **BONE-TEC 2017, International Bone Tissue Engineering Congress** (Munich – Germany; Oct 12th-14th 2017) – oral presentation: Building blocks for bone-tissue engineering: a hybrid 2d-3d system for vascularization of hydrogels

Schools

- Summer School: Biomaterial and Regenerative Medicine (Riva del Garda; July 6th-8th 2015)
- Summer School: Tissue Engineering and Regenerative Medicine (Riva del Garda; July 4th-8th 2016)

Workshops

- **Workshop: IPSP – Industrial Problem Solving with Physics** (Department of Physics, University of Trento, July 21st-26th)

Acknowledgments

I am primarily grateful to my supervisors Prof. Claudio Migliaresi and Dr. Devid Maniglio for their support and their mentoring activity. I want to thank Prof. Antonella Motta for her precious support with the biological experiments and Dr. Walter Bonani for his honest advice and observations. A special thanks to Dr. Volha Liaudanskaya for teaching me the rudiments of cellular biology and to Dr. Mariangela Fedel for the precious summer tutoring.

I am also grateful to the ex-colleagues, current colleagues, and students from Biotech Lab. A big thank you and a wish for a brilliant career and a happy life to all those who have become great friends inside and outside the lab. In particular Lorenzo Moschini, Natascia Cozza, Tianjing Zhao, Thi Duy Hanh, Yuejiao 'Susan' Yang, Massimo Tomaselli, Filippo Benetti, Rosasilvia Raggio, Cristiano Carlomagno, Silvia Chiera, Alessio Bucciarelli, Laura Vettori, Giulia Weiss, Sofia Santi, Luisa Cossu for making this experience so enjoyable.

Next, I would like to acknowledge all the incredible minds I have met during my scientific career: my professors and mentors from Politecnico di Milano, my colleagues and advisors from Ukraine and all the other scientists I was lucky to meet during my Ph.D. adventure.

Moreover, very important, I want to say thanks to all my friends from Trento, Italy, and all around the worlds for their continuous support and inspiration.

Last but not least I am deeply grateful to my parents for always being by my side. I wish my family the strength to face every challenge.